IEA Annex 30 Offshore Code Collaboration Continued (OC4) phase I+II

Final report of the contributions from EUDP 64010-0071

Department of Wind Energy
I-Report

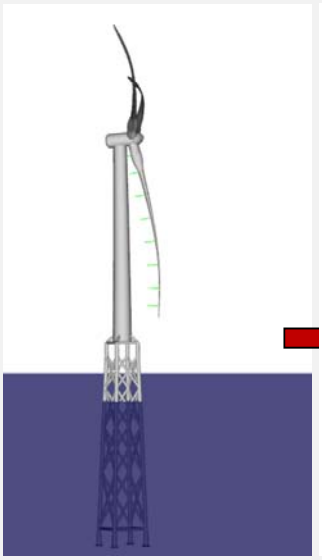

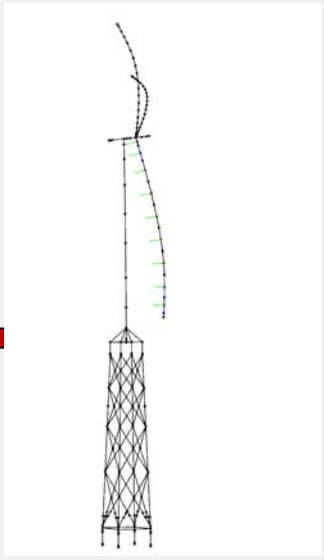

Torben J. Larsen, Anders Yde, David Verelst, Mads M. Pedersen, Anders M. Hansen, Hans Fabricius Hansen

DTU Vindenergi-I-0240(EN)

April 2014

DTU Wind Energy
Department of Wind Energy

Authors: Torben J. Larsen, Anders Yde, David Verelst, Mads M. Pedersen, Anders M. Hansen, Hans Fabricius Hansen
Title: Final report of the contributions from EUDP 64010-0071
Department: Wind Energy

DTU Vindenergi-I-0240(EN)
April 2014

Summary (max 2000 characters):

In this report the results from project IEA Annex 30 Offshore Code Collaboration Continued (OC4) phase II are reported with main attention to the Danish results obtained within the EUDP funded project IEA Annex 30: Offshore Code Collaboration Continued (OC4) 64010-0071. The results from the international comparison is summarized here with respect to the phase 1 addressing a jacket substructure and phase II addressing af semisub version.

Further on, supplementary investigation by DTU Wind Energy is carried out to explain some of the notices differences with respect to both jacket and semisub results. This mainly concerns the influence of super element reduction for the jacket and a more comprehensive comparison of three hydrodynamic approaches using the aeroelastic code HAWC2 for the semisub. Here an engineering approach mainly based on Morisons approach is used for a HAWC2-standalone version, as well as two approaches where HAWC2 is coupled together with a potential flow solution WAMSIM and WAMIT respectively. The theory of these three approaches is also presented. With these approaches it is possible to explain in detail some of the differences seen in the international comparison.

Contract no.:
EUDP 64010-0071

Project no.:

Sponsorship:
Danish Energy Agency, EUDP

Front page:

Pages: 93
Tables: 11
References: 57

Technical University of Denmark
Department of Wind Energy
Frederiksborgvej 399
Building 118
4000 Roskilde
Denmark
Phone 21 32 87 28

tjul@dtu.dk
www.vindenergi.dtu.dk

Preface

In this report the results from project IEA Annex 30 Offshore Code Collaboration Continued (OC4) phase II are reported with main attention to the Danish results obtained within the EUDP funded project IEA Annex 30: Offshore Code Collaboration Continued (OC4) 64010-0071. The results from the international comparison is summarized here with respect to the phase 1 addressing a jacket substructure and phase II addressing af semisub version.

Further on, supplementary investigation by DTU Wind Energy is carried out to explain some of the notices differences with respect to both jacket and semisub results. This mainly concerns the influence of super element reduction for the jacket and a more comprehensive comparison of three hydrodynamic approaches using the aeroelastic code HAWC2 for the semisub. Here an engineering approach mainly based on Morisons approach is used for a HAWC2-standalone version, as well as two approaches where HAWC2 is coupled together with a potential flow solution WAMSIM and WAMIT respectively. The theory of these three approaches is also presented. With these approaches it is possible to explain in detail some of the differences seen in the international comparison.

With this project, the application range for the aeroelastic code HAWC2 was significantly extended as also obtained increased international recognition.

Roskilde, April 2014

Torben J. Larsen
Senior scientist, project leader.

Content

Summary

In this report the results from the project IEA Annex 30 Offshore Code Collaboration Continued (OC4) phase II are reported.

The purpose of the project was to develop and verify existing aero elastic simulation tools for offshore wind turbines mounted at two different sub structures for water depths above 20m. The project was an international corporation consisting of developers and users of the simulation tools for offshore wind turbines within the framework of the international IEA Annex 30, titled "Offshore Comparison of Dynamic Computer Codes and Models". This annex was an extension of the previous Annex 23, which had the purpose of development and verification of computer codes for selected sub structures covering a water depth up to 30m as well as a floating concept suited for water depths above 150m. The unique thing about these annex was the constellation of international experts from the wind turbine environment and conventional oil and gas industry. This led to a distribution of knowledge for all parties causing an increased fidelity in the simulation tools crucial for cost effective offshore wind turbines. With this project, the application range for the aeroelastic code HAWC2 was significantly extended as also obtained increased international recognition.

The project was split in two main tracks. The first contained simulations of a 5MW wind turbine mounted on a jacket at 50m water depth. Benchmark cases were established where the complexity was gradually increased. The first cases covered stand still frequency analysis and steady state load distribution. Wave loads were later introduced and the complexity gradually increased until the final cases with fully turbulent atmospheric inflow, irregular wave loads and a fully flexible construction. The approach of gradually increasing the complexity made it possible to locate the reasons for discrepancies yet still also to include design driving load cases.

The second track contained simulations of a floating turbine mounted on a semi sub. The large dimensions on this semi sub were expected to require consideration of significant radiation/diffraction forces. To solve this, more advanced hydrodynamic tools than the traditional approach using Morison's formula, were used. At DTU Wind Energy, an approach a coupled method between the aeroelastic code HAWC2 and the potential flow solver WAMSIM by DHI/MIT as well as a HAWC2 stand-alone approach using Morison formula and contributions from distributed buoyancy was used. In the final part of the project a third approach was also enabled consisting of a direct coupling between HAWC2 and WAMIT by MIT. As for the jacket simulation cases the complexity was gradually increased from frequency analysis during standstill until full dynamic simulations in time domain. A special case consisting of a loss of mooring line was also included as this special case seemed to be included in the new upcoming IEC standard for floating wind turbines.

One of the main results of the project is the establishment of a database, including the definition of turbine and sub structure as well as the simulation results from the multiple partners. This database enables present and new code developers to compare and verify their results, which is a necessary step on the way to reliable and cost effective wind turbines

Phase I results

In general there is a very fine agreement between the participants regarding the eigenfrequencies of the full system. Especially the first eigenmodes, which are most important for the load response of the substructure is in fine agreement. The higher order modes are agreement within +-10% and it seem as the modal based codes in general predict slightly higher eigenfrequencies than codes solving the full set of degrees of freedom.

With respect to the static load distribution within the jacket there seem to be surprisingly large differences. The differences seen in the jacket corner legs can to some extent be explained by minor differences in modeling of marine growth and for one sensor also different modeling of the grouting connection at sea bed. Earlier in the project even larger differences was seen, which was mainly explained by difference in the way buoyancy was modeled. After some discussions it was clear that the approach of using integration of external water pressure was most accurate with respect to the distributed internal forces in the jacket. This is also the approach that from the start was used in the HAWC2 code. With respect to the internal brace loads in the jacket even larger differences was seen with respect to the static loads. Mean load levels was seen to deviate up to a factor 3. This could to some extend be explained by different modeling of structural beams, where it has previously been found that for static undetermined structures as tripods or even jackets it makes a difference whether Timoshenko or Euler beams are used for the modeling. In a separate study by DTU Wind Energy it was found that the reason for discrepancies could also directly caused by limitation in modal based or super element based approaches. This however depends directly on the way the methods has been implemented, but it seem to be necessary to include a correction term, where the missing high order terms neglected in the modal approach is included as a static load contribution.

The dynamic loading was in rather fine agreement where the fatigue load levels was in agreement within 20%, which is considered acceptable at the present state where only very limited experience with these constructions are present.

A separate study by DTU Wind Energy concluded that the jacket foundation approach may be rather sensitive with respect to loading of steep non-linear waves. This study was based on the exact same wind turbine and jacket used in the OC4 project to which a fine agreement between all codes was seen for linear waves. The study only consisted of numerical simulation, so no final conclusion was drawn, but at least it can be concluded that steep non-linear irregular waves must be included in the design considerations for wind turbines mounted on jacket (or similar) structures.

Phase II results

In general a very fine agreement is seen for all the results with respect to eigen frequencies and free decay transients, which indicates that added mass effects can be well handled by Morsions approach together with additional added mass effects from the heave plates according to (Newman, 1986) and proper consideration of buoyancy.

A fine agreement is also seen when simple wave load cases are applied to the rigid system. The main difference in response is the second order drift forces that are not present using the potential flow methods. A drift force is seen for the HAWC2-standalone due to the wheeler stretched wave profile. This causes a different response in especially the anchor line, where the tension in the upstream line is higher for the HAWC2-standalone than for the coupled versions.

The pitch motion is slightly higher for the HAWC2-standalone version than for the version with WAMIT or WAMSIM when the structure is subjected to linear incoming waves. The consequence of this is a noticeable increase in especially tower bottom loads. When flexibility in the structure is also introduced, where full flexibility in the substructure is only possible with the HAWC2-standalone version, the tower loads increase even further. These results are in line with results seen from the international comparison. It is generally recognized that WAMIT and WAMSIM are significantly more advanced hydrodynamic codes than an engineering approach using Morisons equation on distributed beam elements. However these models are eg rather simple with respect to viscous drag force modeling and so far not capable of handling flexible

structures. From the study in can therefore not be concluded, which approach for this particular system is the best, but only that large differences in tower loads are seen.

Furthermore a comprehensive comparison of three hydrodynamic approaches using the aeroelastic code HAWC2 is presented. Here an engineering approach mainly based on Morisons approach is used for a HAWC2-standalone version, as well as two approaches where HAWC2 is coupled together with a potential flow solution WAMSIM and WAMIT respectively. The theories of these three approaches are also presented. With these approaches it is possible to explain in detail some of the differences seen in the international comparison.

General code improvements

During the project the aeroelastic code HAWC2 was extended with respect to simulations on jackets, which includes both expansions of structural and hydrodynamic aspects. The solver was improved significantly with respect to correct handling of hydrodynamic added mass and a pre-processor specifically aimed for handling the complex design of a jacket was developed. The wave kinematics module was improved so wave kinematics can be pre-calculated in a reduced number of points causing a remarkable speed up. In the final part of the project it was also made possible to condensate the complex jacket structure to a super element. This reduced the degrees of freedom from 700+ to about 20, which makes it possible to simulate fully coupled turbine-jacket simulations at real time, which is about same speed for onshore turbines. The advantage of having the option of whether the structure should be condensed or not has the advantage that the required mode shapes for the condensation can be found using a few initial simulations for a specific problem.

The models used for modeling of dynamic mooring lines were improved with respect to robustness and influence of wave loading. The code HAWC2 was coupled together with the hydrodynamic codes WAMSIM and WAMIT respectively. The project was used to verify these couplings for numerical errors and thereby ensured a useful tool within very short development time. The eigenvalue solver in HAWC2 has been improved so that mooring line contributions as well as contributions from external systems are included from a linearized steady state condition. This also included contributions from WAMIT and/or WAMSIM. Furthermore, it is now possible to reduce the floating substructure to a linearized super element, as for the jacket. This is especially useful related to stability analysis and tuning of control parameters in frequency domain combination with the code HAWCStab2, or simply to carry out time simulations very fast.

.

List of Participants

In the work package in the IEA Annex 30,subtask 2, semi-submersible foundation the following persons have been involved.

From Denmark:
Torben Larsen, Anders Yde, Anders M. Hansen, David Verelst and Mads M. Pedersen, Technical University of Denmark, Roskilde, Denmark
Hans Fabricius Hansen and Anders Wedel Nielsen, DHI, Hørsholm, Denmark
Hans Riber and Cédric Le Cunff PRINCIPIA NORTH Svendborg, Denmark

From Europe:
James Nichols and Ricard Builds, DNV GL, Høvik, Norway
Kristian Sætertrø, Knut Okstad, Fedem Technology A/S, Norway
Tor Anders Nygaard, Institute for Energy Technology, Kjeller, Norway
Zhen Gao, Paul Thomassen NTNU, Norway
Jacob Qvist and Lars Frøyd, 4subsea, Hvalstad, Norway
Chenyu Luan, CeSOS/Nowitech, Trondheim, Norway
Sigrid Ringdalen Vatne and Harald Ormberg,MARINTEK, Trondheim, Norway

Fabian Vorpahl, Wojciech Popko, Adam Zuga, Martin Kohlmeier, Fraunhofer Inst. for Wind Energy, Germany
Raimund Abele, Friedemann Beyer, Daniel Kaufer University of Stuttgart, Stuttgart, Germany
Energy Systems Technology IWES, Bremerhaven, Germany
Andrés Vásquez-Rojas, Jan Dubois, Inst. of steel construction, Leibniz Universität, Hannover, Germany
Heike von Waaden, Repower Systems SE, Osnabrück, Germany

Marten de Ruiter, WMC, The Netherlands
Johann Peringa, ECN, The Netherlands

José Azcona,CENER,Navarra, Spain
Andreas Heege, SAMTECH s.a., Barcelona, Spain

Emre Uzunoglu and Carlos Guedes Soares, CENTEC, Instituto Superior Técnico, Universidade de Lisboa, Portugal
Tiago Duarte and Cyril Godreau, Instituto Superior Técnico, Universidade de Lisboa , Lisbon, Portugal
Marco Alves, WavEC – Offshore Renewables, Lisbon, Portugal

Dimitris Manolas , National Technical Univ. of Athens , Athens, Greece

From US:
Amy Robertson and Jason Jonkman, National Renewable Energy Laboratory,Golden, CO, USA
Xiaohong Chen, ABS, Houston, TX, USA
Kunho Kim, American bureau of shipping, Houston, USA

From Asia:
Wei Shi and Hyunchul Park, POSTECH, Pohang, Korea
Kwang Jin Jung and Hyunkyoung Shin, University of Ulsan, Ulsan, Korea
Atsushi Yamaguchi, University of Tokyo, Tokyo, Japan
Huang Zhiwen, Huang Yutong and Fu Pengcheng, China General Certification Center, Beijing, China
Liu Lei, Goldwind, Beijing, China

Physical meetings in the project

An important part of the project is the sharing of knowledge between the participants, which to a large degree has been done through physical meeting during the project. These meeting has been placed in conjunction with important conferences that people planned on attending. The list of meeting have been shown below

Kick-off meeting, Warsaw, poland, April 26, 2010
Meeting 1 (Kick-off 2), Bremerhaven, Germany, June 8, 2010
Meeting 2, Hamburg, Germany, October 29, 2010
Meeting 3, Maui, Hawaii, USA, June 24, 2011
Meeting 4, Amsterdam, The Netherlands, December 2, 2011
Meeting 5, Rhodes, Greece, June 22, 2012
Meeting 6, Vienna, Austria, Feb 8, 2013
Meeting 7, Nantes, France, June 14, 2013
Meeting 8, Frankfurt, Germany, November 19, 2013

Further on 16 web based meeting has been carried out.

List of publications

Journal papers:

1) F. Vorpahl, M. Strobel, J.M. Jonkman, T.J.Larsen, P. Passon, J. Nichols. Verification of aero-elastic offshore wind turbine design codes under IEA Wind Task XXIII. Wind Energ. (2013). DOI: 10.1002/we.1588

2) Wojciech Popko, Fabian Vorpahl, Adam Zuga, Martin Kohlmeier, Jason Jonkman, Amy Robertson, Torben J. Larsen, Anders Yde, Kristian Sætertrø, Knut M. Okstad, James Nichols, Tor A. Nygaard, Zhen Gao, Dimitris Manolas, Kunho Kim, Qing Yu, Wei Shi, Hyunchul Park, Andrés Vásquez-Rojas, Jan Dubois, Daniel Kaufer, Paul Thomassen, Marten J. de Ruiter, Tjeerd van der Zee, Johan M. Peeringa, Huang Zhiwen and Heike von Waaden. Offshore Code Comparison Collaboration Continuation (OC4), Phase I - Results of Coupled Simulations of an Offshore Wind Turbine With Jacket Support Structure. Journal of Ocean and Wind Energy. Vol. 1, No. 1 February 2014. ISSN: 2310-3604

Conference contributions:

3) Larsen, T.J., Hansen, A.M. Super element formulation of jackets for aero-elastic computations. Danish Wind Industry Annual Event 2014 on March 26-27 in Herning, Denmark

4) W. Popko, F. Vorpahl, A. Zuga, M. Kohlmeier, J. Jonkman, A. Robertson, T. J. Larsen, A.Yde, K. Sætertrø, K. M. Okstad, J. Nichols, T. A. Nygaard, Z. Gao, D. Manolas, K. Kim, Q. Yu, W. Shi, H. Park, A. Vásquez-Rojas, J. Dubois, D. Kaufer, P. Thomassen, M. J. de Ruiter, J. M. Peeringa, H. Zhiwen, H. von Waaden. Offshore Code Comparison Collaboration Continuation (OC4), Phase I – Results of Coupled Simulations of an Offshore Wind Turbine with Jacket Support Structure. Proceedings of the Twenty-second (2012) International Offshore and Polar Engineering Conference Rhodes, Greece, June 17–22, 2012, ISBN 978-1-880653-94–4, ISSN 1098-6189

5) W. Popko, F. Vorpahl, J. Jonkman and A. Robertson. OC3 and OC4 projects – Verification benchmark exercises of the state-of-the-art coupled simulation tools for offshore wind turbines. European Seminar OWEMES 2012

6) Hansen, A.M., Larsen, T.J., Yde, A., Influence of foundation model complexity on the design loads for offshore wtg on jacket foundation. EWEA 2013, Vienna

7) Robertson, J. Jonkman, and W. Musial, F. Vorpahl and W. Popko. Offshore Code Comparison Collaboration, Continuation: Phase II Results of a Floating Semisubmersible Wind System. EWEA Offshore 2013 Frankfurt, Germany November 19–21 2013

8) Robertson, A., Jonkman, J., Quist, J., Chen, X., Armendariz, J.A., Soares, C.G., Luan, C., Yutonn, H., Yde, A., Larsen, T., Nichols, J., Lei, L., Maus, K.E., Godreau, C., Heege, A., Vatne, S.R., Manolas, D., Qin, H., Riber, H., Abele, R., Yamaguchi, A., Pham, A., Alves, M., Kofoed-Hansen, H. Offshore code comparison collaboration, continued: phase II results of a floating semisubmersible wind system. Proceedings of the 33rd International Conference on Ocean, Offshore and Arctic Engineering OMAE2014 June 8-13, 2014, San Francisco, CA, USA

9) Larsen, T.J., Kim, T., Schløer, S., Bredmose, H. Comparison of wave kinematics models for an offshore wind turbine mounted on a jacket substructure. In proceeding of EWEA Offshore 2011, Amsterdam, The Netherlands. Nov. 29 – Dec 1.

Technical reports:

10) Larsen, T.J., Verelst, D., Pedersen, M.M., Hansen, A.M. (2014). Benchmark comparison of load and dynamics of a floating 5MW semisub windturbine, using three different hydrodynamic approaches. DTU Wind Energy Report-I-0239.

11) Larsen, T. J. (2011). Turbulence for the IEA Annex 30 OC4 Project. Technical report, Risø National Laboratory for Sustainable Energy Technical University of Denmark. Risø-I-3206 (EN).

12) Robertson, J. Jonkman, M. Masciola, H. Song, A. Goupee, A. Coulling, and C. Luan. Definition of the Semisubmersible Floating System for Phase II of OC4. Technical report, NREL, 2012.

Phase I:

Phase I addresses benchmark comparison of the 5MW NREL Wind turbine mounted on a jacket foundation.

Methods

A total of 15 different codes participated in the benchmark as listed in Table 1. Some of the codes are standalone codes, where others are coupled approaches between a turbine load code and another specific foundation module eg. FLEX-ASAS and FLEX5-Poseidon. In general the aerodynamic modules are all based on the Blade Element Momentum (BEM) approach, but as always the Devil is in the detail and the implementation of the BEM approaches are not completely identical. However, for these aerodynamically rather simple cases it was previously found in the OC3 project (Vorpahl et.al., 2013) that a sufficient match was present with respect to comparisons of foundation loads.

With respect to the structural formulation there are in general two different approaches, full Finite Beam Element (FEM) and a modal based approach. Some codes used combinations of the two. When going one level deeper into the differences, some codes used a multibody formulation, and some codes a Craig-Bampton, Guyuan or third approach for generating the mode shapes. It is not possible to provide a full overview of all the codes, but for the HAWC2 code, please see (Kim et.al 2013) and for the other codes please see Table 1.

The hydrodynamic forces for the jacket simulation are primarily based on Morisons approach (Morison et. al 1950) with extensions for added mass and buoyancy. Especially there are different approaches with respect to how buoyancy is implemented. In HAWC2, the buoyancy approach is based on pressure integration as explained in the methods section in the phase II chapter which is the correct approach when distributed forces within the structure is targeted. Many other codes used as default some kind of inverse gravity, reduced density or principles from Archimedes, but these methods only ensure the total buoyancy to be correct, not necessarily the distributed forces. Another point for different approaches is how to handle flooded members. In the beginning of the project all codes (except HAWC2) used an increased mass of the steel component for the flooded corner piles. This ensures a correct total mass (steel+water), but the distribution of internal axial forces is not necessarily correct. The explanation is that water inside the legs are not rigidly attached to the steel wall, but will cause pressure in the bottom plate only and therefore only to a very limited level cause axial compression in the legs (assuming the legs are not divided into compartments). After this was presented by DTU, all the other code developers changed their practise. This is described in more details in (Popko et.al 2014).

The wave kinematics is for linear regular and irregular waves based on the Airy Method (Airy, 1841) where the surface elevation issues are accounted for using Wheeler stretching (Wheeler, 1970). The steep waves are accounted for using stream function wave theory (Chaplin, 1980) and (Fenton, 1988). Related to both the IEA OC4 project, but also a Danish PSO project a study of the wave loading on the jacket using fully non-linear and irregular waves was carried out using HAWC2 and presented in (Larsen, 2011) as well as (Bredmose et.al. 2013). These results are however not included in the general benchmark cases, but shows that the jacket construction could be highly sensitive to steep waves causing a high amount of transient vibrations.

Code	Aerodynamics (aero)	Hydrodynamics (hydro)	Control (servo)	Structural (elastic)
3DFloat	BEM or GDW	Airy^{str} or UD Stream + ME	UD	FEM
ADAMS + AeroDyn	BEM or GDW + DS	Airy^{str} or UD or Stream + ME	DLL or UD	MBS
ADCoS-Offshore	BEM + DS	Airy^{str} or UD or Stream + ME	DLL or UD	FEM
ASHES	BEM + DS	Airy^{str} + ME	Internal control system	FEM
Bladed V3.8X	BEM or GDW + DS	Airy^{str} or UD or Stream + ME	DLL or UD	FEM^{p} + Modal/MBS
Bladed V4 Multibody	BEM or GDW + DS	Airy^{str} or UD or Stream + ME	DLL or UD	MBS
FAST-ANSYS	BEM or GDW + DS (AeroDyn)	Airy^{str} or UD + ME	DLL or UD or SM	Support structure: FEM, Turbine: FEM^{p} + Modal/MBS
FEDEM WindPower	BEM or GDW + DS (AeroDyn)	Airy, Airy^{str}, Stream + ME	DLL or UD or Internal control system	MBS/FEM Modal (CMS)
Flex-ASAS	BEM or DS	Airy^{str} or UD + ME	DLL	Modal, FEM
Flex5-Poseidon	BEM or GDW + DS	Airy^{str} or UD or Stream + ME, Interface to WaveLoads	DLL or UD	FEM + Modal
GAST	BEM or 3DFW + DS	Airy^{str} + PF or Stream + ME	DLL or UD	MBS/FEM
HAWC2	BEM or GDW + DS	Airy^{str} or Stream or UD + ME	DLL or UD or SM	MBS/FEM
OneWind	BEM or GDW + DS	Airy^{str} or UD + ME	DLL or UD	MBS/FEM
Phatas-WMCfem	BEM or GDW + DS	Airy^{str} or Stream + ME	DLL or Internal modeling	Rotor-FD, Tower: FEM + Craig Bampton
USFOS-vpOne	BEM + DS	Airy^{str} or Stokes' 5th order or Stream + ME	DLL or UD	FEM

3DFW – Free Wake Vortex particle method
Airy – Airy theory
Airy^{str} – Airy theory with stretching method
BEM – Blade Element Momentum Theory
CMS – Component Mode Synthesis
DLL – External dynamic link library
DS – Dynamic Stall Implementation
FEM – Finite-element method
FEM^{p} – Finite-element method for mode pre-processing only
PF – Linear potential flow with radiation and diffraction
GDW – Generalized Dynamic Wake Theory, there are different formulations of these models that account for dynamic wake, but these differences are not discriminated here.
MBS – Multibody-dynamics formulation
ME – Morison's Formula
Modal – Modal reduced system
Rotor-FD – Nonlinear partial differential equations of the rotating and elastically deforming rotor (slender beams) solved by finite difference method and cubic spline for deformation field.
SM – interface to Simulink with Matlab
Stream – Dean's stream function
UD – User-defined subroutine

Table 1: List of simulation codes included in the phase I benchmark.

Turbine and jacket definition

In the OC4 project, the ”NREL 5-MW Offshore Baseline Turbine” defined by Jonkman et al. (2009) is supported by the UpWind reference jacket model developed by Vemula et al. (2010) and further adopted by Vorpahl et al. (2011) for the needs of this benchmark exercise, see Figure 1. The definition of the jacket support structure, used within the OC4 project, consists of a jacket substructure, a transition piece and a tower. Four legs of the jacket are supported by piles, which are modeled as being clamped at the seabed, see Figure 2. The legs are inclined from the vertical position and stiffened by four levels of X-braces. Additionally, mudbraces are placed just above the mudline to minimize the bending moment at the foundation piles. The jacket and the tower are connected through a rigid concrete transition piece. The elevation of the entire support structure is 88.15 m, whereas the hub height is 90.55 m. The OWT is analysed for a site of 50m water depth.

The definition of the OWT should be as simple as possible to minimize the effort and modeling errors in its implementation in various codes. On the other hand, its complexity should allow it to mimic the structural behaviour of a real OWT and to depict differences in results between the simulation codes. For simplification reasons, it is decided not to include appurtenances on the jacket structure such as boat landings, J-tubes, anodes, cables, ladders etc. Also, joint cans are not taken into account in the setup of the model. At joints, the connecting nodes of elements are defined at the intersection points of the members’ centerlines. This leads to overlap of elements in the analysed jacket. Due to the overlapping members, the mass of the jacket is overestimated by about 9.7 %, though there is only a marginal influence coming from overlapping parts on eigenfrequencies and simulated loading as demonstrated in Kaufer et al. (2010). The additional masses such as: hydrodynamic added mass, water in flooded legs and marine growth, have a strong influence on the dynamic response of the structure, and therefore, are included in the model description. Marine growth mass and hydrodynamic added mass are also slightly overestimated considering the presence of overlapping members, but that was assumed acceptable in the light of this project aiming primarily on the benchmark using identical modeling data.

A visualization of the combined structure through the HAWC modeling is shown in Figure 3.

Figure 1: Illustration of the modeled turbine and jacket foundation.

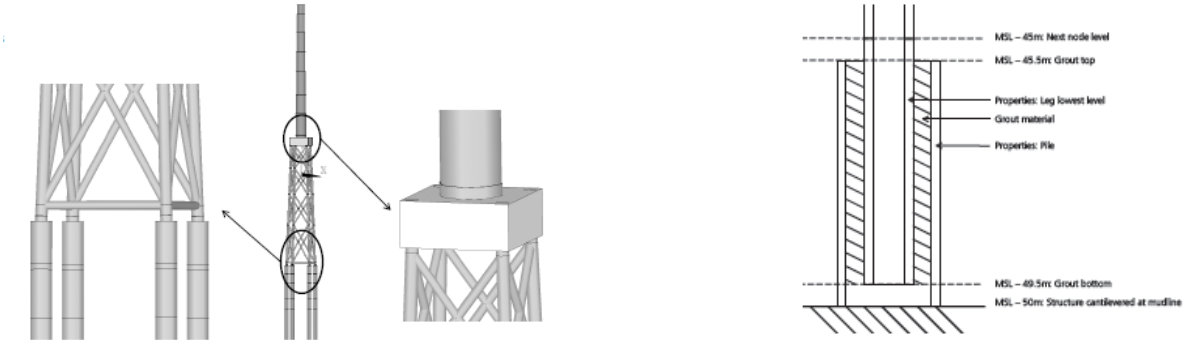

Figure 2: Illustration of details relted to the trasition piece and the pile connections using a grouted connection

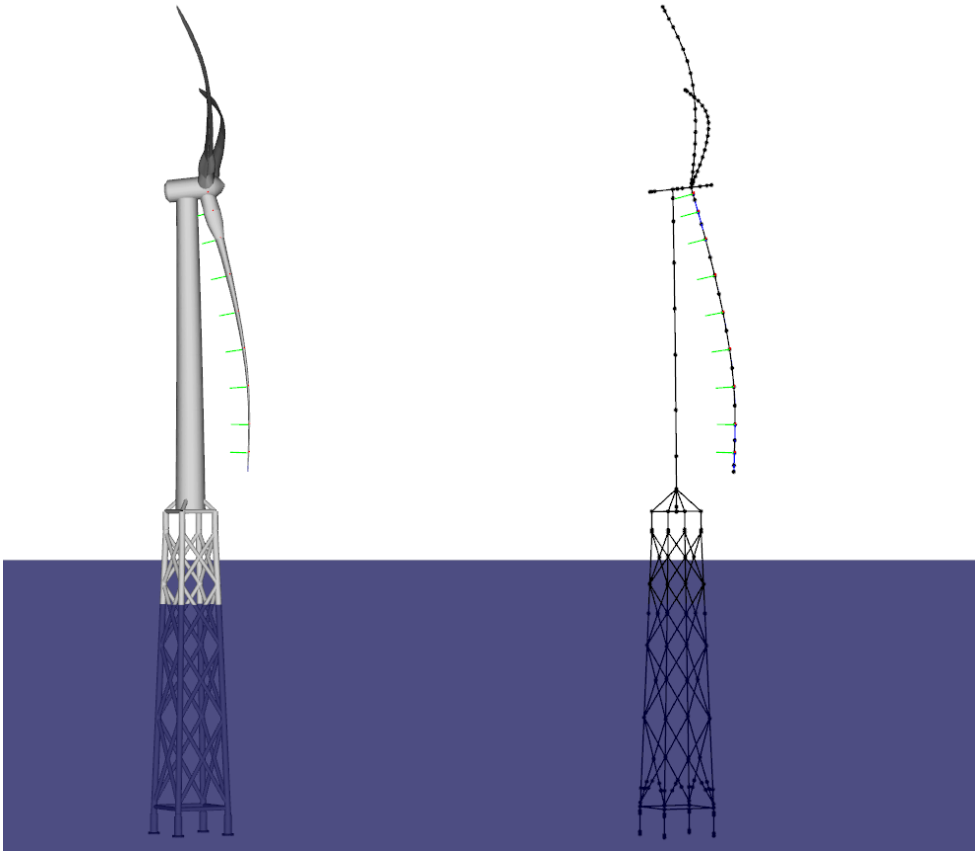

Figure 3: Visualization of the HAWC2 model with the blades in a deflected state. Left: With surface, right: Element and node resolution.

Phase I: Loadcases

A set of load cases was defined starting with very simple standstill conditions without wind or wave loading just to ensure a similar static load level and to compare natural frequencies and component mass during standstill. The next set of cases consisted of again simple load situation, now with a rigid construction subjected to simple wave or wind loading to ensure that the hydro and aerodynamic input was of same magnitude before proceeding to the more complex cases with a fully flexible structure subjected to fully turbulent wind loading during operation and a fully irregular sea state. The load cases can be found in Table 2 to Table 6.

Load Case	Enabled DOF	Wind Conditions	Wave Conditions	Analysis Type	Initial Conditions
1.0a	Support structure	No air	No water	Eigenanalysis, no gravity or damping, natural frequencies and mode shapes	
1.0b	All	No air	No water	Eigenanalysis, no gravity or damping, natural frequencies and mode shapes	$\Omega = 0$ rpm $\Phi = 0$ deg $\Theta = 0$ deg brake applied
1.0c	Support structure	No air	No water	Eigenanalysis, gravity and structural damping included, damped frequencies and mode shapes	
1.0d	All	No air	No water	Eigenanalysis, gravity and structural damping included, damped frequencies and mode shapes	$\Omega = 0$ rpm $\Phi = 0$ deg $\Theta = 0$ deg brake applied

Table 2: Overview of loadcases with a standstill situation with a flexible construction.

Load Case	Enabled DOF	Wind Conditions	Wave Conditions	Analysis Type	Initial Conditions
2.1	None	No air	Still water	Static simulation including gravity and buoyancy to MSL	
2.2	None, Rotor speed and blade pitch via controller	Steady, uniform, no shear, $V_{hub} = 8$ m/s	No water	Periodic time-series solution	$\Omega = 9$ rpm $\Phi = 0$ deg $\Theta = 0$ deg
2.3a	None	No air	Regular Airy: $H = 6$ m, $T = 10$ s	Periodic time-series solution	Wave simulation starts from crest at $x = 0$, $y = 0$ (global system)
2.3b	None	No air	Regular stream function (Dean, 9th): $H = 8$ m, $T = 10$ s	Periodic time-series solution	Wave simulation starts from crest at $x = 0$, $y = 0$ (global system)
2.4a	None, Rotor speed and blade pitch via controller	NTM (Kaimal): $V_{hub} = V_r = 11.4$ m/s $\sigma_x = 1.68$ m/s $\sigma_y = 1.34$ m/s $\sigma_z = 0.84$ m/s $L_{k,x} = 340.20$ m $L_{k,y} = 113.40$ m $L_{k,z} = 27.72$ m $L_c = 340.20$ m Wind shear: $\alpha = 0.14$	No water	PDF, DEL, power spectra	$\Omega = 12.1$ rpm $\Phi = 0$ deg
2.4b	None, Rotor speed and blade pitch via controller	NTM (Kaimal): $V_{hub} = 18$ m/s $\sigma_x = 2.45$ m/s $\sigma_y = 1.96$ m/s $\sigma_z = 1.23$ m/s $L_{k,x} = 340.20$ m $L_{k,y} = 113.40$ m $L_{k,z} = 27.72$ m $L_c = 340.20$ m Wind shear: $\alpha = 0.14$	No water	PDF, DEL, power spectra	$\Omega = 12.1$ rpm $\Phi = 0$ deg
2.5	None	No air	Irregular Airy: $H_s = 6$ m, $T_p = 10$ s, Pierson-Moskowitz wave spectrum	PDF, DEL, power spectra	

Table 3: Overview of loadcases with a rigid construction subjejted to wind and wave loading.

Load Case	Enabled DOF	Wind Conditions	Wave Conditions	Analysis Type	Initial Conditions
3.2	All, Rotor speed and blade pitch via controller	Steady, uniform, no shear: $V_{hub} = 8$ m/s	No water	Periodic time-series solution	$\Omega = 9$ rpm $\Phi = 0$ deg $\Theta = 0$ deg
3.4a	All, Rotor speed and blade pitch via controller	NTM (Kaimal): $V_{hub} = V_r = 11.4$ m/s $\sigma_x = 1.68$ m/s $\sigma_y = 1.34$ m/s $\sigma_z = 0.84$ m/s $L_{k,x} = 340.20$ m $L_{k,y} = 113.40$ m $L_{k,z} = 27.72$ m $L_c = 340.20$ m Wind shear: $\alpha = 0.14$	No water	PDF, DEL, power spectra	$\Omega = 12.1$ rpm $\Phi = 0$ deg

Table 4: Overview of loadcases with a fully flexible construction subjected to wind, but not wave loading.

Load Case	Enabled DOF	Wind Conditions	Wave Conditions	Analysis Type	Initial Conditions
4.3b	Support structure	No air	Regular stream function (Dean, 9th): $H = 8\,\text{m}$, $T = 10\,\text{s}$	Periodic time-series solution	Wave simulation starts from crest at $x = 0$, $y = 0$ (global system)
4.5	Support structure	No air	Irregular Airy: $H_s = 6\,\text{m}$, $T_p = 10\,\text{s}$, Pierson-Moskowitz wave spectrum	PDF, DEL, power spectra	

Table 5: Overview of loadcases with a rigid turbine, a flexible jacket subjected to wave loading only.

Load Case	Enabled DOF	Wind Conditions	Wave Conditions	Analysis Type	Initial Conditions
5.6	All, Rotor speed and blade pitch via controller	Steady, uniform, no shear: $V_{hub} = 8\,\text{m/s}$	Regular stream function (Dean, 9th): $H = 8\,\text{m}$, $T = 10\,\text{s}$	Periodic time-series solution	$\Omega = 9\,\text{rpm}$ $\Phi = 0\,\text{deg}$ $\Theta = 0\,\text{deg}$ wave simulation starts from crest at $x = 0$, $y = 0$ (global system)
5.7	All, Rotor speed and blade pitch via controller	NTM (Kaimal): $V_{hub} = 18\,\text{m/s}$ $\sigma_x = 2.45\,\text{m/s}$ $\sigma_y = 1.96\,\text{m/s}$ $\sigma_z = 1.23\,\text{m/s}$ $L_{k,x} = 340.20\,\text{m}$ $L_{k,y} = 113.40\,\text{m}$ $L_{k,z} = 27.72\,\text{m}$ $L_c = 340.20\,\text{m}$ Wind shear: $\alpha = 0.14$	Irregular Airy: $H_s = 6\,\text{m}$, $T_p = 10\,\text{s}$, Pierson-Moskowitz wave spectrum	PDF, DEL, power spectra	$\Omega = 12.1\,\text{rpm}$ $\Phi = 0\,\text{deg}$

Table 6: Overview of loadcases with a fully flexible construction subjected to both wind and wave loading.

Phase I: Sensors and coordinate systems

The coordinate systems used in the output channels are defined according to the IEC and GL recommendation. For the substructure this means that the x axis is the default wind direction and z is positive upwards, see Figure 4 and Figure 5.

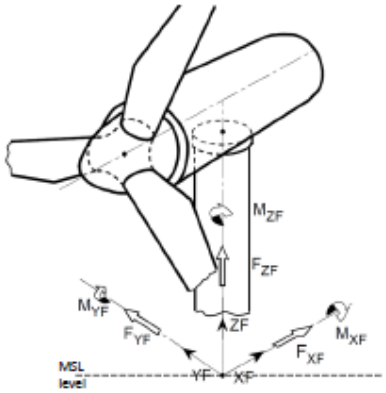

Figure 4: Coordinate system of the tower and substructure

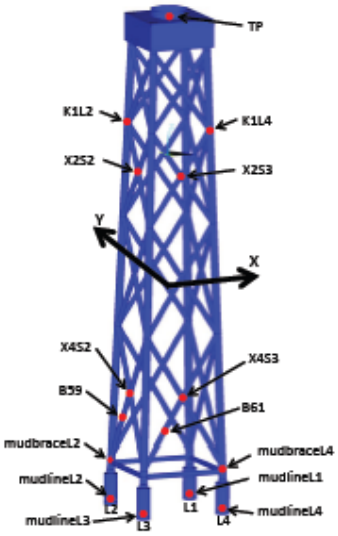

Figure 5: Position of output sensors for the substructure

Phase I: Results

The results presented in this chapter is mainly based on the papers (Popko et.al. 2012) and (Popko et.al. 2014)

The first comparisons addressed natural frequencies and stand still cross sectional load levels. The natural frequencies are shown in Figure 6, where a fine agreement is seen in most cases. The variation in frequency is very low for the first few modes, which are also the most important ones with respect to tower and substructure loads. For the higher modes there in general also an agreement within +/-10%, however it is also clear that it sometimes can be difficult to identify the different mode shapes, which most likely is the reason for the discrepancies of the 1st edgewise collective mode. In the HAWC2 results this mode does not even exist, since collective edge is the same mode as the one denoted 1st drivetrain torsion. (Popko, 2014) concludes that for the higher order modes as the 2nd flap or edgewise mode there seem to be a systematic difference between full FE based codes and modal based codes, where the modal based codes result in slightly higher frequencies. This, however, most likely depends on the detailed implementation and coupling of the mode shapes as illustrated in the DTU Wind Energy study written in the chapter "Phase I: Study of super element reduction impact" below.

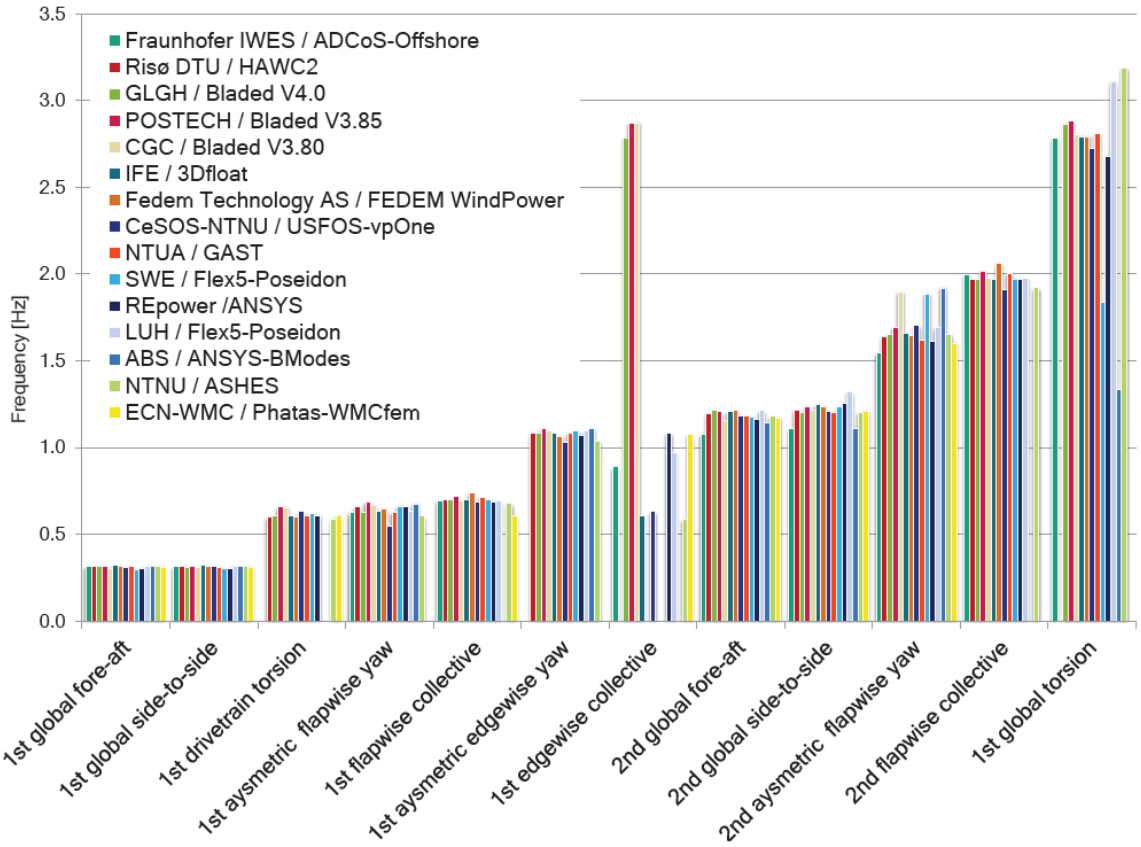

Figure 6: Comparison of natural frequencies.

A general discrepancy in all loadcases is the mean load level inside the jacket. Some of this in explained by difference approached for calculating buoyancy. An example of this can be seen in Figure 7 where the axial load level in a pile is not the same for all participants. It should be noted that during the first rounds of comparison the discrepancy was even larger than shown in Figure 7, but after a constructive discussion the method of using integrated pressure was generally adopted by all and the remaining difference is mainly caused by differences related to pressure forces on the grout connection, small discrepancy in marine growth mass and buoyancy. The method of using a reduced submerged steel mass is not sufficiently accurate for a jacket construction. Further on it can be seen that the time varying vertical forces are not completely identical either, which is explained with small differences in the contribution from the varying dynamic pressure due to the wave motion. The horizontal force variation is however in much better agreement as see in Figure 8.

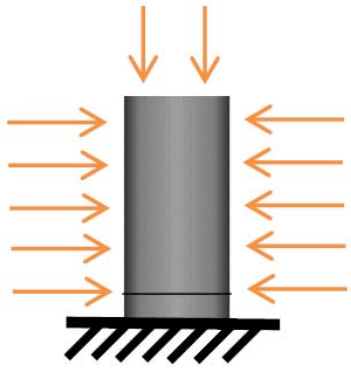

(a) Pile modeled as cut and fixed at the mudline, arrows indicate the areas where pressure is integrated.

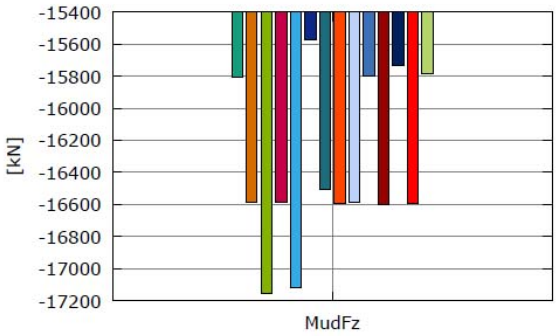

(b) Vertical force at mudline for still water case, LC 2.1.

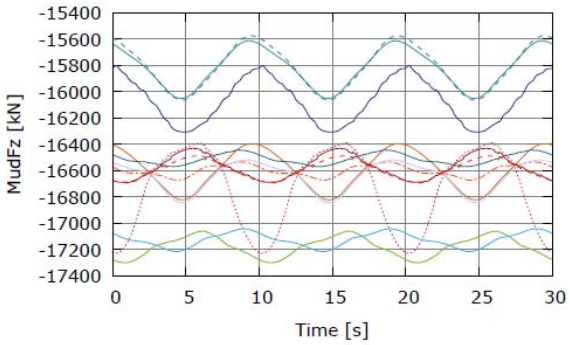

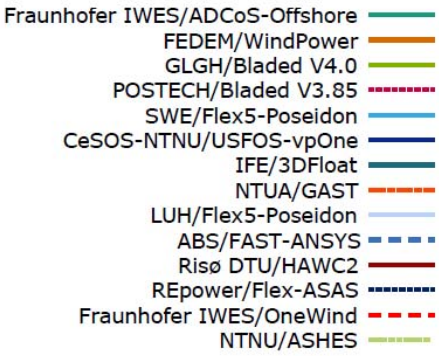

(c) Vertical force at mudline for Airy wave with Wheeler stretching case, LC 2.3a.

Figure 7: Comparison of axial compression in pile 1.

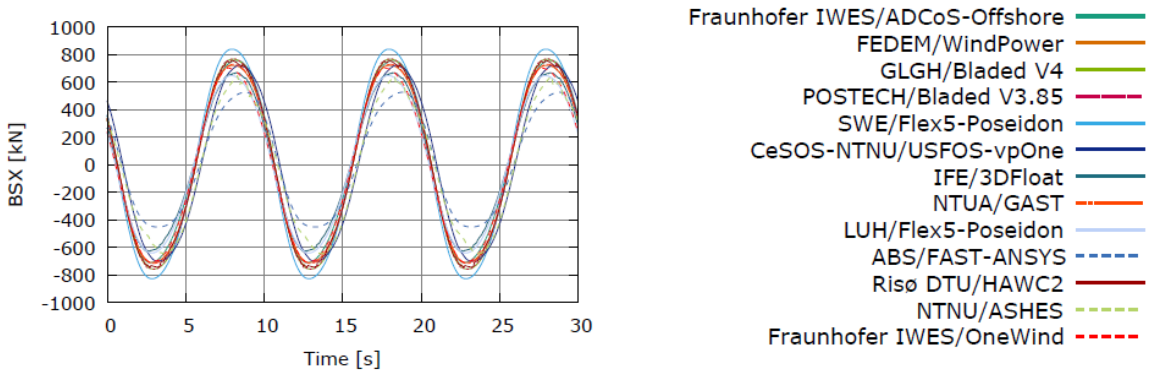

Figure 8: Comparison of fore-after shear force at mudline, loadcase 2.3a.

A comparison of the load level at both tower top and mudline is shown in Figure 9. The structure is subjected to operational aerodynamic forces at 18m/s in case 2.4b. The fatigue load variation is, if the two outliers GAST and ADCoS is neglected, within 20% which is considered a quite fine agreement.

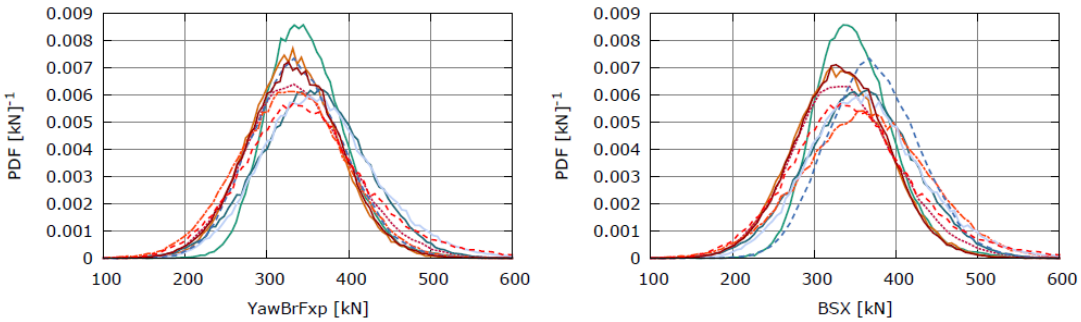

(a) PDF – Tower-top fore-aft shear force. (b) PDF – Fore-aft shear force at mudline.

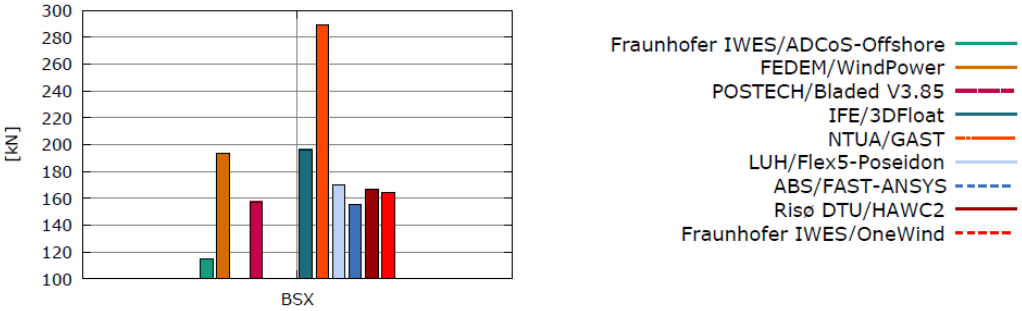

(c) DEL – Fore-aft shear force at mudline.

Figure 9: Comparison of tower and mudline horizontal forces with aerodynamic forces only at 18m/s. Case 2.4b

An example of blade tip deflections is shown in Figure 10 for the few codes capable of handling blade torsion. All codes agree on the phase dependence; however the magnitude differs with a magnitude of 3. This illustrates the complexity for calculating this property even in a simple case at 8m/s without turbulence, which in some cases is quite important since it couples directly to the aerodynamic forces through the angle of attack. The complexity of blade torsion is also seen in Figure 11, where discrepancies in the blade torsion can be seen for the turbulence case 3.4a.

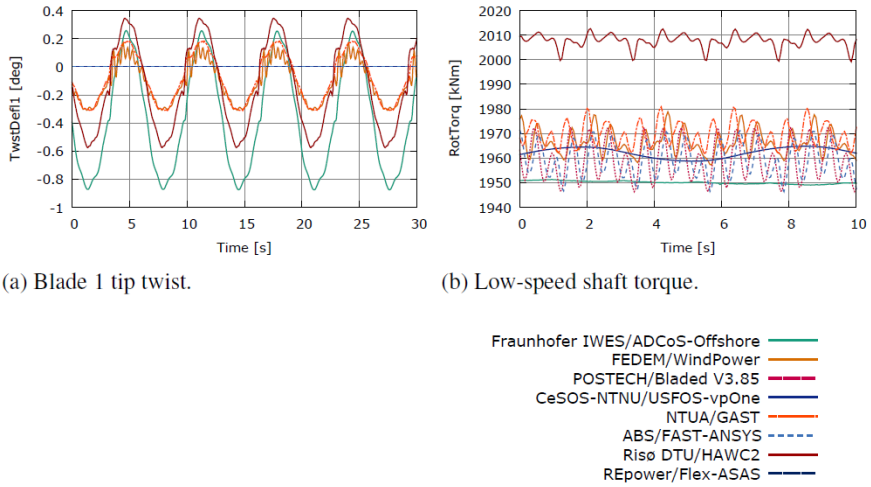

(a) Blade 1 tip twist. (b) Low-speed shaft torque.

Figure 10: Comparison of blade twist angles and rotor speed for loadcase 3.2

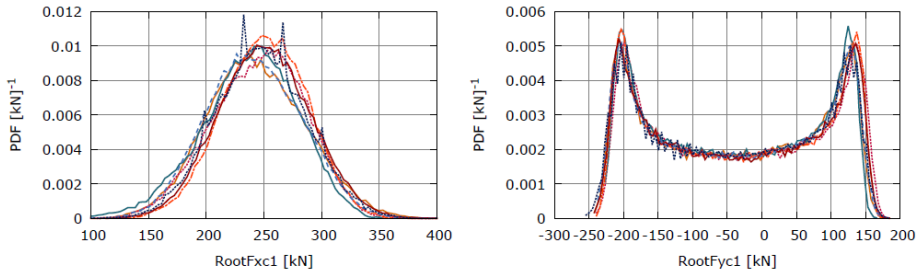

(a) PDF – flapwise shear force at blade root. (b) PDF – edgewise shear force at blade root.

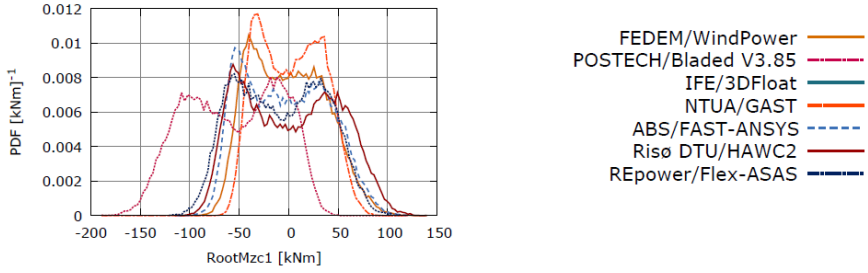

(c) PDF – pitching moment at blade root.

Figure 11: PDF of blade root forces and pitching moment in loadcase 3.4a.

When observing response for the case with a fully flexible sub structure subjected to wave loading, the dynamic behaviour is similarly captured by all codes. This is illustrated in Figure 12 where a special sensor measuring the horizontal out-of-plane motion of an X-joint is compared. This is also seen in Figure 13 and Figure 14 including contributions of irregular waves and combined wind and waves respectively. The most uncertain load is actually the mean load level in the structure, especially seen in the axial force of a brace member, see Figure 13.Some codes have a load level 3 time higher than others! This indicated a fundamental problem with the codes regarding correct handling of a static undetermined structure. It was previously found in the OC3 (Vorpahl et.al 2013)) project that whether beam member for a tripod was modeled as Timoshenko of Bernoulli beam could cause a factor two difference for the distribution of axial loading.

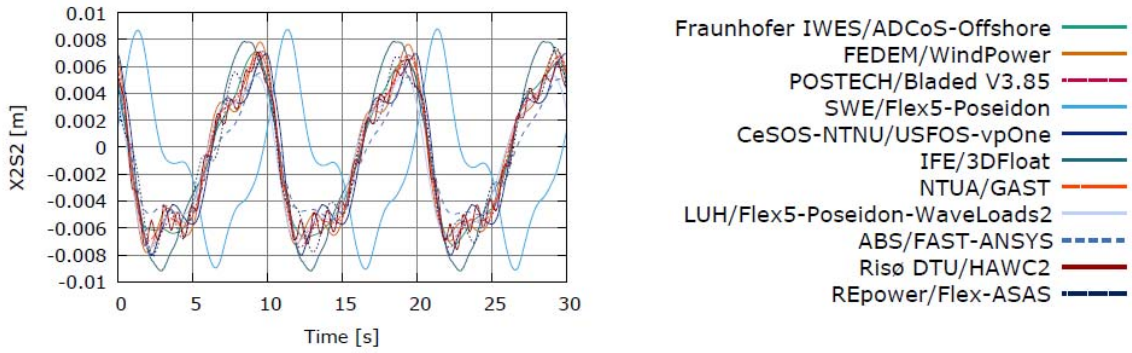

Figure 12: Out-of-plane deflection at center of X-joint at level 2 on side 2, loadcase 4.3b

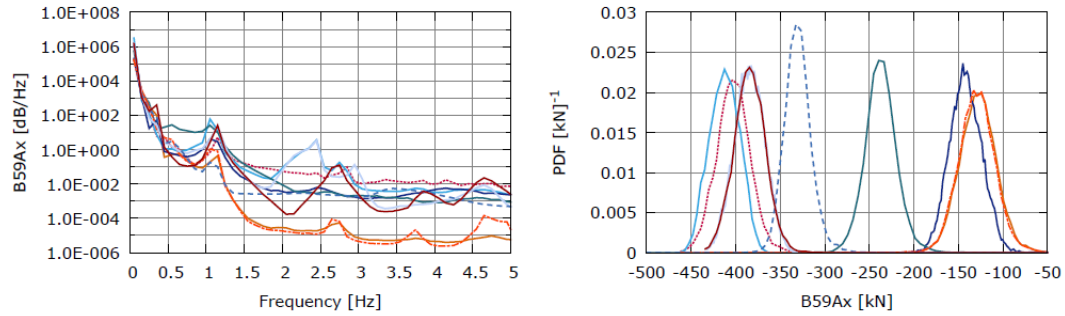

(a) PSD – axial force in B59. (b) PDF– axial force in B59.

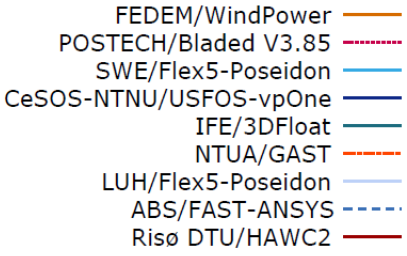

Figure 13: Axial force in center of brace 59, LC 4.5.

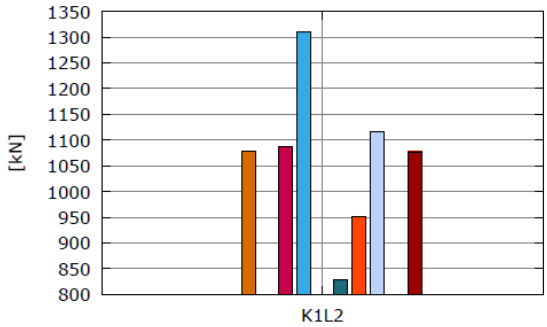

(a) DEL – axial force in Leg 2 at K1L2.

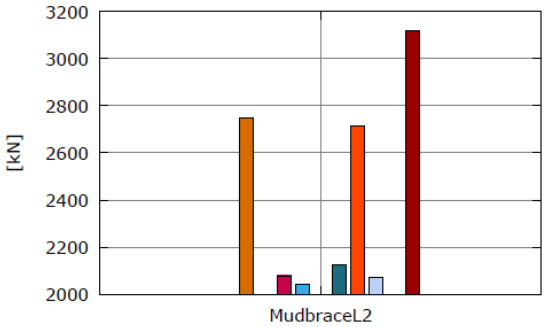

(b) DEL – axial force in Leg 2 at mudbraceL2.

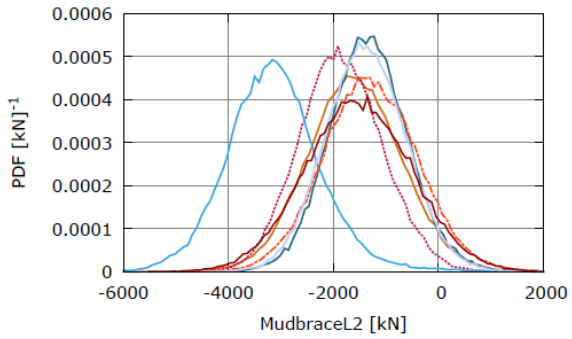

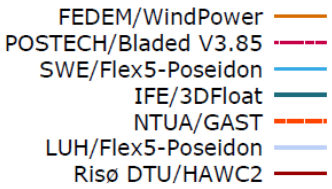

(c) PDF – axial force in Leg 2 at mudbrace level.

Figure 14: Damage equivalent loads at jacket leg, LC 5.7.

Phase I: Study of super element reduction impact

As part of this OC4 project and a parallel research project funded by PSO, a new structural option in HAWC2 was enabled. This approach concerned a reduction of the equations of motions (EOM's) into a reduced number of equations based on a super element reduction technique.

The full description of this approach has been reported in (Bredmose et.al., 2013), but as a small summary the full EOM can (in a simplified form) be rewritten from

$$\mathbf{M}\ddot{\mathbf{x}} + \mathbf{C}\dot{\mathbf{x}} + \mathbf{K}\mathbf{x} = \mathbf{F}(\mathbf{t}) \quad (1)$$

Where **x** is the state vector in physical coordinates and **M**, **C** and **K** is the mass, damping and stiffness matrix respectively.

(1) Can be rewritten to generalized coordinates based on the change in state variables using a transformation matrix **T**.

$$\mathbf{x} = \mathbf{T}\mathbf{y} \quad (2)$$

Where the states **y** are in generalized coordinates and contains a potentially much reduced number of states than contained in **x**.

The reduced set of EOM can be written

$$\mathbf{T}^{\mathbf{T}}\mathbf{M}\mathbf{T}\ddot{\mathbf{y}} + \mathbf{T}^{\mathbf{T}}\mathbf{C}\mathbf{T}\dot{\mathbf{y}} + \mathbf{T}^{\mathbf{T}}\mathbf{K}\mathbf{T}\mathbf{y} = \mathbf{T}^{\boldsymbol{T}}\mathbf{F}(\mathbf{t}) \quad (3)$$

Which can be written in short as

$$\tilde{\mathbf{M}}\ddot{\mathbf{y}} + \tilde{\mathbf{C}}\dot{\mathbf{y}} + \tilde{\mathbf{K}}\mathbf{y} = \tilde{\mathbf{F}}(\mathbf{t}) \quad (4)$$

An essential part of the benefit of the rewriting into generalized coordinates with respect to simulation time and accuracy depends especially of the transformation matrix **T**. This may, depending of the actual physical problem, be generated based on a static Guyan reduction (Guyan, 1964), dynamic modes shapes or a combination thereof.

Within the OC4 project a small study was carried out to investigate how the condensation of the jacket problem should be handled within HAWC2.

Static mode shapes

First the transformation matrix was generated based on a static reduction technique as described in (Guyan, 1964). The principle is that unit loads are applied at the interface node (coupling between the sub structure and the tower) and the corresponding deflection shapes is contained as columns in the transformation matrix **T**. This is illustrated in Figure 15.

As a first evaluation whether the Guyan reduction is a good approach to the definition of the transformation matrix **T**, and finally whether it leads to correct results, the natural frequencies of the combined full turbine and superelement approach was compared to the full DOF approach, shown in Table 7. Here it can be seen that the natural frequencies are well preserved for the combined approach, with small deviance for mode 9 and 10, which are the second flapwise bending modes.

The next comparison was a comparison of time series for selected location at the turbine and within the substructure. The turbine sensors are presented in Figure 16, where a perfect match is seen. However when comparing the internal load in the jacket a deviation to the full solution is seen, see Figure 17. This shows that the Guyan reduction approach is fine with respect to the overall performance, however it is not well suited for analysis of the internal load levels.

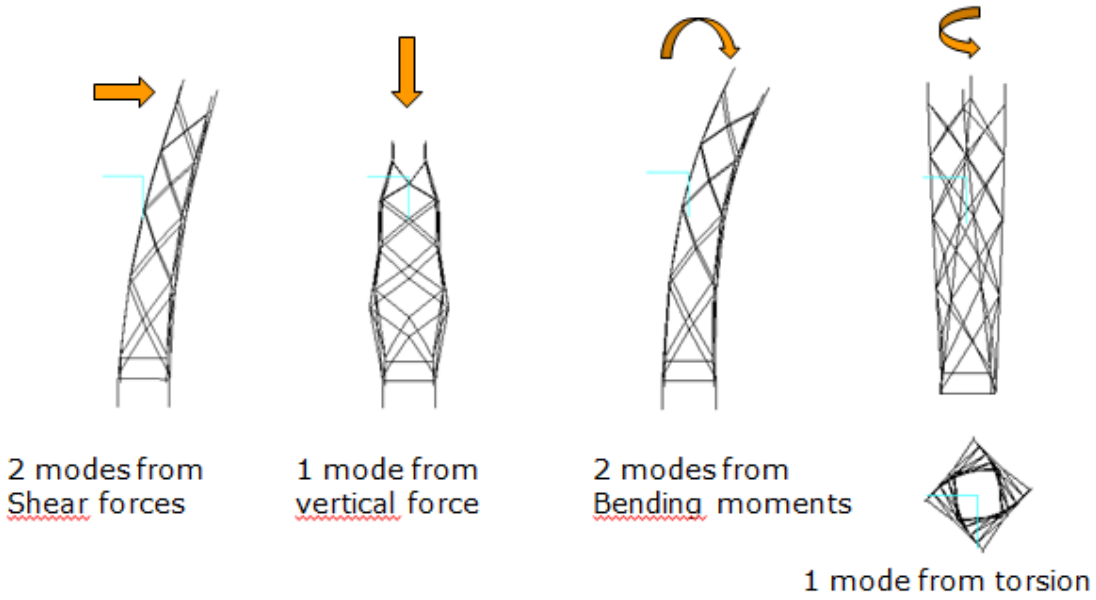

Figure 15: Principles for a static Guyan reduction of the jacket. Unit forces are applied at the interface node to which the corresponsing deflection shapes is derived and used for the transormation matrix.

	Frequency			Damping Log decr		
Mode Nr	Full	Combined	Ratio	Full	Combined	Ratio
1	0.00	0.00	1.00	0.00	0.00	1.00
2	0.32	0.32	1.00	2.63	2.63	1.00
3	0.32	0.32	1.00	2.69	2.69	1.00
4	0.62	0.62	1.00	2.82	2.82	1.00
5	0.66	0.66	1.00	3.18	3.19	1.00
6	0.69	0.69	1.00	3.30	3.30	1.00
7	1.07	1.07	1.00	3.17	3.25	0.98
8	1.08	1.08	1.00	3.41	3.62	0.94
9	1.20	1.17	1.03	9.68	9.37	1.03
10	1.21	1.18	1.03	9.78	9.27	1.06
11	1.64	1.64	1.00	7.36	7.42	0.99
12	1.72	1.72	1.00	13.91	13.91	1.00
13	1.88	1.88	1.00	9.16	9.15	1.00
14	1.97	1.97	1.00	9.24	9.24	1.00
15	2.82	2.74	1.03	15.77	16.54	0.95
16	2.99	2.99	1.00	20.61	20.61	1.00
17	3.63	3.58	1.01	24.06	24.50	0.98
18	3.93	3.79	1.04	17.72	18.49	0.96
19	3.99	3.99	1.00	14.61	14.12	1.03

Table 7: Table of full combined turbine and jacket eigenfrequencies between a full set of DOF and a version where the full turbine model is connected to the static condensated super element. A fine but not perfect match is seen for most frequencies.

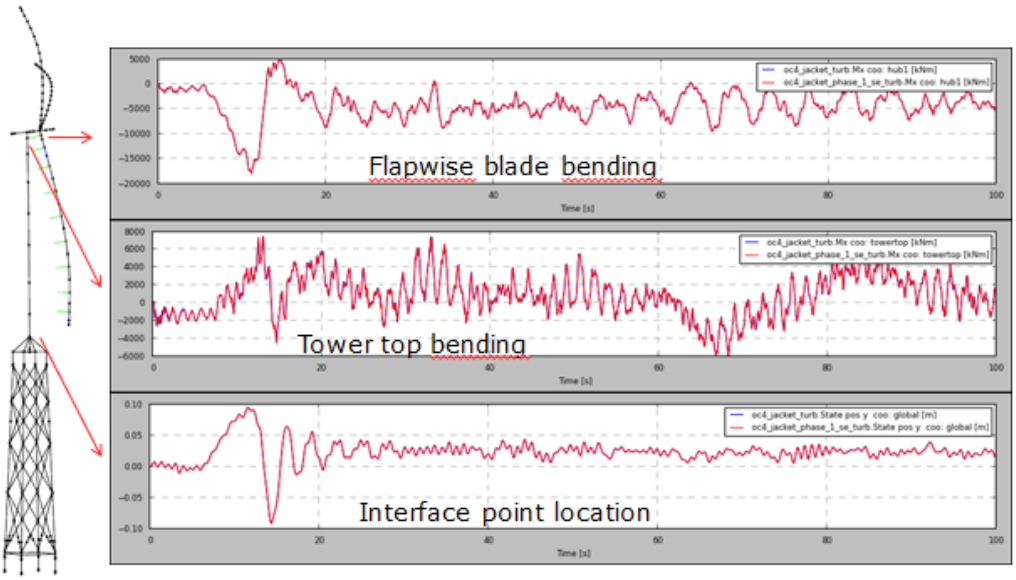

Figure 16: A comparison of a selected number of turbine sensors. Full solution is compared to the combined full turbine and static Guyan condensated super element. A perfect match is seen.

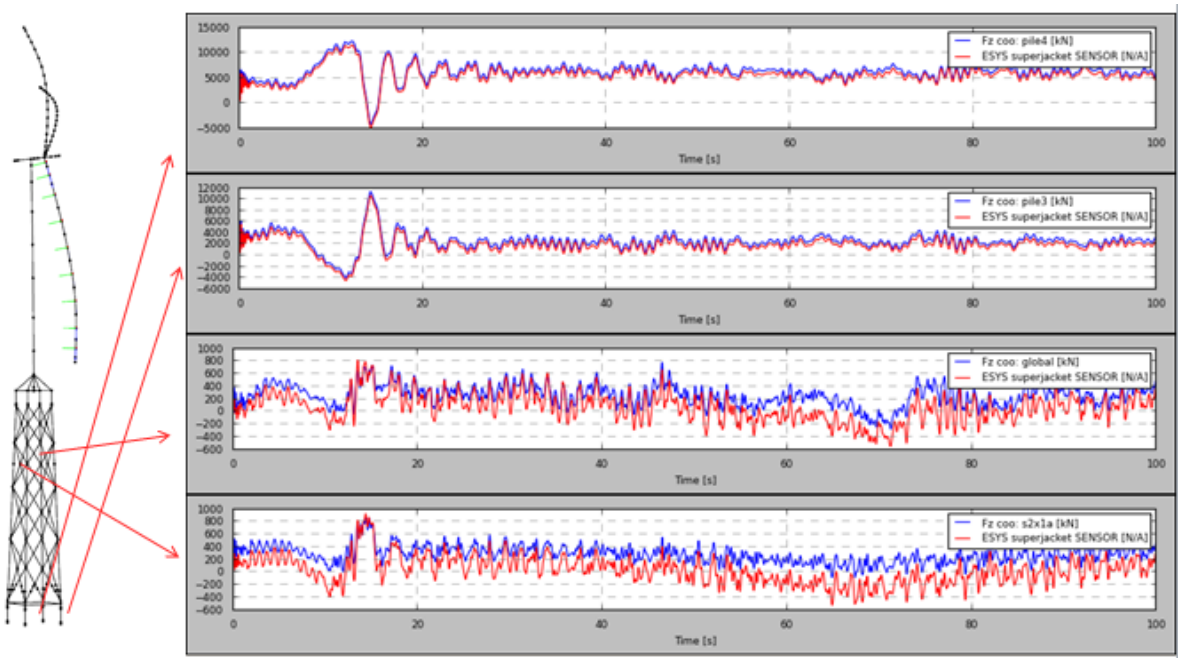

Figure 17: A comparison of a selected number of internal jacket sensors. Full solution is compared to the combined full turbine and static Guyan condensated super element. A deviation in results is seen, especially for the very low frequent (static) contributions.

Dynamic mode shapes

If the super element of the jacket is generated on basis of dynamic mode shapes instead, the immediate question is: Which modes? As a first attempt we tried with the lowest 30 eigenmodes of the jacket only fixed at mudlevel and free at the tower interface point. Examples of such mode shapes can be seen in Figure 18. By comparing the natural frequencies of the full turbine with jacket, see Table 8, it is very clear that the dynamics of the full system is not identical to the target from the full DOF approach and therefore not useful at all.

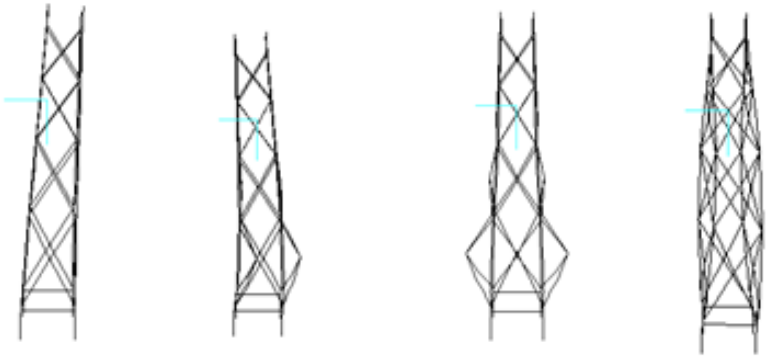

Figure 18: Example of dynamic modes of the jacket without constraint at the interface node.

	Frequency			Damping Log decr		
Mode Nr	Full	Combined	Ratio	Full	Mode Nr	Full
1	0.00	0.00	1.00	0.00	1	0.00
2	0.00	0.00	1.00	0.00	2	0.00
3	0.32	0.35	0.90	2.63	3	0.32
4	0.32	0.36	0.90	2.69	4	0.32
5	0.62	0.63	0.99	2.82	5	0.62
6	0.66	0.66	1.00	3.18	6	0.66
7	0.69	0.69	1.00	3.30	7	0.69
8	1.07	1.07	1.00	3.17	8	1.07
9	1.08	1.08	1.00	3.41	9	1.08
10	1.20	1.14	1.05	9.68	10	1.20
11	1.21	1.19	1.02	9.78	11	1.21
12	1.64	1.66	0.99	7.36	12	1.64
13	1.72	1.72	1.00	13.91	13	1.72
14	1.88	1.88	1.00	9.16	14	1.88
15	1.97	1.97	1.00	9.24	15	1.97
16	2.82	2.76	1.02	15.77	16	2.82
17	2.99	2.99	1.00	20.61	17	2.99
18	3.63	3.58	1.01	24.06	18	3.63
19	3.93	3.69	1.06	17.72	19	3.93

Table 8: A comparison of natural frequencies for the full solution and a combined approach with full turbine and super element. the super element has in this case be generated based on dynamic mode shapes of the jacket only.

Combined static and dynamic modes

If we combine the static and dynamic mode shapes from the previous two test cases the performance is only worse, see Table 9. This approach is not suitable either.

	Frequency			Damping Log decr		
Mode Nr	Full	Combined	Ratio	Full	Mode Nr	Full
1	0.00	0.00	1.00	0.00	0.00	1.00
2	0.00	0.00	1.00	0.00	0.00	1.00
3	0.32	0.30	1.07	2.63	2.47	1.07
4	0.32	0.31	1.03	2.69	2.60	1.03
5	0.62	0.59	1.05	2.82	2.91	0.97
6	0.66	0.66	1.00	3.18	3.19	1.00
7	0.69	0.69	1.00	3.30	3.28	1.00
8	1.07	1.06	1.01	3.17	3.42	0.93
9	1.08	1.07	1.01	3.41	3.95	0.86
10	1.20	1.14	1.05	9.68	8.60	1.13
11	1.21	1.17	1.03	9.78	9.32	1.05
12	1.64	1.43	1.14	7.36	8.04	0.91
13	1.72	1.72	1.00	13.91	13.91	1.00
14	1.88	1.88	1.00	9.16	9.16	1.00
15	1.97	1.97	1.00	9.24	9.24	1.00
16	2.82	2.33	1.21	15.77	13.48	1.17
17	2.99	2.99	1.00	20.61	20.61	1.00
18	3.63	3.50	1.04	24.06	28.73	0.84
19	3.93	3.56	1.10	17.72	24.72	0.72

Table 9: A comparion of natural frequencies for the full solution and a combined approach with full turbine and super element. the super element has in this case be generated based on a combination of static and dynamic mode shapes of the jacket only. The dynamic modes are generated without constraint at the tower interface node.

Static and dynamic modes using the Craig-Bampton approach

A classic method for the generation of super elements is the Craig-Bampton approach (Craig and Bampton, 1968). With this approach the transformation matrix is generated based on a static and dynamic approach. In contrast to the previous attempt the dynamic modes are generated with fixed constraints at the interface node. The static modes are still derived using fixed constraints at mudlevel and no constraints at the interface node where the unit load are applied. The lowest 25 dynamic modes have been included together with the 6 static modes.

When observing a comparison of natural frequencies for the full turbine-jacket system a very good agreement is seen in Table 10. For the lowest 17 modest there is a perfect match which is indeed impressive.

However when observing the final load within a brace member, see Figure 19, there is still a mismatch in the load level between the full DOF approach and the super element approach. This finding could be the explanation for the difficulties of finding the same load level within the static undetermined jacket structure seen in the OC4 results.

	Frequency			Damping Log decr		
Mode Nr	Full	Combined	Ratio	Full	Mode Nr	Full
1	0.00	0.00	1.00	0.00	0.00	1.00
2	0.00	0.00	1.00	0.00	0.00	1.00
3	0.32	0.32	1.00	2.63	2.63	1.00
4	0.32	0.32	1.00	2.69	2.69	1.00
5	0.62	0.62	1.00	2.82	2.82	1.00
6	0.66	0.66	1.00	3.19	3.19	1.00
7	0.69	0.69	1.00	3.30	3.30	1.00
8	1.07	1.07	1.00	3.26	3.25	1.00
9	1.08	1.08	1.00	3.66	3.63	1.01
10	1.16	1.17	1.00	9.32	9.36	1.00
11	1.17	1.18	1.00	9.18	9.25	0.99
12	1.63	1.63	1.00	7.45	7.45	1.00
13	1.72	1.72	1.00	13.91	13.91	1.00
14	1.88	1.88	1.00	9.16	9.16	1.00
15	1.97	1.97	1.00	9.24	9.24	1.00
16	2.68	2.68	1.00	17.25	17.22	1.00
17	2.99	2.99	1.00	20.61	20.61	1.00
18	3.33	3.56	0.93	26.02	24.87	1.05
19	3.45	3.58	0.96	28.28	17.56	1.61

Table 10: A comparion of natural frequencies for the full solution and a combined approach with full turbine and super element. the super element has in this case be generated based on a combination of static and dynamic mode shapes of the jacket using the Craig-Bampton approach. The dynamic modes are generated with fixed constraints at the tower interface node.

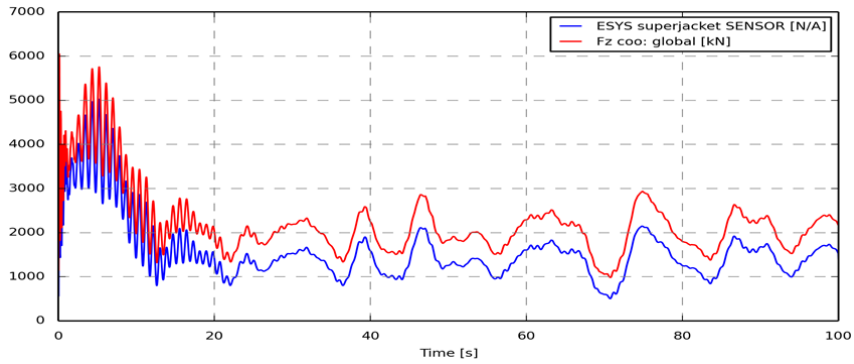

Figure 19: A comparison of the load in a brace member. Full DOF solution is compared to the combined full turbine and Craig-Bampton condensated super element. A deviation in results is still seen, especially for the very low frequent (static) contributions.

The missing part.

From the OC4 comparison it is very clear that large differences in load level are seen in the mean loads within the static undetermined jacket structure. Some part can perhaps be caused by different approaches for buoyancy and other external loads, however it could also be that the approach using condensated super elements, modal based formulation or Guyan reduced descriptions is problematic with respect to static undertermined problems.

At least for the super element generated using HAWC2, there are some problematic issues. However, this problem is actually not new at all. In 1979 similar issues was addressed with respect to an oil rig model and a solution was presented by Hansteen and Bell (Hansteen and Bell, 1979).

The basic idea is that the high frequent modes, that are neglected in the analysis is included in the solution as a static loading. More precisely this is formulated by inserting a new state variable in the basic equations

$$\mathbf{M\ddot{x} + C\dot{x} + Kx = F(t)} \tag{5}$$

$$\mathbf{x = T_h y_h + T_x y_x} \tag{6}$$

Where the index h indicates the modeshapes from 1 to n (highest selected mode) and the index x is for the remaining mode shapes.

The solution of finding $\mathbf{y_h}$ is still based on the problem

$$\mathbf{T_h^T M T_h \ddot{y}_h + T_h^T C T_h \dot{y}_h + T_h^T K T_h y_h = T_h^T F(t)} \tag{7}$$

Where the remainder $\mathbf{y_x}$ is subsequently found based on the residual force $\mathbf{F_x}$.

$$\mathbf{F_x = F - K T_h y_h} \tag{8}$$

Where the final state vector **x** is found

$$\mathbf{x = K^{-1} F_x + T_h y_h} \tag{9}$$

This approach was verified in the Hansteen and Bell paper with respect to wave load on an oil rig, shown in Figure 20. This still needs to be fully verified for the jacket substructure within HAWC2 and will be done in the near future.

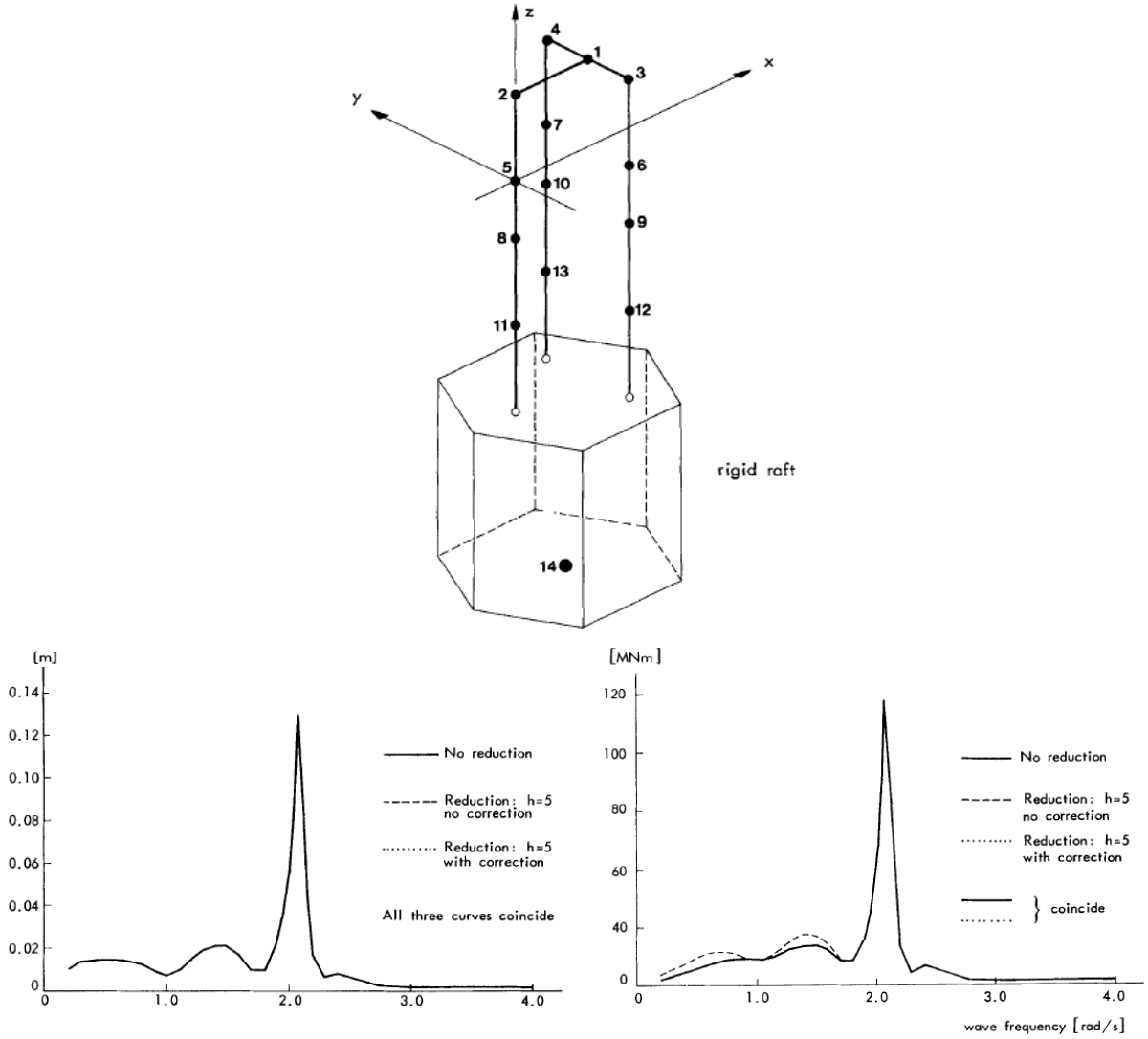

Figure 20: Verification of modified super element approach for an oil rig (top) subjected to wave loading. A lower left is seen a fine agreement for a node state both with and without modifications, whereas at lower right the bending moment is seen only to fit for the low frequencies with a full or modified modal approach. From Hansteen and Bell, 1979.

The impact of steep non-linear waves on the jacket substructure

In (Larsen et.al., 2011) and (Bredmose et.al, 2013) a wind turbine mounted on a jacket was investigated with respect to the influence of nonlinear wave load contributions. The study was carried out for a stand still situation where the turbine is stopped and the blades are pitched 90deg. The investigated standstill situation is with waves in a direction directly towards the wind turbine direction. Since the blades are pitched, the aerodynamic contribution was considered very low and aerodynamic loads on the tower were also neglected. This load condition is considered highly relevant for offshore turbines and is known to be problematic for monopile configurations since the total level of structural, aerodynamic and hydrodynamic damping generally is very low at stand still.

The load increase from the nonlinear waves is pronounced and seen to increase the load level for all the simulated wave cases. For small significant wave heights the increase in load level is likely to be caused by ”springing” where ”ringing” is seen for the large significant wave heights. It is however difficult to really identify whether it is ”springing” or ”ringing” that causes the high response for the nonlinear waves, which is illustrated in Figure 21, however it is clear that the structural response occurs when the wave is very steep. The increased load effect was seen for all sensors on the structure but is especially pronounced for the tower bottom bending load and the leg load in the upper part of the substructure. For the cases with small significant wave heights, the increased high frequency content in the nonlinear waves seem to cause a general small increase in loads, which fits very well with the springing affected loads. The mechanism is however different for the large significant waves where ringing occur. Here the single large waves in the irregular wave train is of a magnitude large enough to excite the structure and cause large transients after the wave passing. The excitation is mainly on the first structural frequency at 0.32Hz and due to the low amount of damping, the vibration levels become large. Since the turbine is at standstill and the blades are pitched 90deg, the aerodynamic damping on the structure is minimal, and there is only contribution from damping originating from the structure, hydrodynamics and soil. In order to see the influence of damping levels, results was obtained for damping levels between 2 and 10% expressed a a log. decrement, which represent the expected range of efficient damping for a turbine mounted on a monopile. For all cases a significant increase in loads are seen for the nonlinear wave loads. The load increase could be to an increased level of a factor of 2-3 compared to the approach using linear wave theory. This really indicates the importance of these nonlinear wave situations for sites where steep nonlinear waves occurs, as eg. in the inner Danish waters.

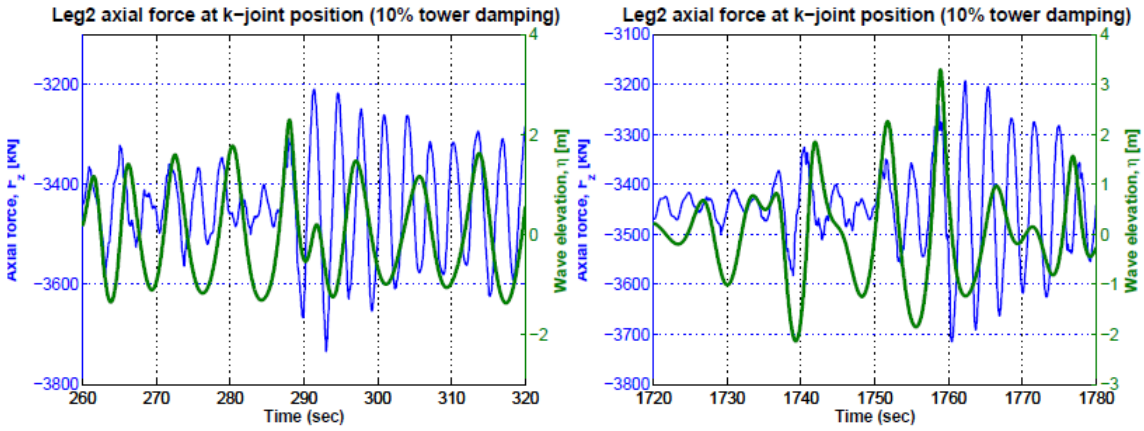

Figure 21: High transient load is seen in the jacket when steep non-linear irregular waves are applied, from (Bredmose et.al., 2013).

Phase II:

In phase II, the 5MW turbine is simulated in combination with a floating semi submersible structure.

Methods

In this chapter the three different approaches for modeling the floating wind turbine are presented. Special attention is on the hydrodynamic aspects as the wind turbine modeling is identical for all three approaches. A description and general validation of HAWC2 can be found in (Kim et.al, 2013) and (Larsen et.al., 2013).

The anchor line model is identical for all three approaches. It consists of a fully dynamic nonlinear chain-element model, originally described in (Kallesøe and Hansen, 2011). The model contains a structural description of a chain module with elements only capable of transferring axial forces and includes effects of large rotations as well as hydrodynamic added mass and drag. A set of vertical nonlinear springs is used from mudline and downward to ensure correct handling of bottom contact. Above mudline the spring's stiffness is zero corresponding to floating conditions. The mooring line will for low motions of the cables correspond to a static non-linear mooring line solution, but in the simulation also dynamic effects of the line movement in the water is included. The inertial of the line itself is included as well as viscous drag. It is assumed that the added hydrodynamic mass effects are neglectable.

As part of this EUDP project, the mooring line module was extended for inclusion of wave forces from the incoming wave field using Morison's formula. Furthermore a general python script was created which enables an easy creating of the otherwise rather complex input data for the mooring line module.

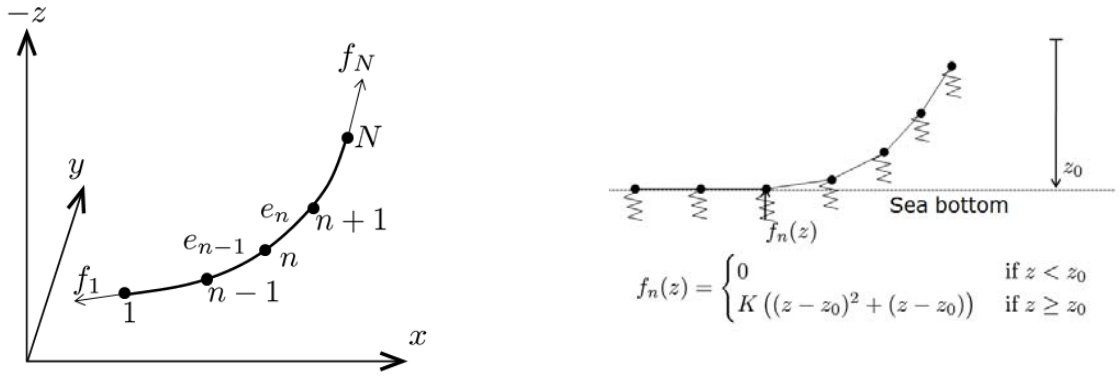

Figure 22. illustration of the non-linear mooring line model (left) and the handling of the sea bottom contact problem (right). From (Kallesøe and Hansen, 2011)

HAWC2-Standalone

In the basic version of the program HAWC2, hydrodynamic forces can be included quite similarly to how other distributed external force from aerodynamics and gravity are included. As default the wave kinematics are calculated from a separate module a bit similar to how turbulent wind is generated for the wind loading. The wave velocities and accelerations are converted to external forces on the structure using Morison's formula and there are also contribution for added mass and drag effects of heave plates, buoyancy forces and influence of flooded water.

In the calculation of hydrodynamic forces, it is assumed that the structure is assembled from slender members with a local diameter much less than the length of the incoming wave. A set of calculation points is distributed along the structure. In these calculation points, the hydrodynamic forces are calculated with an engineering approach with contribution from different load generating effects.

First of all the Morison formula (10) is used for calculating the wave forces dF.

$$dF = \rho A\dot{U} + \rho C_a A_R \dot{U}_{rel} + \tfrac{1}{2}\rho D C_d U_{rel}\left|U_{rel}\right| \qquad (10)$$

The Froud-Krylov contribution is included in the term $\rho A\dot{U}$, the added mass effects in the term $\rho C_a A_R \dot{U}_{rel}$ and the viscous drag from the term $\frac{1}{2}\rho D C_d U_{rel}|U_{rel}|$. ρ is the density of water, A is the cross sectional area, $\dot{U}$ is the water acceleration, C_A is the added mass coefficient related to the shape dependent cross sectional area A_R. $\dot{U}_{rel}$ is the relative acceleration between wave and structure, D is the diameter of the cross section and U_{rel} is the relative velocity between wave and structure.

The added mass and drag from the heave plate is included as a separate concentrated end effect with an added mass based on a sphere (Newmann,1986), see Figure 23. From this figure it can be seen that the added mass coefficient for a circular disc is 0.65.

The heave plate also contributes with viscous drag forces (2), especially important for the heave motion. The drag coefficient used in the HAWC2 simulations is 2.4.

$$F_d = \frac{1}{2}\rho A C_d U_{rel}|U_{rel}| \qquad (11)$$

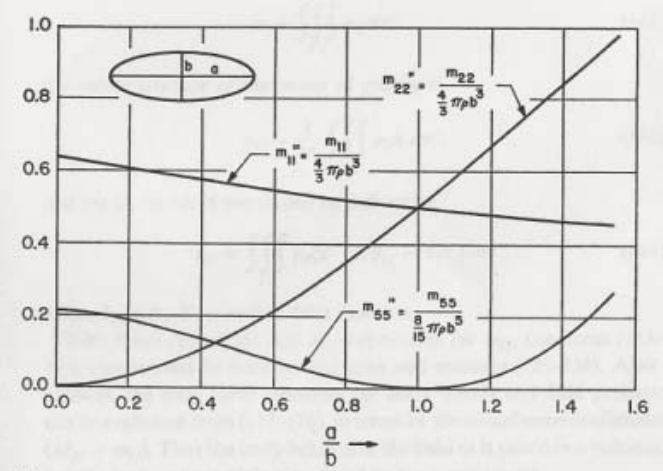

4.8
Added-mass coefficients for a spheroid, of length $2a$ and maximum diameter $2b$. The added mass m_{11} corresponds to longitudinal acceleration, m_{22} to lateral acceleration in the equatorial plane, and m_{55} denotes the added moment of inertia, for rotation about an axis in the equatorial plane. In the upper figure, the coefficients are nondimensionalized with respect to the mass and moment of inertia of the displaced volume of the fluid, and in the lower figure with respect to the same quantities for a sphere of radius b.

Figure 23. Added mass effects of a sphere, from (Newman, 1986). If 'a' equals zero then the expression can be used for a thin circular disc. Heave notation is m_{11}.

Buoyancy is found based on an approach equivalent to integration of external pressure forces. This is done in order to ensure a correct force distribution so that internal cross sectional forces in the structure can be found. The local buoyancy forcing per length of the structure is found as written in (13) and (14) for cross sectional forces and moments respectfully. An essential part is the orientation of the beam expressed as the orientation matrix A (z along the beam, x and y perpendicular and orthogonal to z). The offdiagonal terms $A_{3,1}$ and $A_{3,2}$ only contains values when the beam is not vertical. Conicity is expressed as the change in Area S per length z $\frac{\partial S}{\partial z}$. Gravity acceleration is denoted g.

In the end of the beams, or where changes in area occur, concentrated forces are inserted according to (3).

$$\boldsymbol{F}_{b,end}(3) = \rho g S(z - z_0) + S p_{dyn} + \tfrac{1}{2}\rho C_{d,axial} S U_{rel}|U_{rel}| \qquad \textbf{(12)}$$

$$\vec{F}_b = -g\rho \begin{Bmatrix} A_{3,1}S \\ A_{3,2}S \\ -\frac{\partial S}{\partial z}(z - z_0) + \frac{\partial S}{\partial z} p_{dyn} \end{Bmatrix} \qquad (13)$$

$$\vec{M}_b = -g\rho \left\{ \begin{array}{c} -A_{3,2} \dfrac{\partial r}{\partial z} \pi r^3 \\ A_{3,1} \dfrac{\partial r}{\partial z} \pi r^3 \\ 0 \end{array} \right\} \qquad (14)$$

HAWC2-WAMSIM

The vessel response model WAMSIM developed by DHI, Denmark is capable of simulating wave-induced motion of a moored or freely floating structure in the time domain. The wave exiting force is calculated assuming a superposition of long-crested (uniform along one horizontal dimension) waves. The results of each WAMSIM simulation are presented as time-series of motions for surge, sway, heave, roll, pitch and yaw and as forces in the mooring lines and vessel diffraction forces. The radiation/diffraction code WAMSIM for calculating floating body dynamics is based on the frequency-domain program WAMIT for the calculation of the hydrodynamic quantities (Bingham, 2000), (Christensen, 2008), (Hansen, 2009). The structure in WAMSIM is assumed to behave as a rigid body.

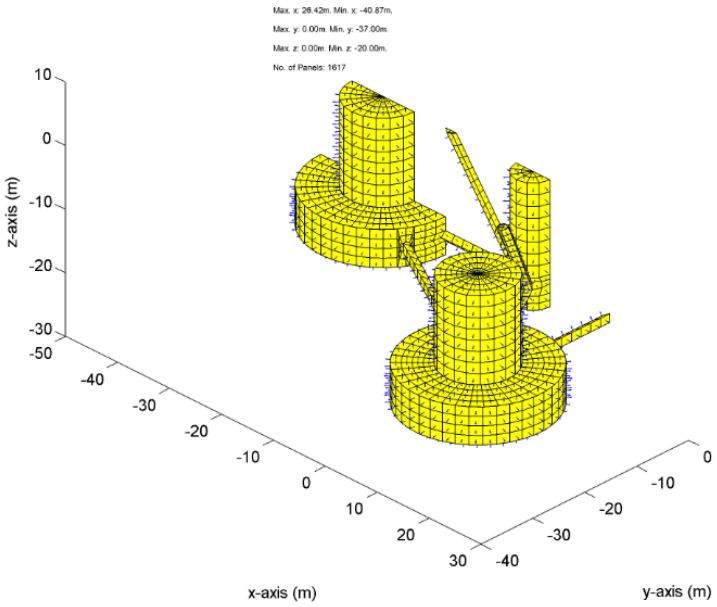

Figure 24. The WAMSIM model of the semi sub platform. Symmetry about the y = 0 plane is exploited

The following short general description of WAMSIM is taken from (Hansen et.al., 2009). The hydrodynamic interaction between the fluid and floating bodies is assumed to be well described by linear potential theory (i.e. an inviscid and irrotational flow, with the free surface and body boundary conditions satisfied to first order). That is to say, despite any nonlinear effects, which may have been important in producing the conditions at the bodies; all nonlinear terms are ignored in the free surface boundary conditions in the local vicinity of the bodies, as well as in the expressions for fluid pressure and force on the bodies. This is a good approximation as long as the parameter kH/tanh(kh) << 1 Assuming the body motions remain small, the equations of motion for the body dynamics for the N degrees of freedom can be written in the following convolution form:

$$\sum_{k=1}^{N}\left[\left(\mathbf{M_{jk}}+\mathbf{a_{jk}}\right)\ddot{\mathbf{x}}_{\mathbf{k}}(t)+\int_0^t \mathbf{K_{jk}}(t-\tau)\ddot{\mathbf{x}}_{\mathbf{k}}(\tau)d\tau+\mathbf{C_{jk}}\mathbf{x_k}(t)\right]=\mathbf{F_{jD}}(t)+\mathbf{F_{jnl}}(t),\qquad j=1,2\ldots,N \quad (15)$$

All non-linear external forces, such as those due to viscous/frictional damping, are included via the term $F_{jnl}(t)$. The rest of this equation describes the inertia, hydrostatic restoring forces, and hydrodynamic forces on the bodies to first order in the body motion and the wave steepness. The bodies' linear inertia and hydrostatic restoring matrices are $\mathbf{M_{jk}}$ and $\mathbf{C_{jk}}$,

respectively. The forces due to radiated waves generated by the bodies' motions are expressed as a convolution of the radiation impulse response functions, $\mathbf{K}_{jk}$, with the body velocity (plus the impulsive contributions, $\mathbf{a}_{jk}$, which come from the t=0 limit of the radiation problem, and are proportional to acceleration). A cross sectional view of the semisub can be seen in Figure 24. The transfer functions (RAO) can be seen in Figure 25 and Figure 26.

Buoyancy is handled by integration on the submerged volume, where it is assumed that the initial position corresponds to a steady state equilibrium. The mass of the system is set to match this submerged volume mass in line with the assumption of steady state equilibrium. A simple and practical approach in many cases, but for the coupled approach to HAWC2 this caused some practical issues since the mass of the submerged volume is not necessarily the same when the turbine and anchor loads are assembled through the HAWC2 coupling. This had some importance for loadcase 1.2 where the steady state solution was to be found and fictitious forces had to be applied to ensure a correct heave position.

Coupling of HAWC2 with WAMSIM

The coupling of the models has been performed by letting a special version of WAMSIM interact with an interface for external models included in HAWC2, originally presented in (Larsen, 2011). The frame for connecting the external DOF's in the WAMSIM frame has been done using the multibody approach in similar way as the core of HAWC2 is build. First the external mass and stiffness matrix is set up in its own coordinates system. Secondly a set of six constraints are set to ensure fixed connection in translation and rotation at the coupling point. These constraints are updated at every time step and iteration and the derivative of the constraint with respect to the external system DOF are evaluated. The same solver (Newmark beta) used in the core of the code is also applied to the external system and therefore solved in an integrated way with the HAWC2 equations of motion. The special WAMSIM model has been compiled as a dynamically linked library (dll) that is activated and controlled by HAWC2. A number of modifications has been made to WAMSIM in order to return the right quantities to HAWC2 at the right times. The coupled model involves the following steps:

1. Mass matrices and stiffness matrices of the floating foundation are calculated by WAMSIM and delivered to HAWC2.
2. HAWC2 sets up mass and stiffness matrices for the entire system including wind turbines and floating foundation.
3. HAWC2 sets up mass and stiffness matrices for the entire system including wind turbines and floating foundation.
4. The simulation is initiated by HAWC2. A WAMSIM subroutine is called by HAWC2, with HAWC2's guess on the state of the system (ie. velocities and position in 6 DOF's) and the constraint force at the model interface (ie. forces from wind turbines on foundation). The subroutine uses parts of the WAMSIM routine for solving body equations of motion to returns the state differentiated with respect to time (ie. accelerations and velocities). All hydrodynamics incl. added mass and forcing from incident waves are included in this step.
5. The iterative solver of HAWC2 will repeat Step 3 with new guesses of the state vector until the calculated residuals are acceptable. When the acceptance criteria are met it will proceed to the next time step, and step 3 is repeated for this time step.

The convergence with this approach is in general very good and convergence is obtained within 1-2 iterations. The impact on simulation time with the coupled system to WAMSIM has not been noticeable.

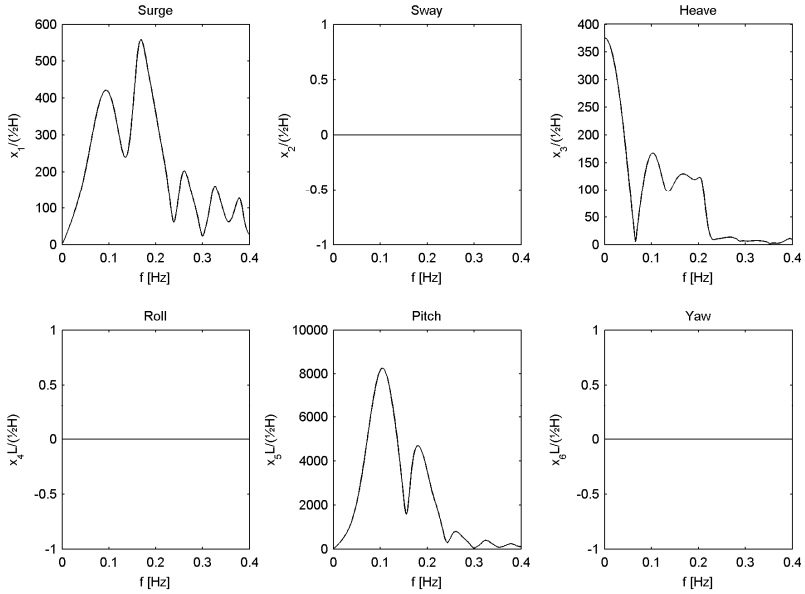

Figure 25. WAMSIM transfer function for 0deg wave heading

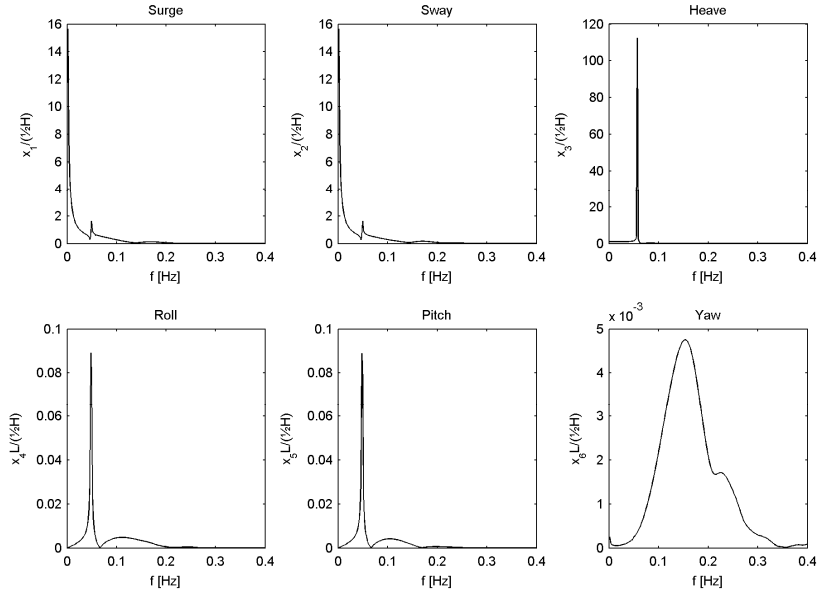

Figure 26. WAMSIM transfer function for 45deg wave heading

HAWC2-WAMIT

A newly developed stand-alone HAWC2 interface to WAMIT, similar to HAWC2-WAMSIM coupling, has also been used in the OC4 project. The interface reads WAMIT output files directly and uses these as input to a HAWC2-WAMIT module via the HAWC2 external system DLL interface (Called ESYSWamit on the following pages).

ESYSWamit can model rigid body floating structures limited to 6 degrees of freedom (DOF), 3 displacements and 3 rotations. The structural mass of the floating structure is included ESYSWamit and allows arbitrary positioning of center of gravity and rotational inertia. The necessary constraints are implemented in ESYSWamit which allows coupling the floating structure to the wind turbine model to enable integrated simulation of the total floating wind turbine system.

The wave input to ESYSWamit is taken directly from the wave definition built into HAWC2 which allows other wave-dependent HAWC2 modules (e.g. the mooring lines) to share the same wave environment.

ESYSWamit implements the 6-DOF rigid body equations of motion for the floating structure and applies the following external forces to the structure:

- Gravity (in COG)
- Buoyancy (in COB, provided by WAMIT output)
- Linear and non-linear damping forces (user specified)
- Linear stiffness (user specified)
- Hydrostatic forces (provided from WAMIT output)
- Radiation forces (provided from WAMIT output)
- Diffraction forces (wave forces) (provided from WAMIT output)
-

The gravity and buoyancy forces and centers are independent which allows the floating structure to be in static equilibrium when external components interact with the structure (e.g. when a wind turbine is put on top of it). The user-specifies damping and stiffness forces are implemented for flexibility reasons to allow the user to interact with the system in a simple manner, e.g. to model simple mooring systems or to fit model behavior to measured response. The hydrostatic forces are read from file and added to the linear stiffness matric for the system.

The radiation and diffraction forces are really the main concern in the ESYSWamit implementation. Both force components are implemented as convolution integrals based on the frequency response functions (FRFs) provided by WAMIT.

The radiation forces are output from WAMIT as the FRFs of hydrodynamic forces driven by the movement of the structure in all 6 DOFs. For each DOF, 6 FRFs are provided, one for each force component. This gives, in principle, 36 FRFs for the radiation force component, but due to symmetry conditions many of these are either equal or zero.

Similar to the radiation forces, the diffraction forces are also provided by WAMIT as FRFs, however, driven by the wave elevation instead of the movement of the structure. Since there is only one driving parameter (the wave elevation), the diffraction forces are described by 6 FRFs, however, 6 FRFs for each wave direction. Presently, ESYSWamit can only handle one wave direction per simulation, but future plans include an interpolation scheme which can handle changes in wave direction during the simulation.

An example of one of the radiation FRFs provided by WAMIT output is shown in Figure 27- the upper plot shows the amplitude and the lower plot shows the phase of the surge radiation force driven by the surge acceleration. The force is in phase with the acceleration at zero and at infinite frequency, but in-between the force amplitude and phase is seen to be highly frequency dependent. The blue line is the WAMIT output directly read from file – the red dots wil be mentioned later.

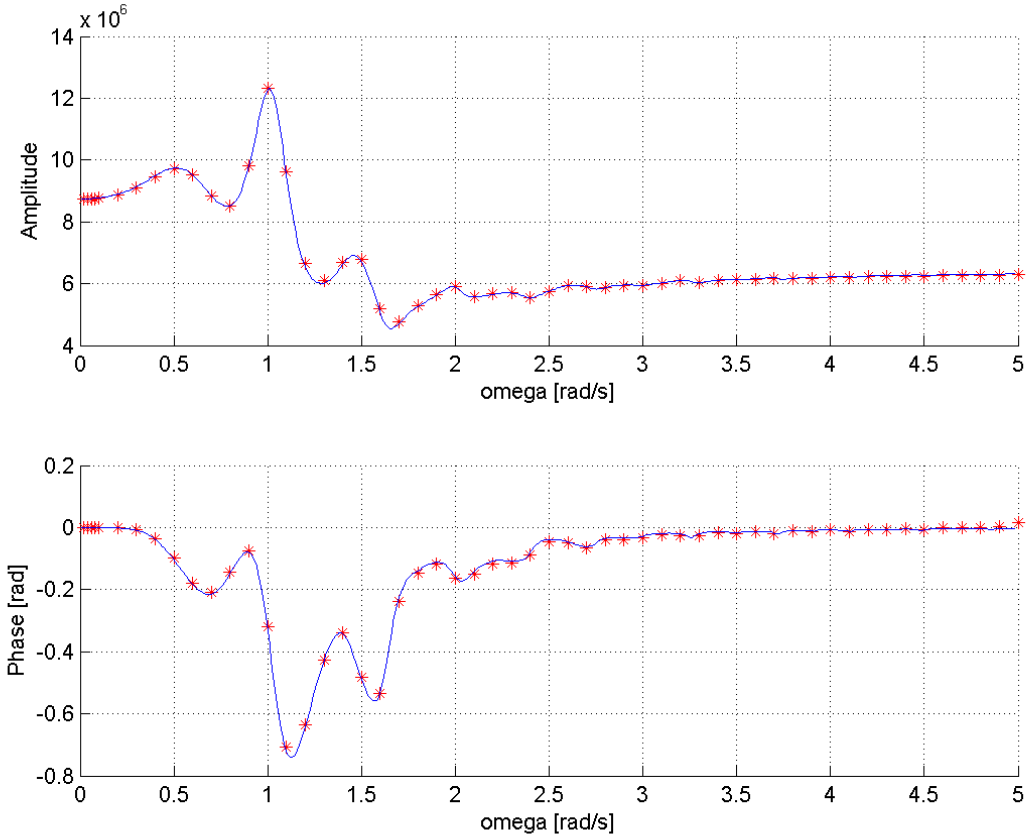

Figure 27: Surge / surge radiation FRF.

To go from the frequency domain forces defined by the FRFs to time domain is done by convolution. In general, the convolution integral is defined as:

$$\mathbf{F(t)} = \int_{\mathbf{0}}^{\infty} \mathbf{K(t-\tau)X(\tau)d\tau} \qquad (16)$$

where K(t) is the impulse response function (IRF) which is found by the inverse Fourier transform of the corresponding FRF, and X(t) is the driving parameter, i.e movement of the floating structure in case of radiation forces and wave elevation in case of diffraction forces. ESYSWamit calculates the IRFs related to both radiation and diffraction forces in the same way by an implementation of a method called Filon integration. An example of one of the radiation IRFs is shown in Figure 28 and one of the diffraction IRFs is shown in Figure 29.

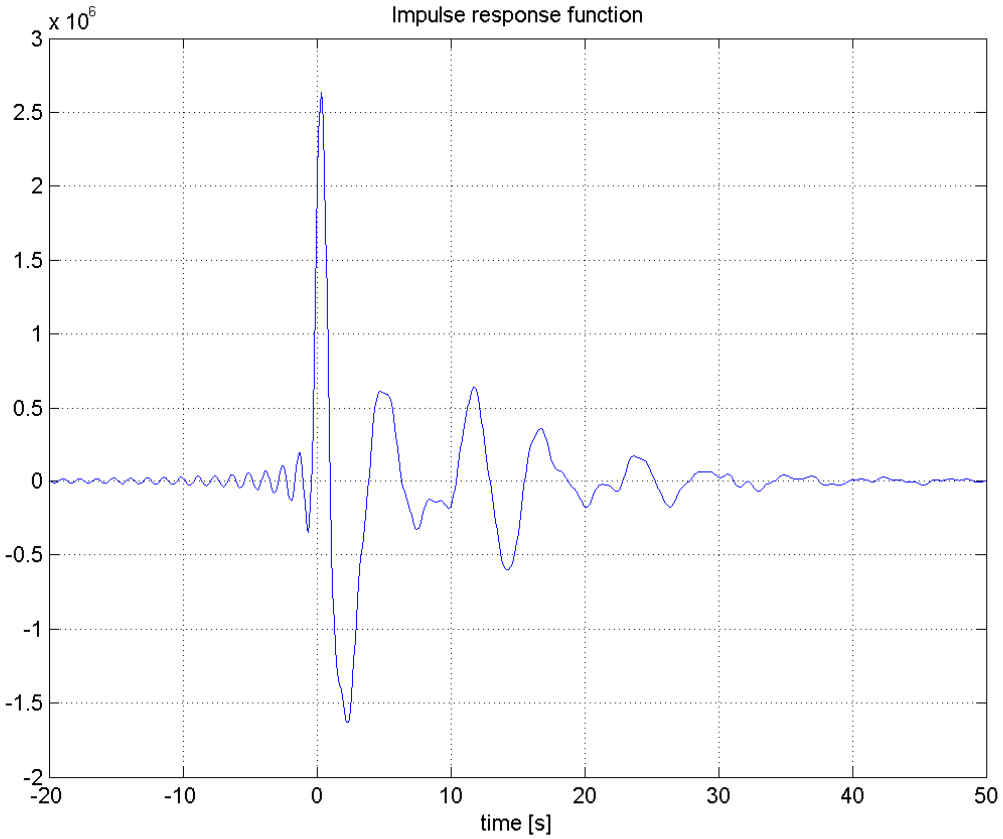

Figure 28: Surge/surge radiation IRF

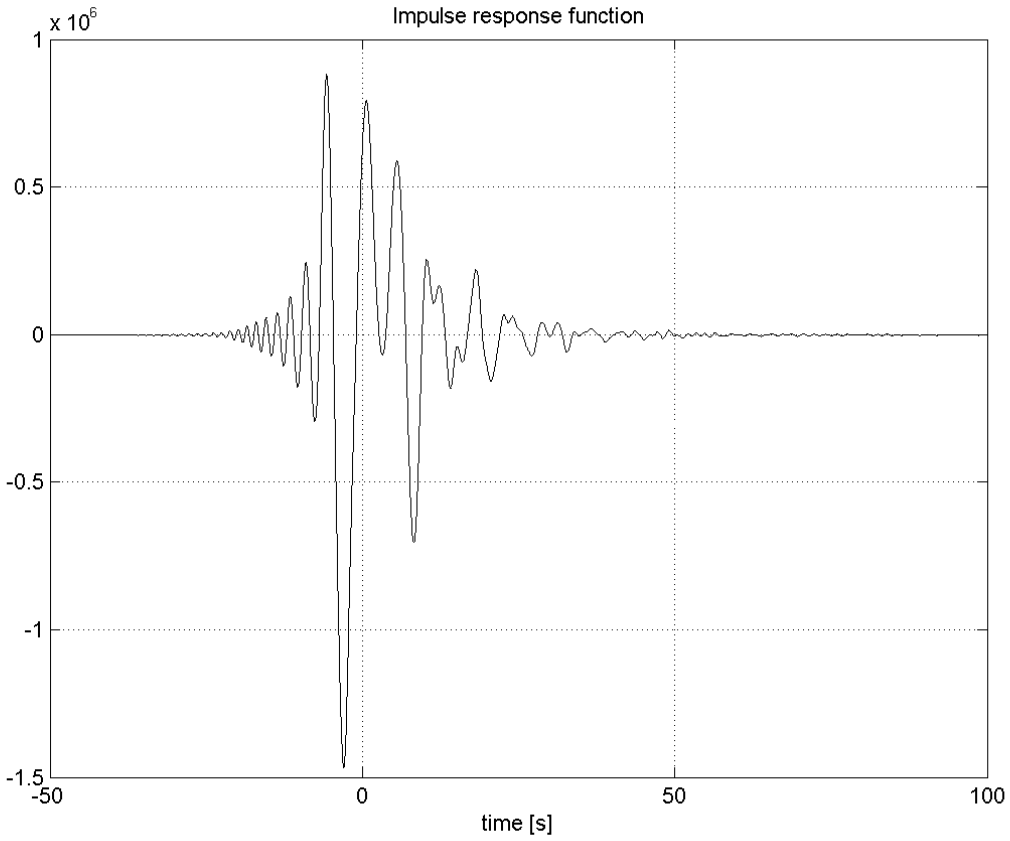

Figure 29: Surge diffraction IRF.

One general difference between the radiation and the diffraction IRFs is that the radiation IRFs must be equal to zero for t<0 while the diffraction IRFs extend towards negative time. From the definition of the convolution integral in (6) it is seen that if the IRFs are non-zero for negative time, the force at present will be dependent on future values of the driving parameter. In case of the diffraction forces, the IRF shows that the force at present is dependent of the wave elevation in the future which is only natural because the structure can feel the waves approaching the structure. However, for the radiation forces which are dependent on the movement of the structure, the force cannot be dependent on how the structure will move before the movement has actually taken place. This is called causality and the radiation FRFs must obey causality otherwise they are un-physical. In Figure 28 it is seen that the radiation IRF does have non-zero values for time<0, however small. This small contribution is caused by truncation of the frequency range when calculating the IRFs by inverse Fourier transformation using the Filon integration scheme and in the validation described next, the influence is shown to be negligible.

A validation of the implementation of the radiation and diffraction transformation into time domain has been made in the following way: Several simulations of the ESYSWamit model were made with HAWC2 where the structure was forced to move harmonically at varying frequencies. After the first transient period of the simulation has passed, the force response also become harmonic, and the amplitude and phase of the harmonic response is plotted on top of the corresponding FRF provided by WAMIT input. The result of this validation procedure has produced the red dots in Figure 27: Surge/surge radiation FRF. (the blue line is the

corresponding FRF from WAMIT). The correspondence between the input FRF and simulated FRF is good and shows that the radiation forces calculated by ESYSWamit can be trusted. The same procedure with varying wave frequency and fixed structure has been followed and the same correspondence between input FRF and simulated FRF was found for the diffraction forces (not shown herein). To conclude, both radiation forces and diffraction forces produced by ESYSWamit are indeed trustworthy.

Loadcases

The loadcases was set up where the complexity was gradually increased. The first cases covered stand still frequency analysis and steady state load distribution. Wave loads were later introduced and the complexity gradually increased until the final cases with fully turbulent atmospheric inflow, irregular wave loads and a fully flexible construction. The approach of gradually increasing the complexity made it possible to locate the reasons for discrepancies yet still also to include design driving load cases. The list of load cases are shown in Table 11. Case 1.x are standstill situation with no external forces from waves of wind. Steady state loads and position if found together with eigenfrequencies and decay transients. Case 2.x are also standstill situations with a rigid turbine and a substructure with flexible mooring lines. Wave loads are applied. Case 3.x covers situation with a fully flexible construction submitted to both wind and wave loads. Furthermore, a load case where the transfer function from wave motion is found. This term is also denoted response amplitude operator (RAO).

Load Case	Description	Enabled DOFs	Wind Condition	Wave Condition
1.1	Eigenanalysis	All	No air	Still water
1.2	Static equilibrium	All	No air	Still water
1.3a	Free decay, surge	Platform and moorings	No air	Still water
1.3b	Free decay, heave	Platform and moorings	No air	Still water
1.3c	Free decay, pitch	Platform and moorings	No air	Still water
1.3d	Free decay, yaw	Platform and moorings	No air	Still water
2.1	Regular waves	Support structure	No air	Regular Airy: H = 6 m, T = 10 s
2.2	Irregular waves	Support structure	No air	Irregular Airy: H_s = 6 m, T_p = 10 s, γ=2.87, JONSWAP spectrum
2.3	Current only	Support structure	No air	Surface = 0.5 m/s, $1/7^{th}$ power law decrease with depth
2.4	Current and regular waves	Support structure	No air	Regular Airy: H = 6 m, T = 10 s; Current at surface = 0.5 m/s, $1/7^{th}$ power law
2.5	50-year extreme wave	Support structure	No air	Irregular Airy: H_s = 15.0 m, T_p = 19.2 s, γ=1.05, JONSWAP spectrum
2.6	RAO estimation, no wind	Support structure	No air	Banded white noise, PSD =1 m^2/Hz for 0.05-0.25 Hz
3.1	Deterministic,	All	Steady,	Regular Airy: H = 6 m, T = 10 s

	below rated		uniform, no shear: V_{hub} = 8 m/s	
3.2	Stochastic, at rated	All	Turbulent (Mann model): V_{hub} = V_r (11.4 m/s)	Irregular Airy: H_s = 6 m, T_p = 10 s, γ=2.87, JONSWAP spectrum
3.3	Stochastic, above rated	All	Turbulent (Mann model): V_{hub} = V_r (18 m/s)	Irregular Airy: H_s = 6 m, T_p = 10 s, γ=2.87, JONSWAP spectrum
3.4	Wind/wave/current	All	Steady, uniform, no shear: V_{hub} = 8 m/s	Regular Airy: H = 6 m, T = 10 s; Current at surface = 0.5 m/s, $1/7^{th}$ power law
3.5	50-year extreme wind/wave	All	Turbulent (Mann model): V_{hub} = V_r (47.5 m/s)	Irregular Airy: H_s = 15.0 m, T_p = 19.2 s, γ=1.05, JONSWAP spectrum
3.6	Wind/wave misalignment	All	Steady, uniform, no shear: V_{hub} = 8 m/s	Regular Airy: H = 6 m, T = 10 s, direction = 30^0
3.7	RAO estimation, with wind	All	Steady, uniform, no shear: V_{hub} = 8 m/s	Banded white noise, PSD =1 m^2/Hz for 0.05-0.25 Hz
3.8	Mooring line loss	All	Steady, uniform, no shear: V_{hub} = 18 m/s	Regular Airy: H = 6 m, T = 10 s
3.9a	Flooded column	All	No air	Still water
3.9b	Flooded column	All	Turbulent (Mann model): V_{hub} = V_r (18 m/s)	Irregular Airy: H_s = 6 m, T_p = 10 s, γ=2.87, JONSWAP spectrum
RAO = Response Amplitude Operator		DOF = Degree of Freedom	V_{hub} = hub-height wind speed V_r = rated wind speed PSD = power-spectral density	H = wave height H_s = significant wave height T = wave period T_p = peak-spectral wave period γ = peak enhancement factor

Table 11: Overview of loadcases for the semi sub simulations.

Phase II: Sensors and coordinate systems

In this report, the coordinate system as used in the HAWC2 simulations has been used directly. Please pay attention that these orientation may differ compared to sensor used in joint papers within the international rojects members as it was there decided to use a more common IEC set of coordinates.

The HAWC2 coordinate system is defined with the global z coordinate pointing downwards, the global y-direction in the direction of the default wind and wave direction and x horizontally to the side. Further on, each body on the structure has its own coordinate that is defined by the choise of the user. In this particular case, the structure is typically defined along the z-axis of the body coordinate system. The coordinate systems are shown in Figure 31 and Figure 32.

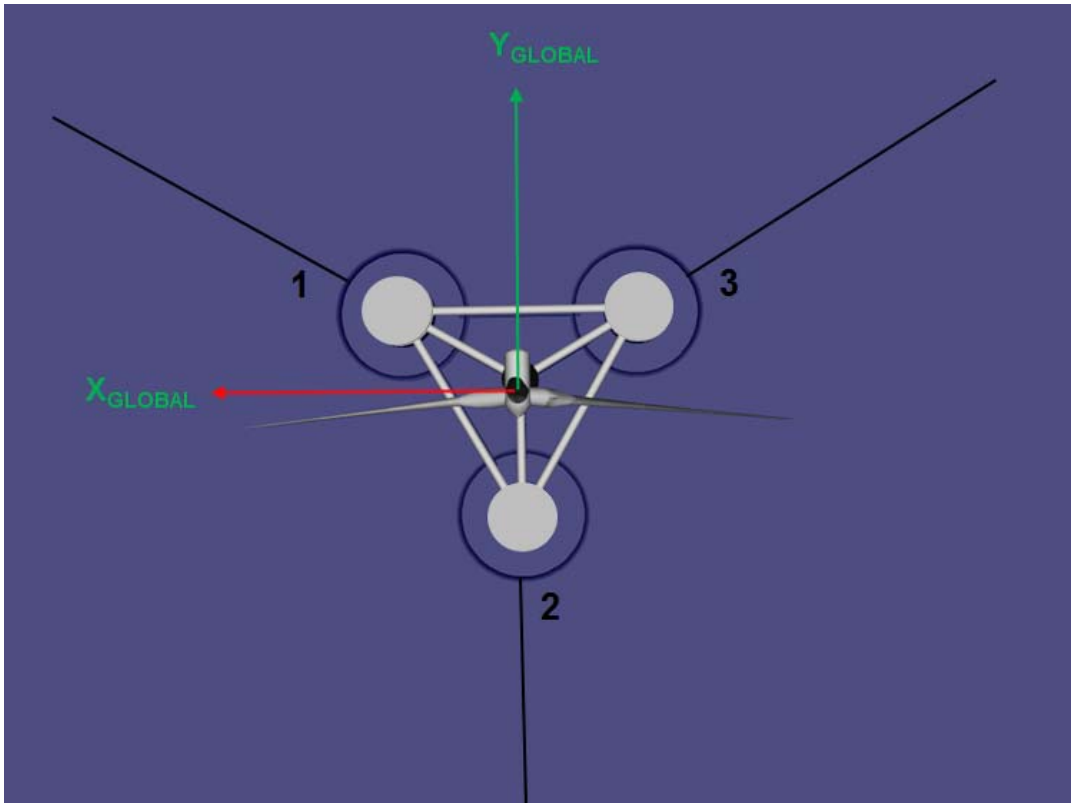

Figure 30 Global coordinate system and numbering order for columns and mooring lines

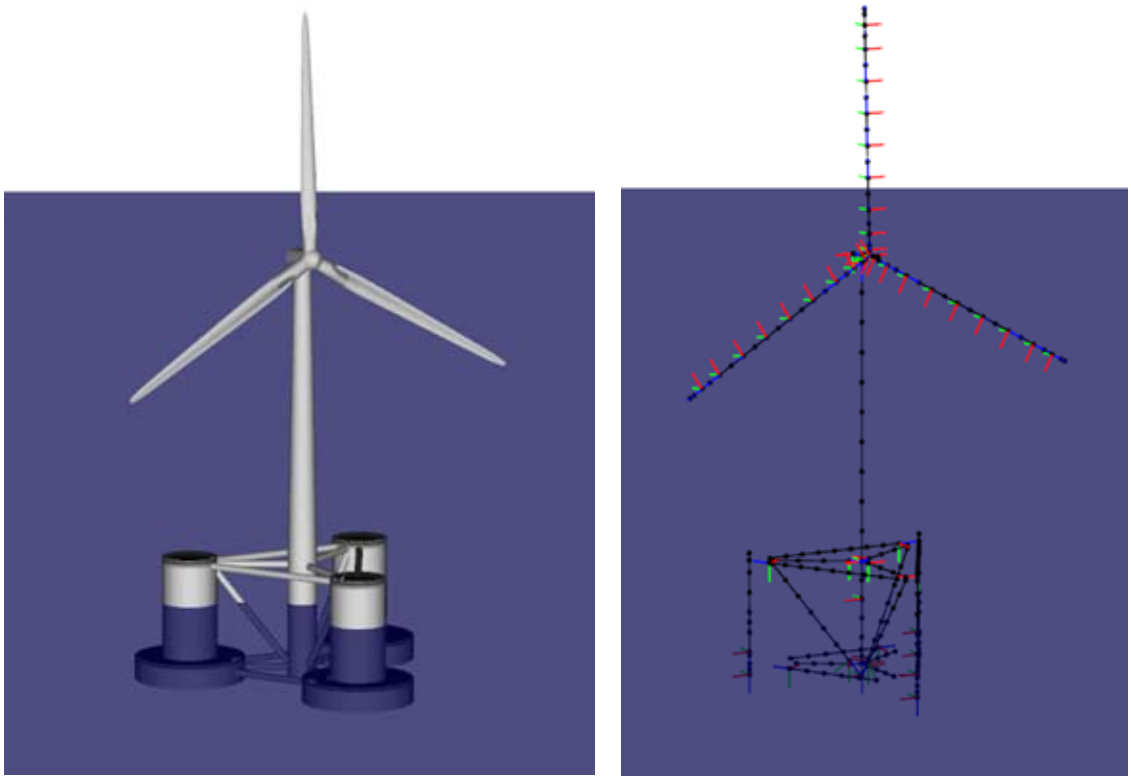

Figure 31: Body coordinates of the full system. X, Y and Z

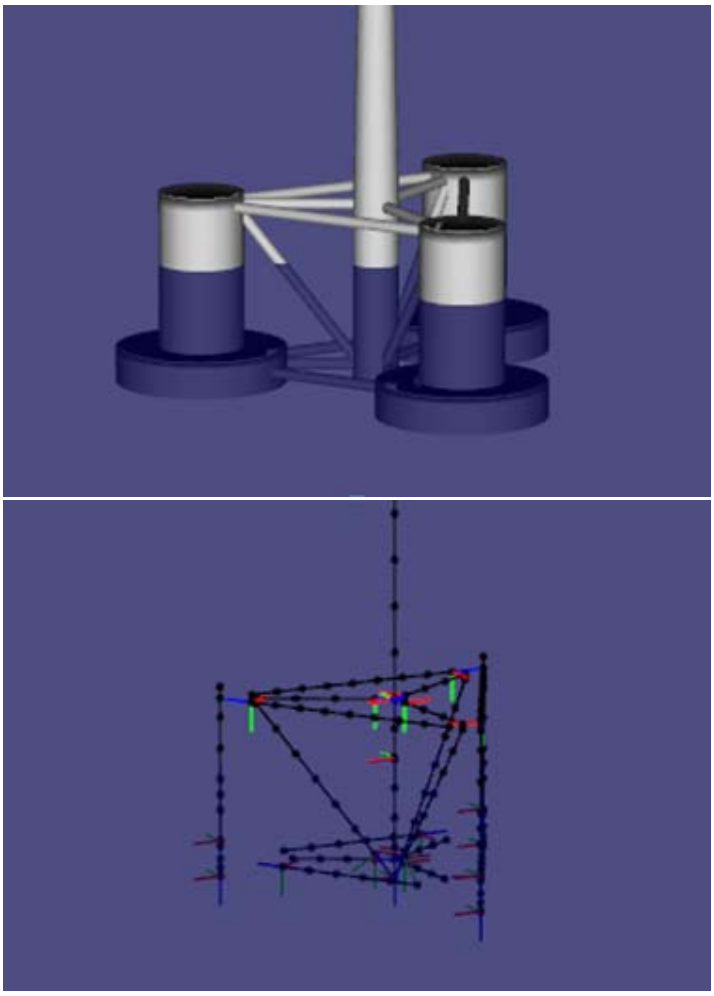

Figure 32: Body coordinates of the semi sub. X, Y and Z. The bodies are in all cases modeled along the direction of –Z (opposite direction of Z).

Phase II: Results

Phase II: Case 1.1: Steady state condition

The first and most basic case was the full system in a standstill situation, steady water and without wind loading. The dynamics of the system was investigated through eigenvalue analysis. In order to enable this, a new eigenvalue solution approach was implemented in HAWC2 which made it possible to perform the eigenvalue analysis at a time where a steady state equilibrium was obtained and also that it was possible to solve the full problem including contribution from structural flexibility, fully dynamic anchorline flexibility, buoyancy and gravity.

In general there is a fairly good agreement with respect to the natural frequencies and except of a few outliers a match within 5% was obtained.

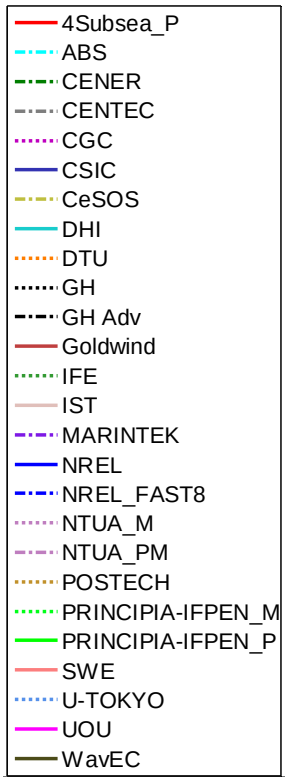

Figure 33: Participants line notations used in Figure 34. DTU is the HAWC2-standalone results.

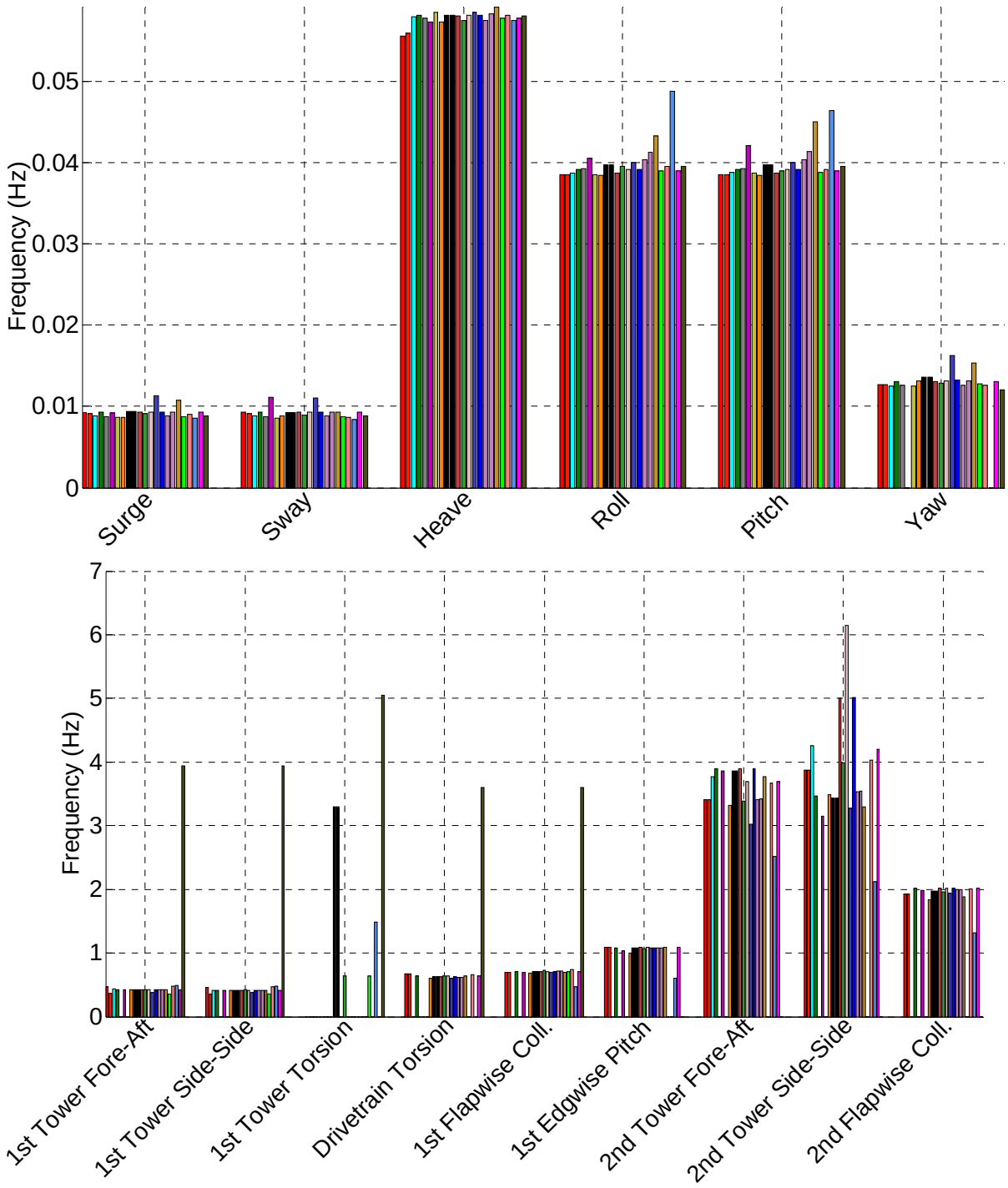

Figure 34: Full-system natural frequencies from LC 1.1. IEA international results.

Case 1.3: Free decay test

Case 1.3 is a decay test with an initial displacement of the structure of 22m in the surge direction. A very fine agreement is seen both for the international comparison as for the three versions of HAWC2.

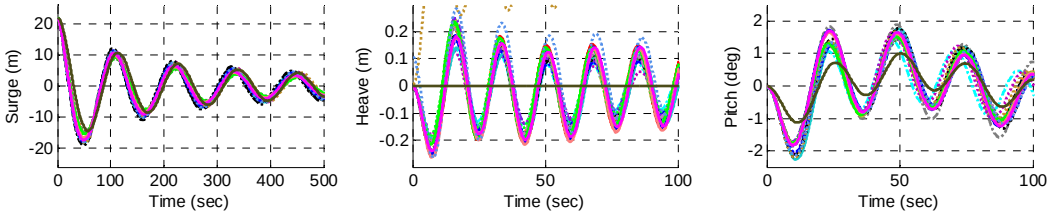

Figure 35: Surge free decay (LC 1.3a), platform motion response. IEA international results

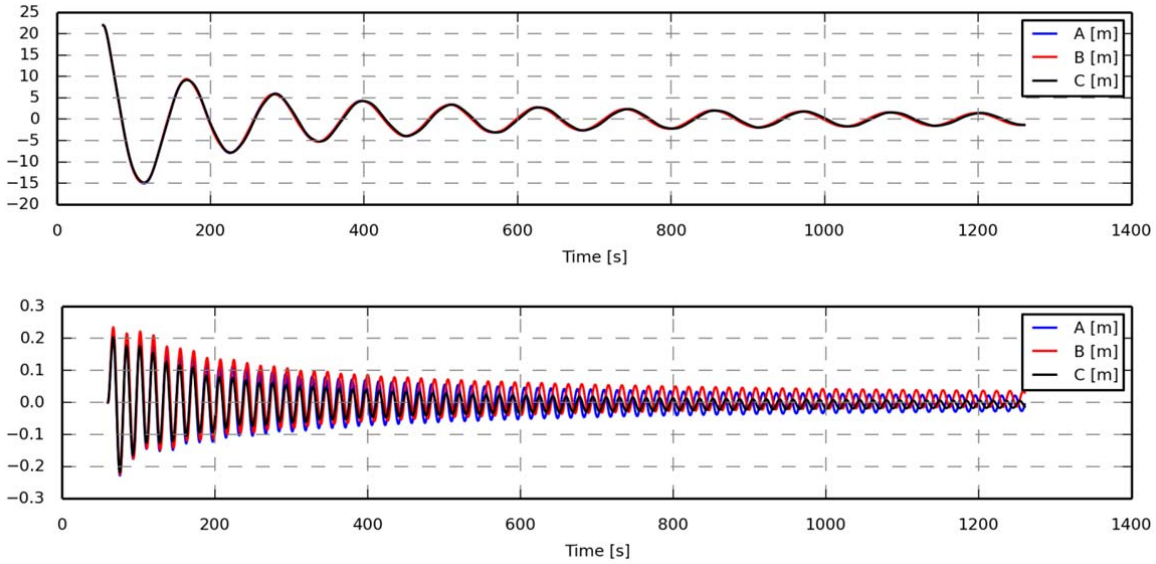

Figure 36: Case 1.3a. Surge and heave. A is HAWC2-WAMIT, B is HAWC2-WAMSIM and C is HAWC2-StdAlone

Case 1.3b is a decay test with an initial displacement of the structure of 6m in the heave direction. A very fine agreement for all methods is seen for the heave response, whereas in the corresponding pitch rotation, differences are seen. Two distinct levels of amplitude is seen. From the three version of HAWC2 it can be seen that the different response in pitch is a consequence of whether Morison or a potential solution is used. A higher level of drag in the Morison approach, not present in the potential flow solutions may very well be the reason for the differences.

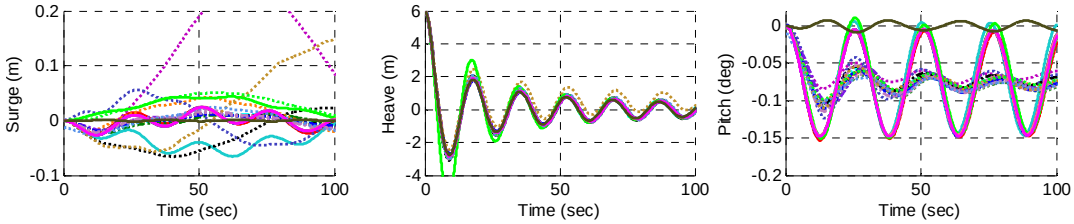

Figure 37:Heave free decay (LC 1.3b), platform motions response. IEA international results.

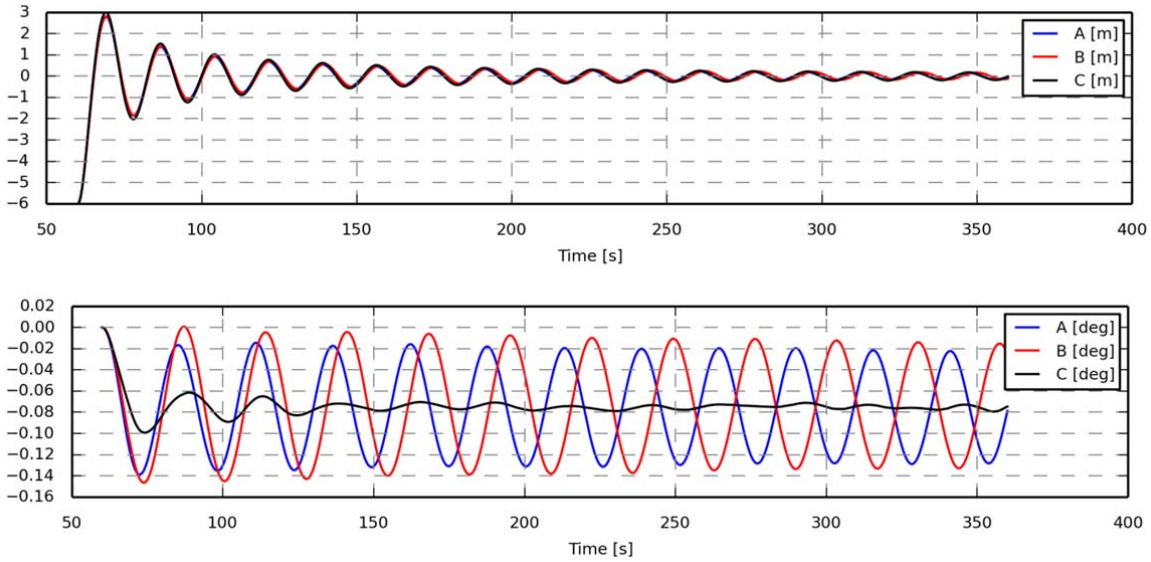

Figure 38: Case 1.3b. Heave and pitch. A is HAWC2-WAMIT, B is HAWC2-WAMSIM and C is HAWC2-StdAlone

Case 1.3c is a pitch decay test with an intial rotation of 8deg. A difference in pitch frequency is seen between the three HAWC2 versions. The HAWC2-WAMSIM approach results in a lower frequency. The reason for this is most likely caused by the approach of handling mass and buoyancy in WAMSIM as explained in the theory chapter HAWC2-WAMSIM. A too high mass is probably the outcome of the assumption of substructure mass being identical to the mass of the submerged volume of water by the substructure compensated by external fictive forces, since the actual mass of the substructure is significantly lower. When the mass is too high, the inertia is also too high and therefore the pitch frequency too low. This is however a small thing to update in WAMSIM, but is important to be aware about.

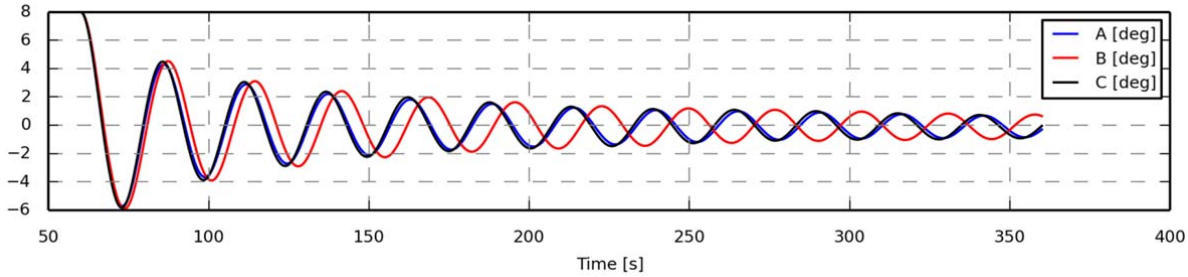

Figure 39: Case 1.3c. Pitch rotation. A is HAWC2-WAMIT, B is HAWC2-WAMSIM and C is HAWC2-StdAlone

Case 1.3d is a yaw decay test with a initial yaw rotation of 8deg. Three approaches in HAWC2 lead to same frequency, but slightly different damping levels. The method using Morisons approach also has the highest damping.

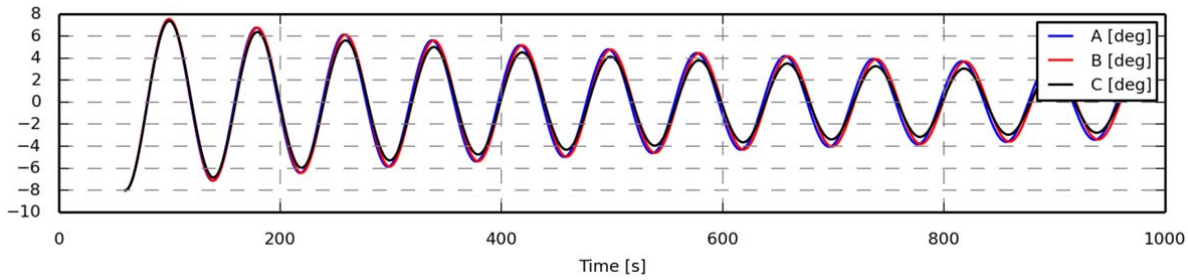

Figure 40: Case 1.3d. Yaw rotation. A is HAWC2-WAMIT, B is HAWC2-WAMSIM and C is HAWC2-StdAlone

Case 2.1: Linear waves on a rigid structure

In this case the structure is rigid, but the mooring lines flexible. Linear waves are applied with a wave height of 6m with a time period of 10s. In Figure 42 a drift force is seen for the Morison based simulations causing a different surge position as well as different anchor line tensions. This is explained by the wheeler stretching of the wave. A small phase difference is also seen. It can also be seen that the pitch motion is higher for the Morison based approach.

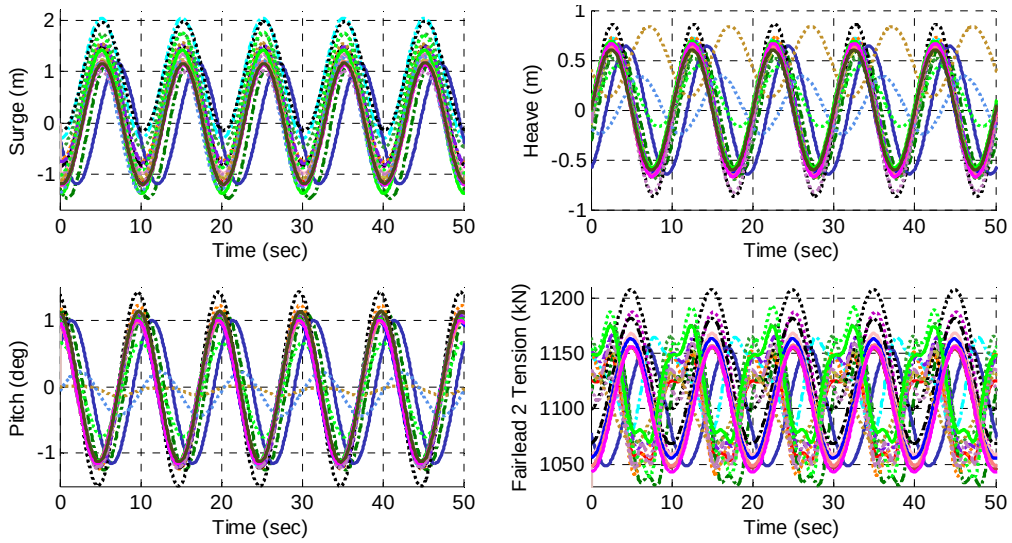

Figure 41: Regular wave simulation (LC 2.1), H = 6 m, T = 10 s. IEA international results.

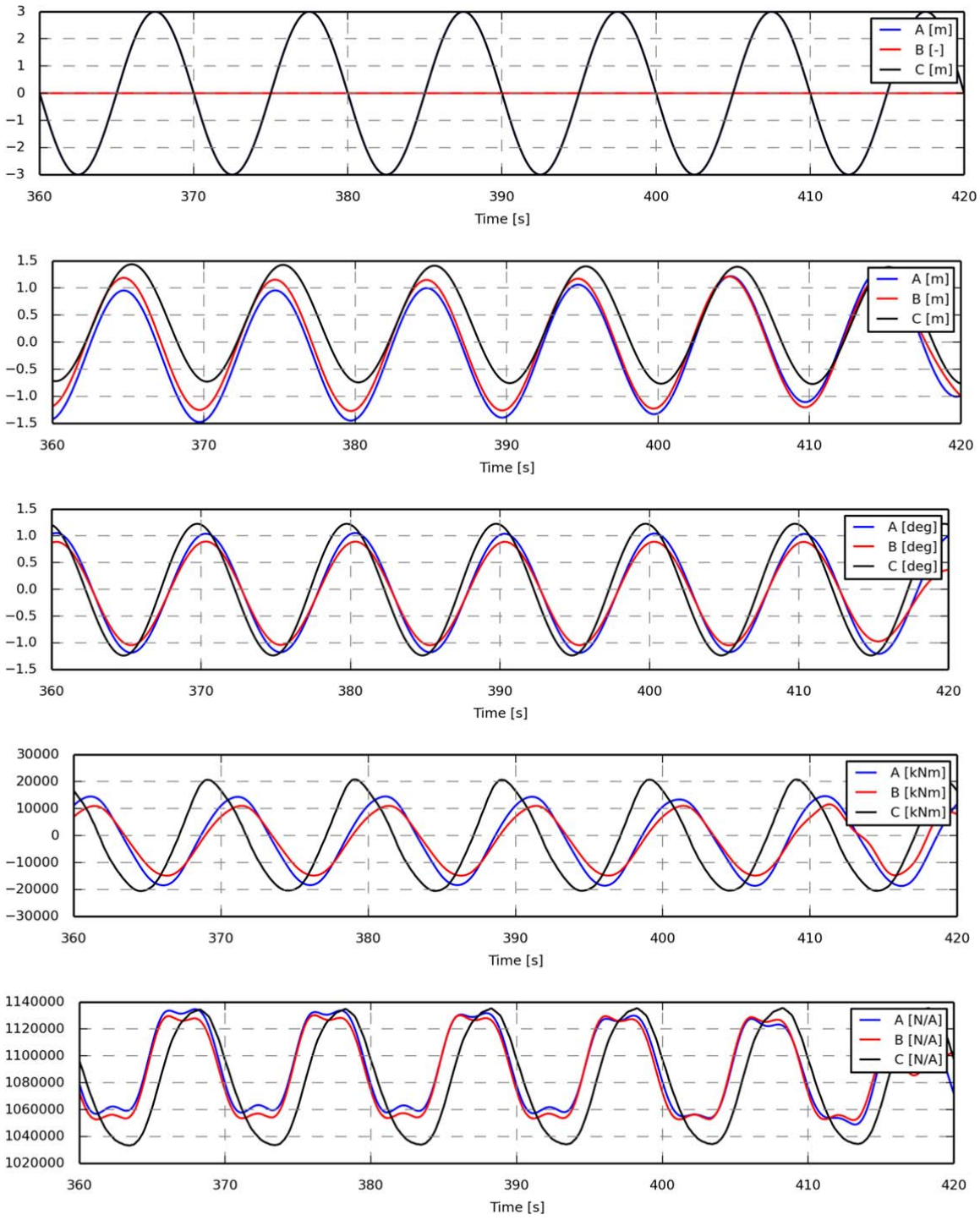

Figure 42: Case 2.1. Wave elevation, surge, pitch, tower Mx, axial force line 1 top. A is HAWC2-WAMIT, B is HAWC2-WAMSIM and C is HAWC2-StdAlone. Even though the wave height is not outputted for HAWC2–WAMSIM it is still present.

Case 2.2: Regular waves on a flexible substructure

Rigid turbine at standstill. Flexible substructure and moorings submitted to irregular Airy wave forces. Hs = 6 m, Tp = 10 s, γ=2.87, JONSWAP spectrum.

In this case a significantly different response is observed for the pitch and surge motion of the structure when Morisons approach is used compared to the potential flow solutions. The increased pitch motion has a direct consequence in term of increased tower bending moments and increased anchor line tension. Since the surge motion is reduced it seem as the effective forcing point on the substructure is located at a lower position for the potential flow methods than for the Morsions approach. One explanation could be the slight wave non-linearity from wheeler stretching only applied with the Morison approach. Since the consequence is large, this is a point that need to be validated with experiments at later stage.

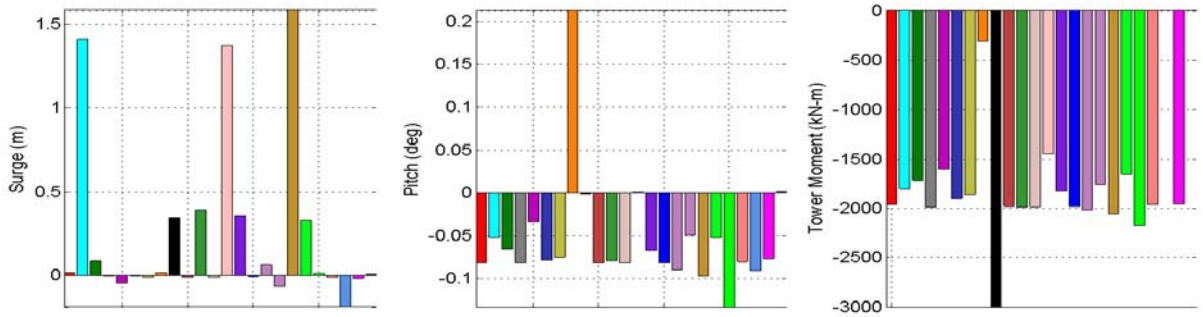

Figure 43. Irregular wave simulation (LC 2.2), H_s = 6 m and T_p = 10 s, mean value of response. IEA international results

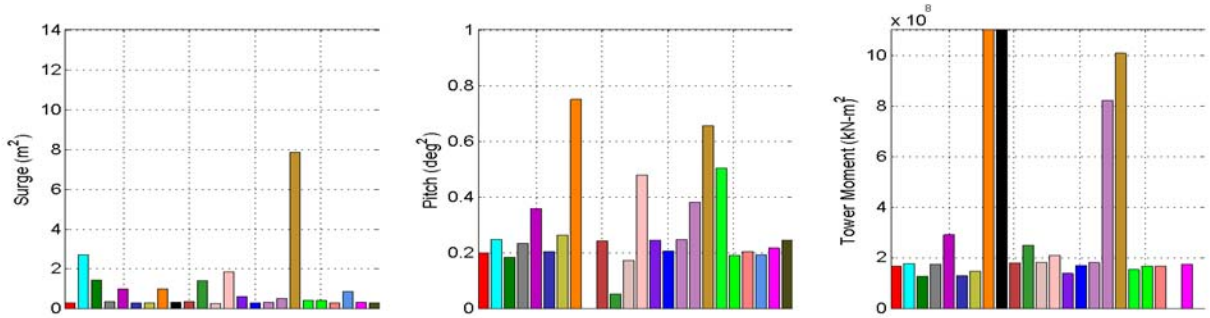

Figure 44. Irregular wave simulation (LC 2.2), Hs = 6 m and Tp = 10 s, variance of response. IEA international results

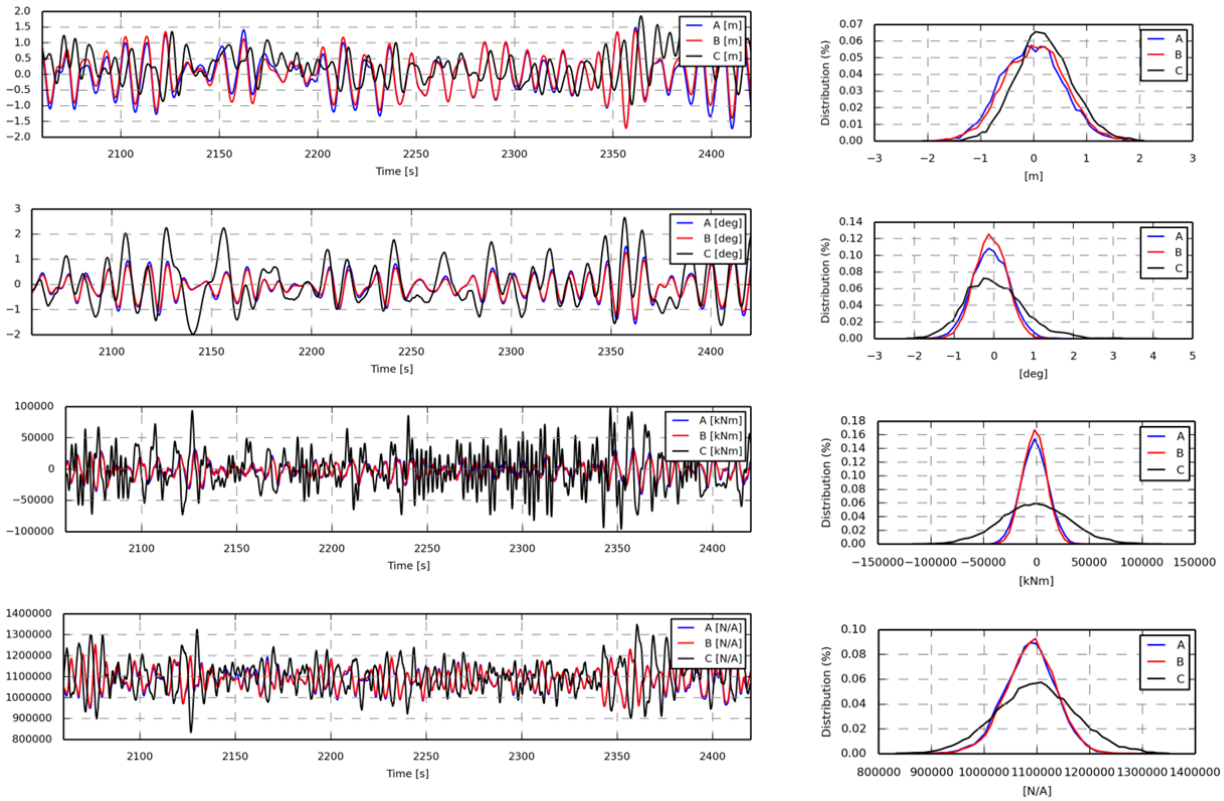

Figure 45: Case 2.2. Surge, pitch, Mx tower bottom, Line 2 axial force. A is HAWC2-WAMIT, B is HAWC2-WAMSIM and C is HAWC2-StdAlone. Left is a zoom of the time signal, right is the distribution function.

Case 2.5: Iregular waves on a flexible substructure

This loadcase is with a rigid turbine, but flexible mooring and substructure (Morison based versions). Irregular waves from a 50 year sea state is included. : Hs = 15.0 m, Tp = 19.2 s, γ=1.05, JONSWAP spectrum.

The Morison based results gives a higher response in pitch motion causing higher tower loads as also seen in load case 2.2.

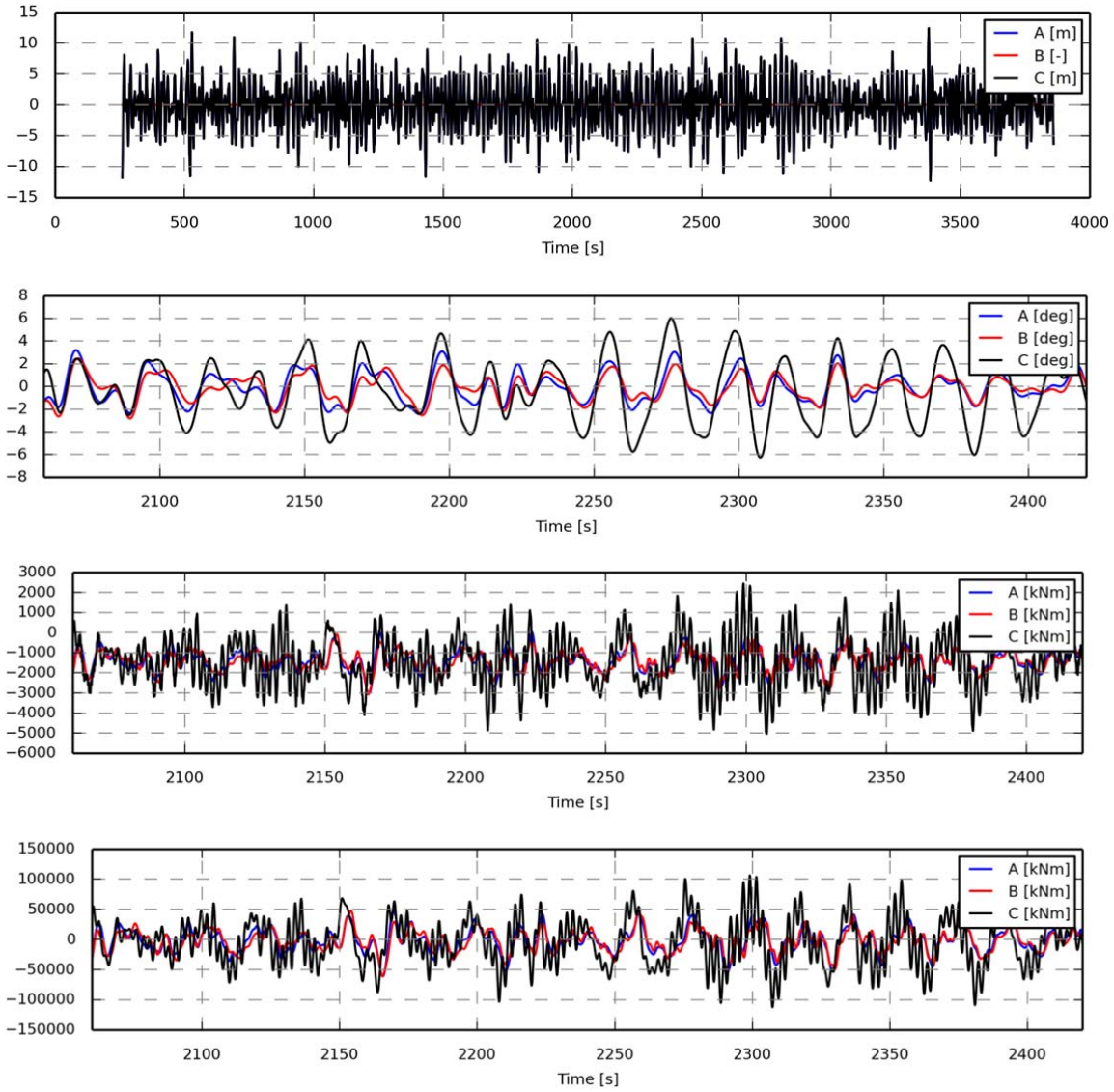

Figure 46: Case 2.5. Wave elevation, surge, pitch, tower bottom Mx. A is HAWC2-WAMIT, B is HAWC2-WAMSIM and C is HAWC2-StdAlone

Case 3.2: Iregular waves on a fully flexible structure at 11.4m/s

In this load case, the structure is fully flexible (potential flow methods with rigid substructure though). The turbine is operating at 11.4m/s in turbulent inflow and the waves are irregular with Hs = 6 m, Tp = 10 s, γ=2.87, jonswap spectrum.

It can be seen that the fully flexible HAWC2-stdalone solution results in higher pitch motions of the structure, which can be seen to cause larger variations in rotor speed, power production and blade pitch angle. The tower loads agree very well in the top of the tower and side-side, but the fore-aft tower bottom loads larger variations are seen in the HAWC2-stdalone edition with the flexible semisub and Morison approach.

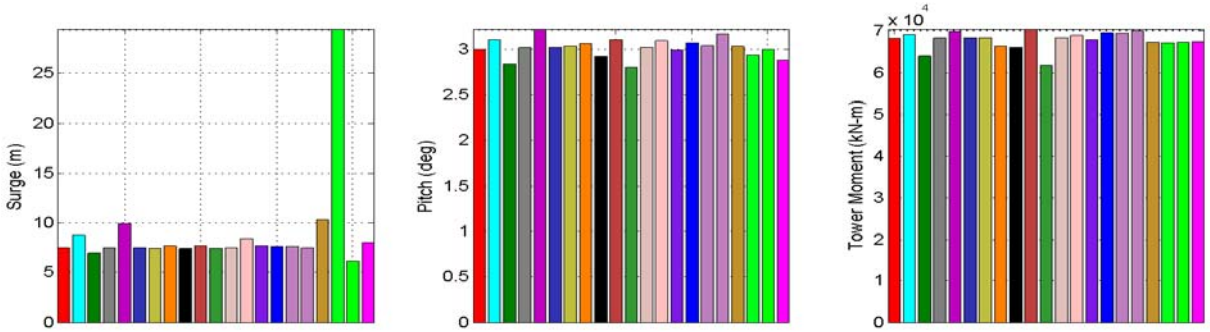

Figure 47. Irregular wave simulation with wind (LC 3.2), Hs = 6 m, Tp = 10 s, V=11.4 m/s, mean value of response. IEA international results

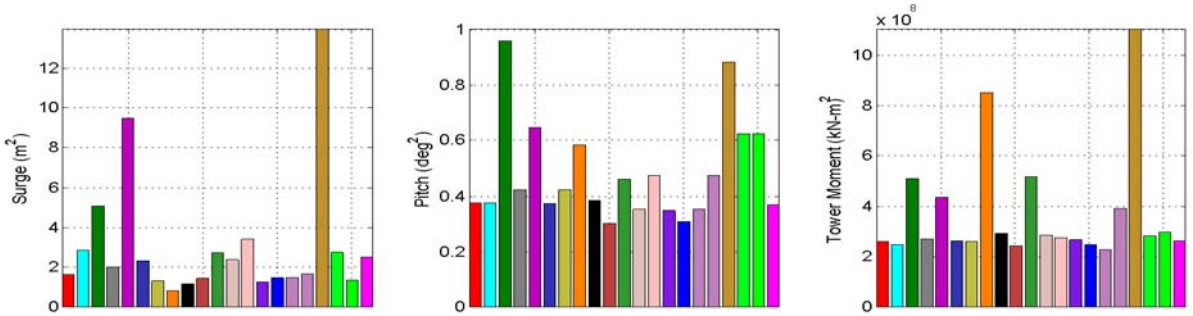

Figure 48. Irregular wave simulation with wind (LC 3.2), Hs = 6 m, Tp = 10 s, V=11.4 m/s, variance of response. IEA international results

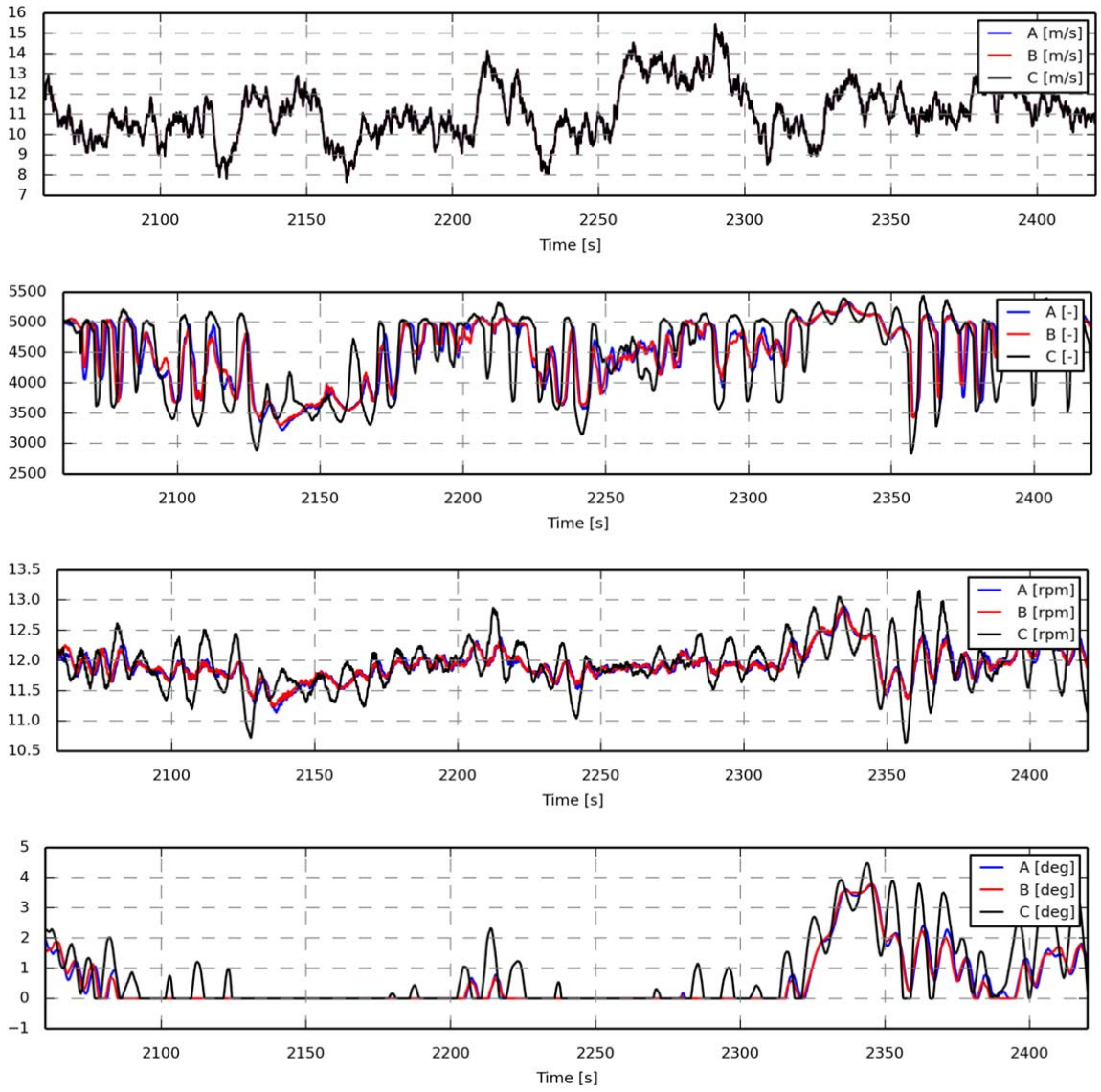

Figure 49: Case 3.2. Wind, Electrical power, rotor speed, blade pitch angle. A is HAWC2-WAMIT, B is HAWC2-WAMSIM and C is HAWC2-StdAlone.

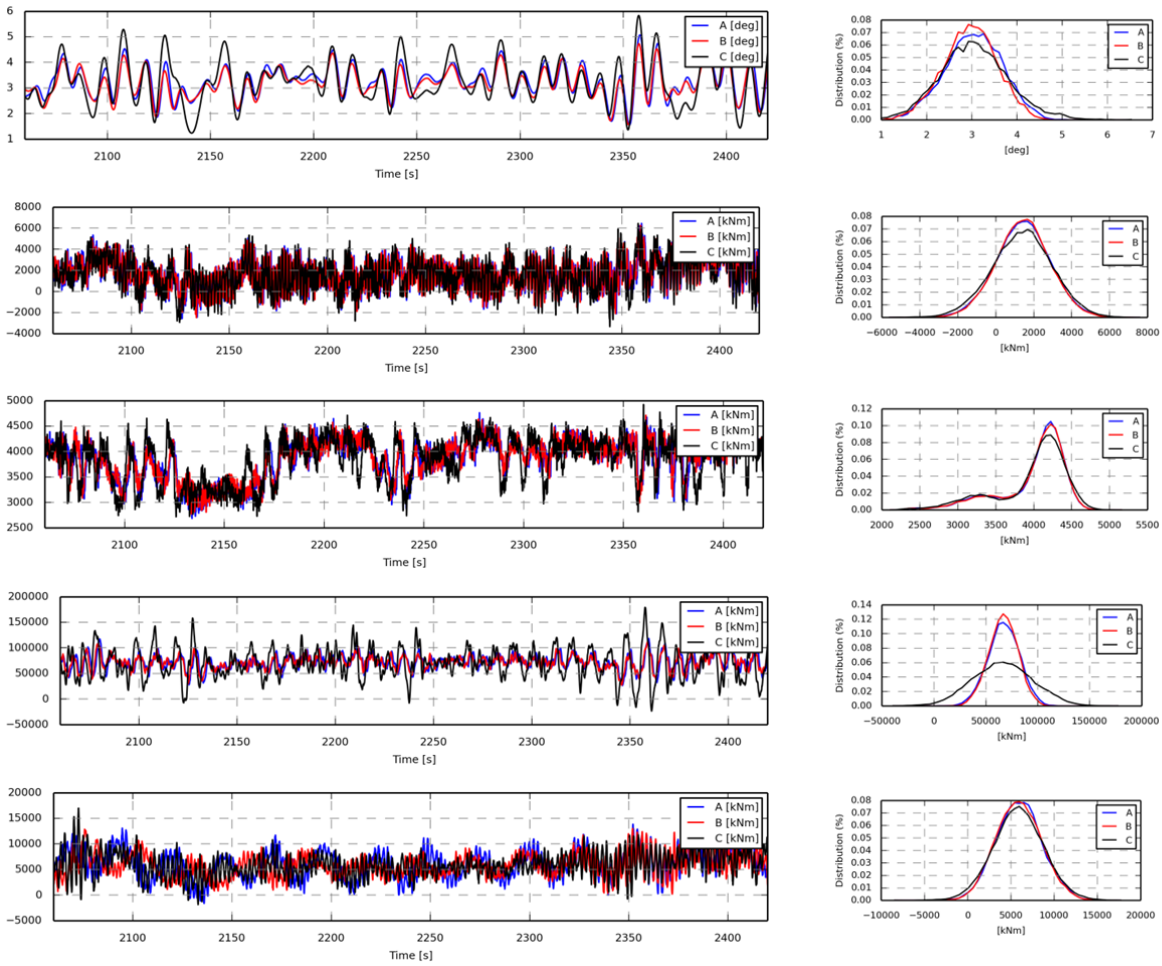

Figure 50: Case 3.2. Pitch, Mx tower top, My tower top, Mx tower bottom. A is HAWC2-WAMIT, B is HAWC2-WAMSIM and C is HAWC2-StdAlone. Left is a zoom of the time signal, right is the distribution function.

Case 3.3: Iregular waves on a fully flexible structure at 18m/s

In this load case, the structure is fully flexible (potential flow methods with rigid substructure though). The turbine is operating at 18m/s in turbulent inflow and the waves are irregular with Hs = 6 m, Tp = 10 s, γ=2.87, jonswap spectrum.

As for case 3.2 it can be seen that the fully flexible HAWC2-stdalone solution results in higher pitch motions of the structure, which can be seen to cause larger variations in rotor speed, power production and blade pitch angle. The tower loads agree very well in the top of the tower and side-side, but the fore-aft tower bottom loads larger variations are seen in the HAWC2-stdalone edition with the flexible semisub and Morison approach.

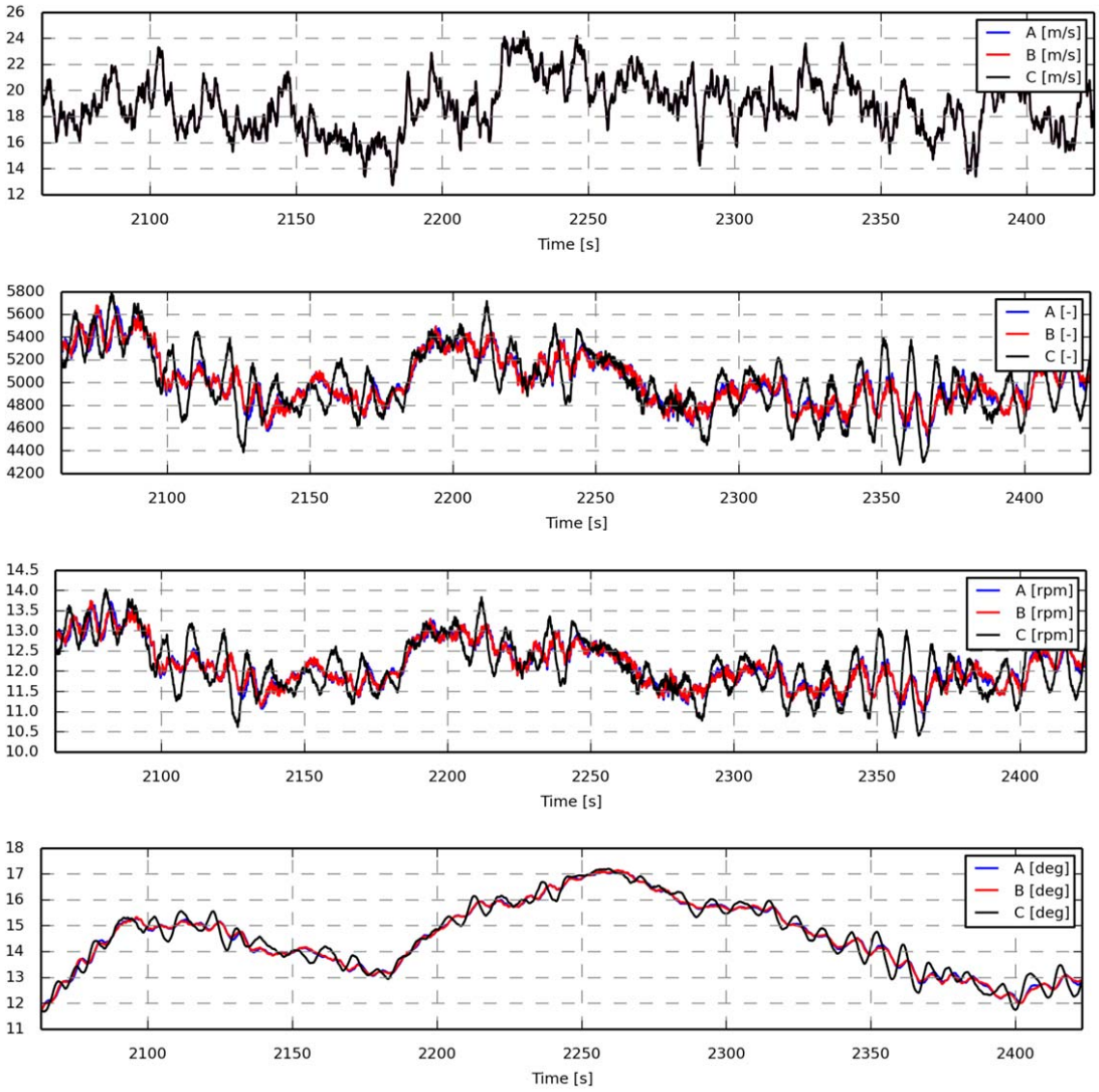

Figure 51: Case 3.3. Wind, Electrical power, rotor speed, blade pitch angle. A is HAWC2-WAMIT, B is HAWC2-WAMSIM and C is HAWC2-StdAlone.

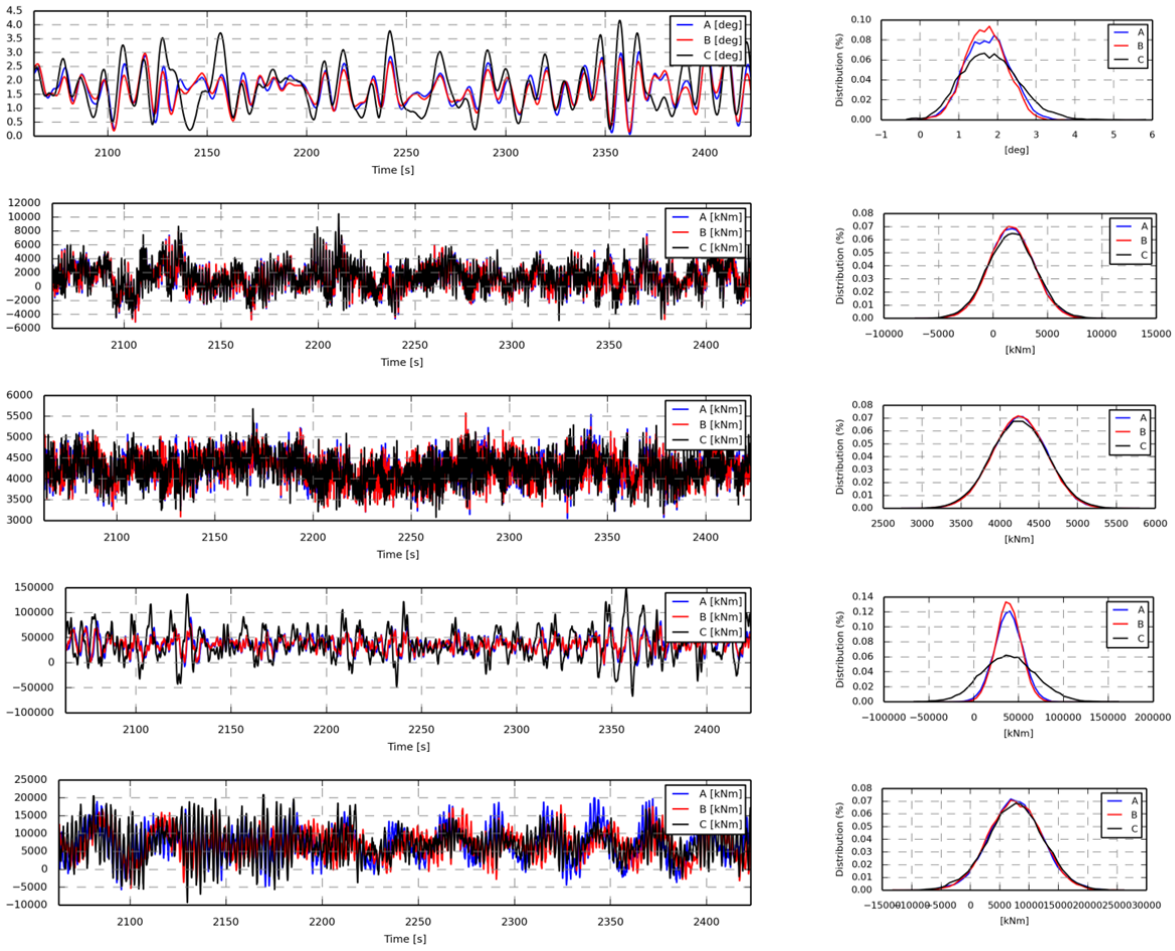

Figure 52: Case 3.3. Pitch, Mx tower top, My tower top, Mx tower bottom. A is HAWC2-WAMIT, B is HAWC2-WAMSIM and C is HAWC2-StdAlone. Left is a zoom of the time signal, right is the distribution function.

Case 3.5: Iregular waves on a fully flexible structure at 47.5m/s

In this load case, the structure is fully flexible (potential flow methods with rigid substructure though). The turbine at stand still with the blades pitched 90deg. The wind speed is 47.5m/s in turbulent inflow and the waves are irregular with Hs = 15 m, Tp = 19.2 s, γ=1.05, jonswap spectrum.

Again larger pitch motion is seen for the HAWC2-stdalone with Morison approach compared to the rigid semisub with potential flow theory. This results in higher tower loads, whereas the anchor line tension is more unaffected.

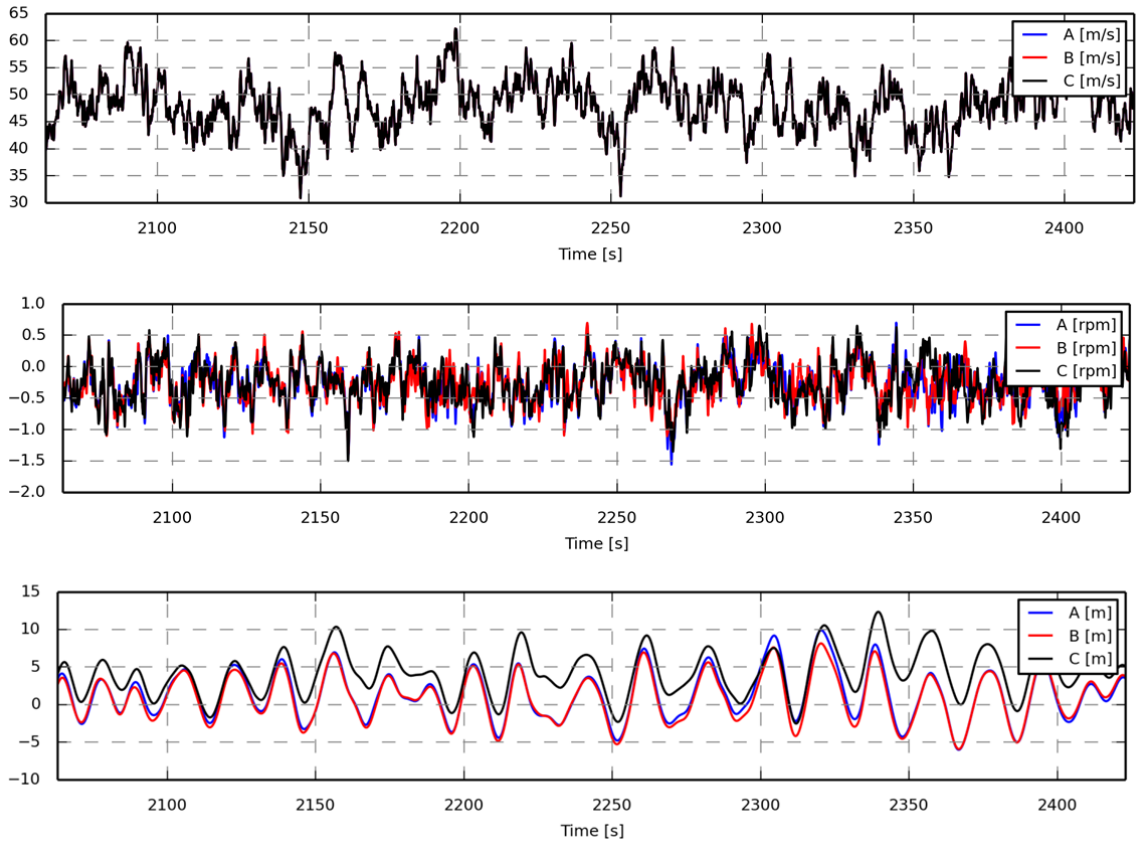

Figure 53: Case 3.5. Wind speed, rotor speed, surge. A is HAWC2-WAMIT, B is HAWC2-WAMSIM and C is HAWC2-StdAlone.

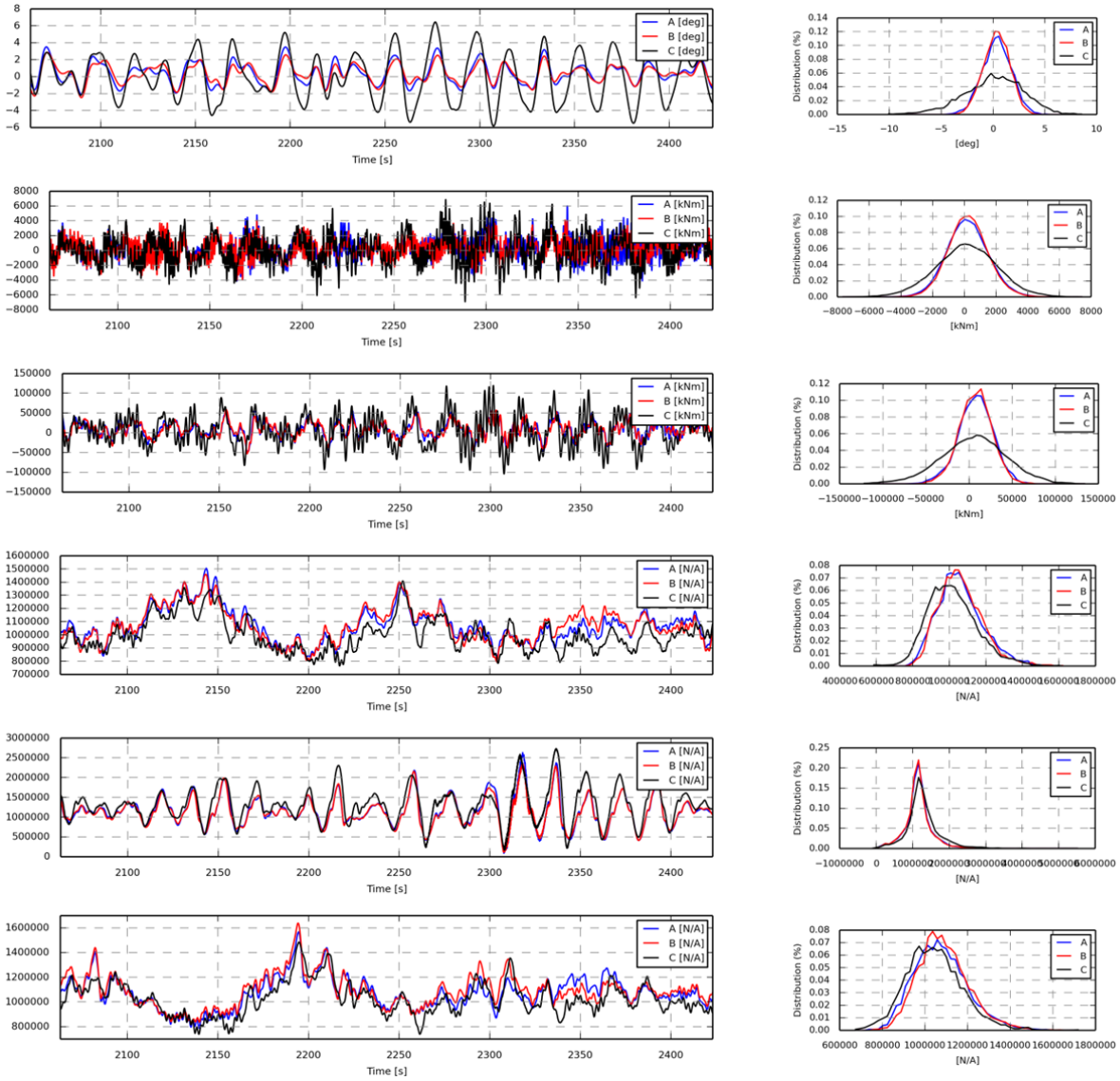

Figure 54: Case 3.5. Pitch, Mx tower top Mx tower bottom, line 1, line 2, line 3. A is HAWC2-WAMIT, B is HAWC2-WAMSIM and C is HAWC2-StdAlone. Left is a zoom of the time signal, right is the distribution function.

Case 3.9a: Flooded compartment, no waves

LC 3.9 examines the response of the semi during a damage scenario where water has flooded a compartment within one of the offset columns. Water is added to both Base Column 1 and Upper Column 1. For Base Column 1, the column is completely flooded, which results in the addition of 3.82e5 kg of water. Upper Column 1 is flooded up to 9.33 m above the base of that column, which means an addition of 1.704e5 kg of water.

It was not directly possibly to adjust the water ballast in the hydrodynamic codes WAMSIM and WAMIT, and therefore these results does not result in a skew orientation of the semi sub. The impact can be seen from the HAWC2-standalone results where the offset is included. The semisub is seen to have a pitch angle of 7deg and a roll angle of 4deg due to the water offset, which directly causes extra loads on the tower bottom.

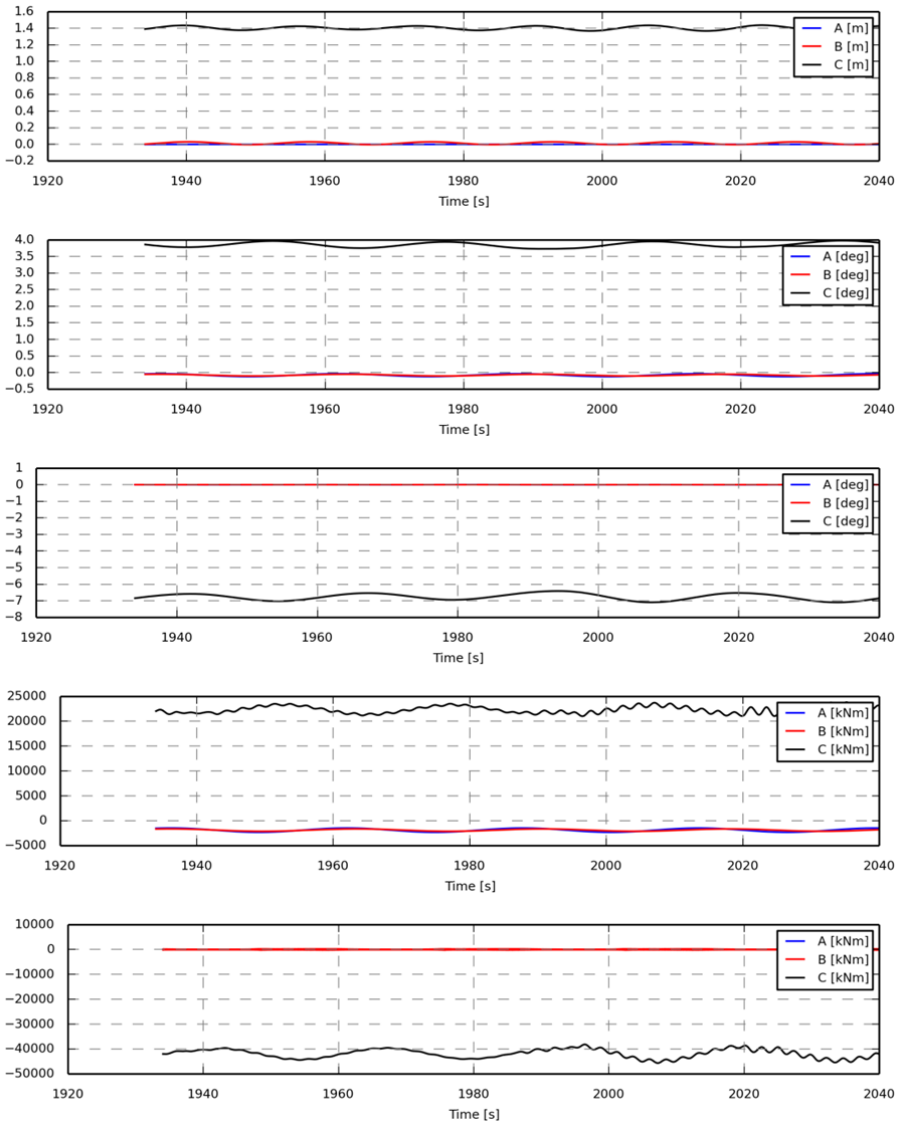

Figure 55: Case 3.9a. Heave, pitch, roll,Mx tower bottom, My tower bottom. A is HAWC2-WAMIT, B is HAWC2-WAMSIM and C is HAWC2-StdAlone

Case 3.9b: Flooded compartment, iregular waves

This loadcase is also with flooded compartments as for case 3.9a, but here the turbine is operating at 18m/s with turbulent inflow and irregular waves Hs = 6 m, Tp = 10 s, γ=2.87, jonswap spectrum.

It was not directly possibly to adjust the water ballast in the hydrodynamic codes WAMSIM and WAMIT, and therefore these results does not result in a skew orientation of the semi sub which explain the main result differences.

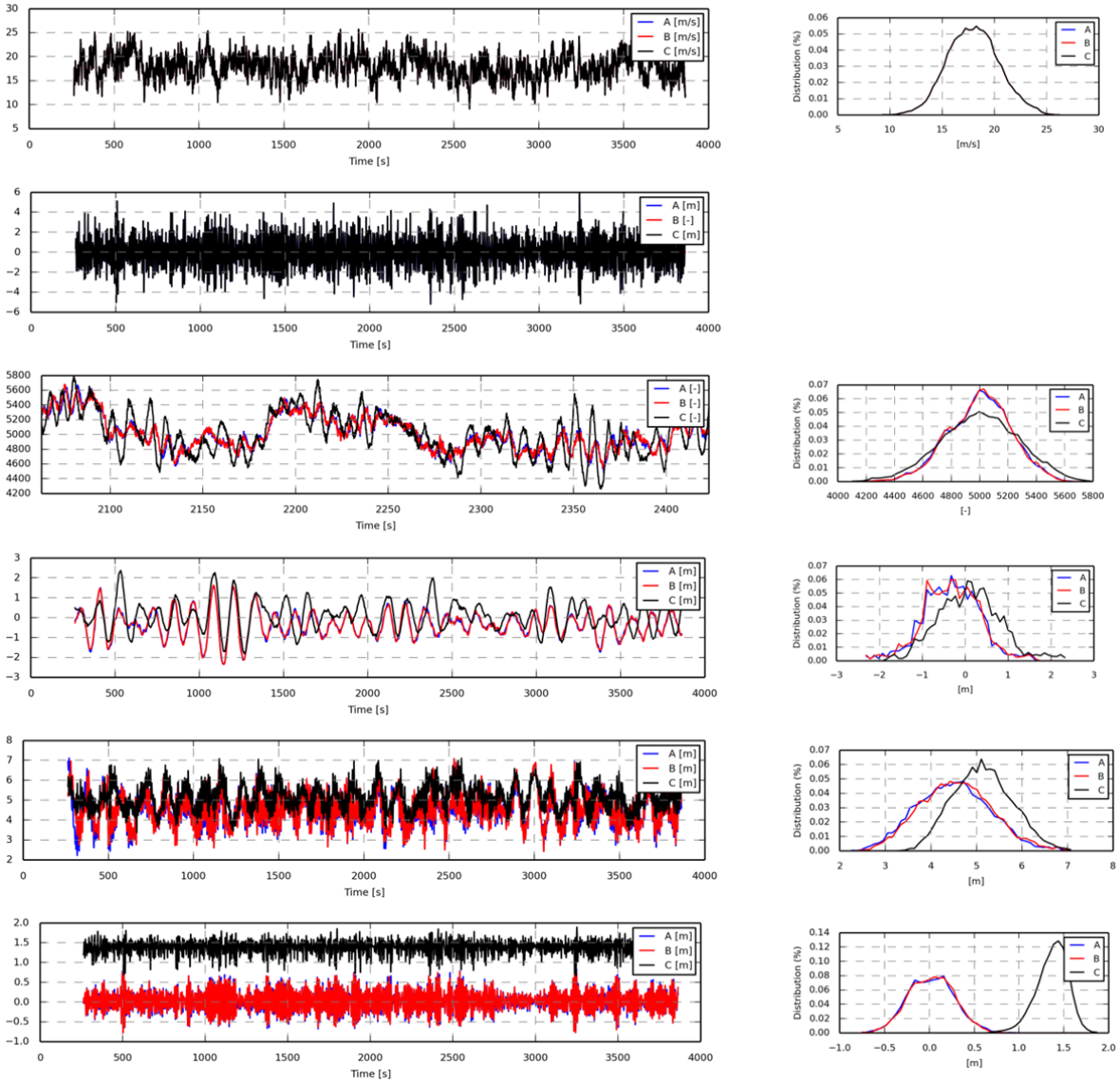

Figure 56: Case 3.9b. Wind speed, Wave height, Electrical power, sway, surge, heave. A is HAWC2-WAMIT, B is HAWC2-WAMSIM and C is HAWC2-StdAlone. Left the time signal, right is the distribution function

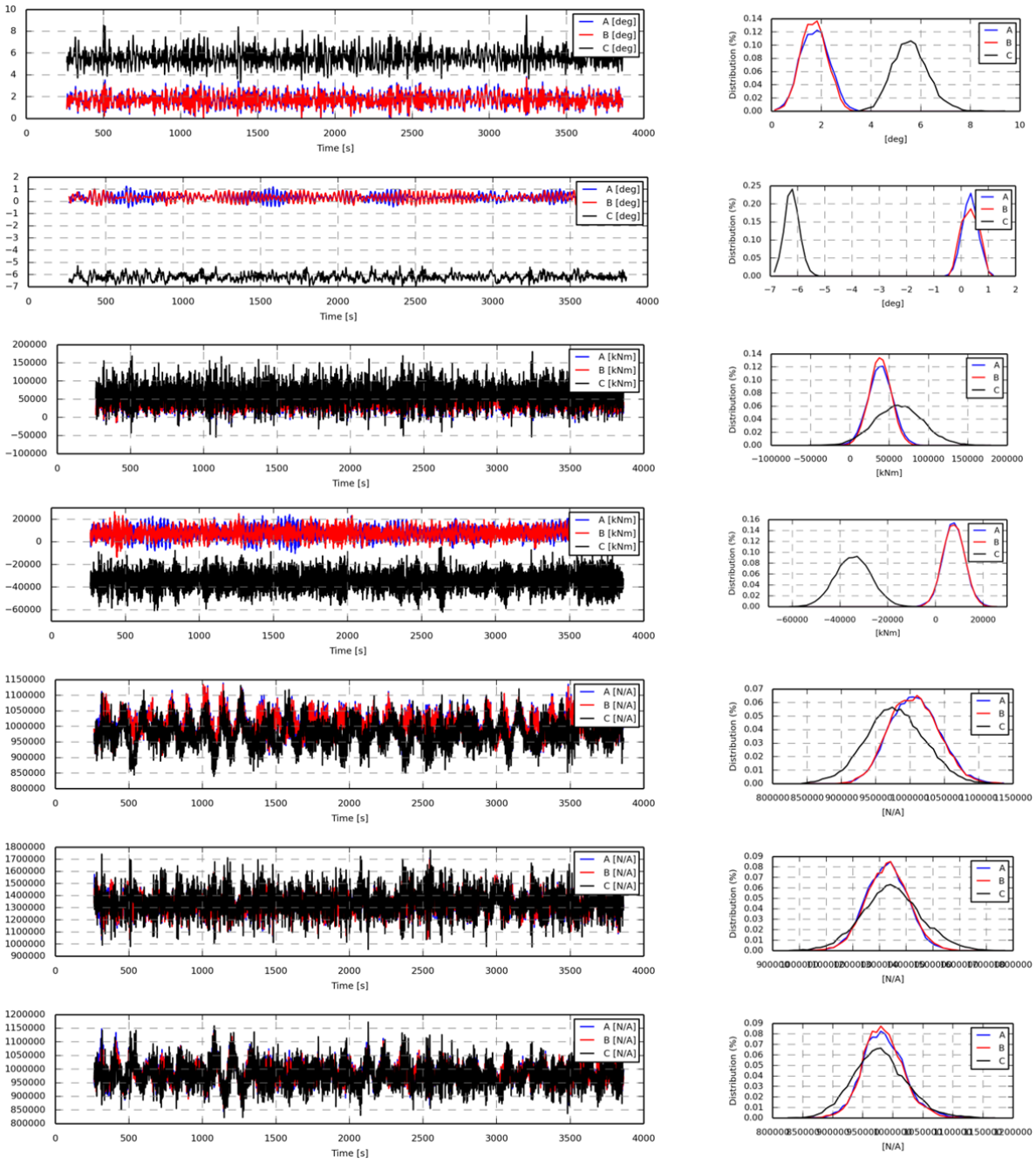

Figure 57: Case 3.9b. Pitch, roll, Mx tower bottom, My tower bottom, Fz line 1, Fz line 2, Fz line 3. A is HAWC2-WAMIT, B is HAWC2-WAMSIM and C is HAWC2-StdAlone. Left the time signal, right is the distribution function

Acknowledgements

The work presented in this report is funded by the EUDP project IEA Annex 30: Offshore Code Collaboration Continued (OC4) under project number 64010-0071 which is gratefully acknowledged.

References

G.B. Airy (1841), Tides and waves, Encyclopaedia Metropolitana

Bingham, H.B. (2000): A hybrid Boussineq-panel method for predicting the motion of a moored ship., page 40:21-38, Publisher Coastal Engineering.
Henrik Bredmose, Jesper Mariegaard, Bo Terp Paulsen, Bjarne Jensen, Signe Schløer,
Torben Juul Larsen, Taesong Kim and Anders, Melchior Hansen (2013). The wave loads project. DTU Wind Energy Report E–0045. December 2013

J.R. Chaplin (1980), Developments of stream-function theory, Coastal Engineering Vol 3 p 179-205, 1980

Craig, R. R., Bampton, M.C.C. (1968) Coupling of substructures for dynamic analysis. AIAA journal. Vol 6 no. 7, 1968.

Christensen, E., Jensen, B., Mortensen, S., Hansen, H. and Kirkegaard, J. (2008) Numerical simulation of ship motion in offshore and harbour areas. In OMAE2008-57206, Proc. ASME 27th Int Conf. on Offshore Mechanics and Artic Engineering, Estoril, Portugal. ASME.
Hansen, H.F., Carstensen, S. and Christensen, E.D. (2009) Multi-Vessel Interaction in Shallow Water. In OMAE2009-79161, Proc. ASME 28th Int Conf. on Offshore Mechanics and Artic Engineering, Honolulu Hawaii, USA. ASME

J.D. Fenton (1988), The numerical solution of steady water wave problems, Computers & Geosciences, Vol 14 no 3 p 357-368, 1988

Guyan, R. J. (1964) Reduction of stiffness and mass matrices. AIAA journal vol 3, No 2, 1964

Kallesøe, B. and Hansen, A. (2011). Dynamic mooring line modeling in hydro-aero-elastic wind turbine simulations, ISOPE-2011, Maui, Hawaii, USA, June 19-24, 2011.

Kim, T., Hansen, A. M., & Branner, K. (2013). Development of an anisotropic beam finite element for composite wind turbine blades in multibody system. *Renewable Energy*, *59*, 172-183. 10.1016/j.renene.2013.03.033

Larsen, T.J, Kallesøe, B., Hansen, H.F. (2011) Dynamics of a Floating Wave Energy Platform with Three Wind Turbines Operating, ISOPE-2011, Maui, Hawaii, USA, June 19-24, 2011.

T.J. Larsen, H. A. Madsen, G. Larsen, K. S. Hansen (2013). Validation of the Dynamic Wake Meander Model for Loads and Power Production in the Egmond aan Zee Wind Farm. Wind Energy, 16, 2013, pp. 605–624. DOI: 10.1002/we.1563

Newman, J. (1986). Marine Hydrodynamics. Cambridge University Press.
Robertson, A., Jonkman, J., Quist, J., Chen, X., Armendariz, J.A., Soares, C.G., Luan, C., Yutonn, H., Yde, A., Larsen, T., Nichols, J., Lei, L., Maus, K.E., Godreau, C., Heege, A., Vatne, S.R., Manolas, D., Qin, H., Riber, H., Abele, R., Yamaguchi, A., Pham, A., Alves, M., Kofoed-Hansen, H. (2014) Offshore code comparison collaboration, continued: phase II results of a floating semisubmersible wind system. Proceedings of the 33rd International Conference on Ocean, Offshore and Arctic Engineering OMAE2014 June 8-13, 2014, San Francisco, CA, USA

J.M. Morison, M.P. O'Brien,J.W. Johnson and S.A. Schaaf (1950), The force exerted by surface waves on piles, Transaction of the American institute of mining and metallurgical engineers, Vol 189 p (149-154), 1950

F. Vorpahl, M. Strobel, J.M. Jonkman, T.J.Larsen, P. Passon, J. Nichols. Verification of aero-elastic offshore wind turbine design codes under IEA Wind Task XXIII. Wind Energ. (2013). DOI: 10.1002/we.1588

J.D. Wheeler (1970), Method for Calculating Forces Produced by Irregular Waves, Journal of petroleum technology. Vol 249 p. (359-367),1970

Wojciech Popko, Fabian Vorpahl, Adam Zuga, Martin Kohlmeier, Jason Jonkman, Amy Robertson, Torben J. Larsen, Anders Yde, Kristian Sætertrø, Knut M. Okstad, James Nichols, Tor A. Nygaard, Zhen Gao, Dimitris Manolas, Kunho Kim, Qing Yu, Wei Shi, Hyunchul Park, Andrés Vásquez-Rojas, Jan Dubois, Daniel Kaufer, Paul Thomassen, Marten J. de Ruiter, Tjeerd van der Zee, Johan M. Peeringa, Huang Zhiwen and Heike von Waaden. Offshore Code Comparison Collaboration Continuation (OC4), Phase I - Results of Coupled Simulations of an Offshore Wind Turbine With Jacket Support Structure. Journal of Ocean and Wind Energy. Vol. 1, No. 1 February 2014. ISSN: 2310-3604

W. Popko, F. Vorpahl, A. Zuga, M. Kohlmeier, J. Jonkman, A. Robertson, T. J. Larsen, A.Yde, K. Sætertrø, K. M. Okstad, J. Nichols, T. A. Nygaard, Z. Gao, D. Manolas, K. Kim, Q. Yu, W. Shi, H. Park, A. Vásquez-Rojas, J. Dubois, D. Kaufer, P. Thomassen, M. J. de Ruiter, J. M. Peeringa, H. Zhiwen, H. von Waaden. Offshore Code Comparison Collaboration Continuation (OC4), Phase I – Results of Coupled Simulations of an Offshore Wind Turbine with Jacket Support Structure. Proceedings of the Twenty-second (2012) International Offshore and Polar Engineering Conference Rhodes, Greece, June 17–22, 2012, ISBN 978-1-880653-94–4, ISSN 1098-6189

Appendix A: Larsen, T.J. (2011)

Risø DTU

DTU

Turbulence for the IEA Annex 30 OC4 project

Appendix B: Vorpahl, F et. Al. (2014)

Wind Energy

WIND ENERGY
Wind Energ. 2014; **17**:519–547
Published online 18 March 2013 in Wiley Online Library (wileyonlinelibrary.com). DOI: 10.1002/we.1588

RESEARCH ARTICLE

Verification of aero-elastic offshore wind turbine design codes under IEA Wind Task XXIII

Fabian Vorpahl[1], Michael Strobel[1], Jason M. Jonkman[2], Torben J. Larsen[3], Patrik Passon[4] and James Nichols[5]

[1] Fraunhofer Institute for Wind Energy and Energy System Technology IWES, Bremerhaven, Germany
[2] National Renewable Energy Laboratory, Golden, Colorado, USA
[3] Risø DTU National Laboratory for Sustainable Energy, Roskilde, Denmark
[4] Rambøll Wind Energy, Esbjerg, Denmark
[5] GL Garrad Hassan, Bristol, UK

ABSTRACT

This work presents the results of a benchmark study on aero-servo-hydro-elastic codes for offshore wind turbine dynamic simulation. The codes verified herein account for the coupled dynamic systems including the wind inflow, aerodynamics, elasticity and controls of the turbine, along with the incident waves, sea current, hydrodynamics and foundation dynamics of the support structure.

A large set of time series simulation results such as turbine operational characteristics, external conditions, and load and displacement outputs was compared and interpreted. Load cases were defined and run with increasing complexity to trace back differences in simulation results to the underlying error sources. This led to a deeper understanding of the underlying physical systems. In four subsequent phases—dealing with a 5-MW turbine on a monopile with a fixed foundation, a monopile with a flexible foundation, a tripod and a floating spar buoy—the latest support structure developments in the offshore wind energy industry are covered, and an adaptation of the codes to those developments was initiated.

The comparisons, in general, agreed quite well. Differences existed among the predictions were traced back to differences in the model fidelity, aerodynamic implementation, hydrodynamic load discretization and numerical difficulties within the codes. The comparisons resulted in a more thorough understanding of the modeling techniques and better knowledge of when various approximations are not valid. More importantly, the lessons learned from this exercise have been used to further develop and improve the codes of the participants and increase the confidence in the codes' accuracy and the correctness of the results, hence improving the standard of offshore wind turbine modeling and simulation.

One purpose of this paper is to summarize the lessons learned and present results that code developers can compare to. The set of benchmark load cases defined and simulated during the course of this project—the raw data for this paper—is available to the offshore wind turbine simulation community and is already being used for testing newly developed software tools. Despite that no measurements are included, the large number of participants and the—in general—very fine level of agreement indicate high trustworthy results within the physical assumptions of the codes and the simulation cases chosen. Other cases, such as large prebend flexible blades, large wind shear, large yaw error or transient maneuvers, may not show the same level of agreement. These cases were deliberately left out because the focus is on the specific offshore application. Further on, this benchmark study includes participating codes and organizations by name (contrary to several previous benchmark studies) that gives the reader a chance to find results from one particular code of interest. Copyright © 2013 John Wiley & Sons, Ltd.

KEYWORDS

offshore wind turbine; aero-servo-hydro-elastic analysis; code verification; monopile; tripod; floating spar buoy

Correspondence
Fabian Vorpahl, Fraunhofer Institute for Wind Energy and Energy System Technology IWES, Am Seedeich 45, 27572 Bremerhaven, Germany.
E-mail: fabian.vorpahl@fraunhofer.iwes.de

Received 8 June 2011; Revised 24 October 2012; Accepted 5 December 2012

Appendix C: Vorpahl et.al. (2013)

Fraunhofer IWES

Technical Report

Description of a basic model of the 'UpWind reference jacket' for code comparison in the OC4 project under IEA Wind Annex 30

Authors
Dipl.-Ing. Fabian Vorpahl
MSc Wojciech Popko
Dipl.-Ing. Daniel Kaufer

July 19, 2013

Appendix D Vorpahl and Popko (2013)

Technical Report

Description of the load cases and output sensors to be simulated in the OC4 project under IEA Wind Annex 30

Authors
Dipl.-Ing. Fabian Vorpahl
MSc Wojciech Popko

July 19, 2013

Appendix E Larsen, T.J. et.al. (2011)

Comparisons of wave kinematics models for an offshore wind turbine mounted on a jacket substructure

†Torben J. Larsen*, †Taeseong Kim
†Risø DTU, National Laboratory for Sustainable Energy,
Technical University of Denmark

‡Signe Schløer and ‡Henrik Bredmose
‡DTU, Mechanical Engineering,
Technical University of Denmark

EWEA Offshore 2011
Amsterdam, The Netherlands
29th November - 1st December 2011

Abstract

The purpose of this study is to investigate the dynamic influence of wave loads for wind turbines placed at intermediate water depths (40-60m) using a jacket substructure. We analyze whether nonlinear wave loading may lead to "ringing", which is a transient excitation of structural modes with much larger amplitudes than seen for linear wave kinematic models. Full interaction between dynamics of the wind turbine and the substructure is included in the study performed for a standstill situation using the fully flexible aeroelastic code HAWC2. Wave loads are modeled using classic methods like Airy and stream function theory, but also a new and more advanced fully nonlinear irregular model has been applied. This nonlinear wave model solves the 3D Laplace equation for the velocity potential with nonlinear boundary conditions at the free surface and an impermeability condition on the sea bed on a variable depth, representing state-of-the-art within nonlinear irrotational wave modeling. The results show a significant increase in dynamic load contribution by the nonlinear waves.

1 Introduction

Within the offshore wind industry there is a general trend towards constantly increasing turbine sizes and siting conditions at water depth above 30m, which has a direct consequence for the design of the applied substructure. Until now, mainly gravity based concrete foundations and monopile have been utilized. However, for increasing water depth and turbine sizes other concepts seem competitive. Especially hydrodynamic transparent designs like the jacket construction attain increased attention since they appear to be cost effective for intermediate water depths. For very deep water, floating designs seem to be the only feasible design.

In general the wave loads are more simple to simulate for deeper waters where small waves are described very well with the linear Airy method [1]. This simple wave model has the benefits of being easily extended to irregular wave trains with and without wave spreading. An improvement of the kinematics near the free surface is obtained by mapping the wave kinematics from the sea bed to the still water level onto the full water column stretching from from the sea bed to the instant wave surface height. This is referred to as the Wheeler stretching [2]. Steep waves (though not breaking) can be represented using stream function theory [3] and [4], which provides a fully nonlinear solution for regular waves on constant depth. These methods are especially applied for investigation of extreme load in storm situation. An offshore wind turbine however differs from most other offshore structures by

*e-mail: tjul@risoe.dtu.dk

Appendix F Popko, W. et.al (2014)

Journal of Ocean and Wind Energy (ISSN 2310-3604)
Copyright © by The International Society of Offshore and Polar Engineers
Vol. 1, No. 1, February 2014, pp. 1–11

http://www.isope.org/publications

Offshore Code Comparison Collaboration Continuation (OC4), Phase I—Results of Coupled Simulations of an Offshore Wind Turbine with Jacket Support Structure

Wojciech Popko[1], Fabian Vorpahl[1]*, Adam Zuga[1], Martin Kohlmeier[1], Jason Jonkman[2], Amy Robertson[2], Torben J. Larsen[3], Anders Yde[3], Kristian Sætertrø[4], Knut M. Okstad[4], James Nichols[5], Tor A. Nygaard[6], Zhen Gao[7], Dimitris Manolas[8]*, Kunho Kim[9], Qing Yu[9], Wei Shi[10], Hyunchul Park[10], Andrés Vásquez-Rojas[11], Jan Dubois[11], Daniel Kaufer[12], Paul Thomassen[13], Marten J. de Ruiter[14], Tjeerd van der Zee[14], Johan M. Peeringa[15], Huang Zhiwen[16], Heike von Waaden[17]

[1]Fraunhofer Institute for Wind Energy and Energy System Technology IWES, Bremerhaven, Germany; [2]National Renewable Energy Laboratory, Golden, CO, USA; [3]Technical University of Denmark, Department of Wind Energy, Roskilde, Denmark; [4]Fedem Technology AS, Trondheim, Norway; [5]Garrad Hassan & Partners Ltd., Bristol, UK; [6]Institute for Energy Technology, Kjeller, Norway; [7]Centre for Ships and Ocean Structures at the Norwegian University of Science and Technology, Trondheim, Norway; [8]National Technical University of Athens, Zografou, Greece; [9]American Bureau of Shipping, Houston, TX, USA; [10]Pohang University of Science and Technology, Pohang, Korea; [11]Institute of Steel Construction at Leibniz Universität Hannover, Hannover, Germany; [12]Endowed Chair of Wind Energy at the Institute of Aircraft Design at Universität Stuttgart, Stuttgart, Germany; [13]Norwegian University of Science and Technology, Trondheim, Norway; [14]Knowledge Centre WMC, Wieringerwerf, The Netherlands; [15]Energy Research Centre of the Netherlands, Petten, The Netherlands; [16]China General Certification, Beijing, China; [17]REpower Systems SE, Osnabrück, Germany

In this paper, the exemplary results of the IEA Wind Task 30 Offshore Code Comparison Collaboration Continuation (OC4) Project – Phase I, focused on the coupled simulation of an offshore wind turbine (OWT) with a jacket support structure, are presented. The focus of this task has been the verification of OWT modeling codes through code-to-code comparisons. The discrepancies between the results are shown and the sources of the differences are discussed. The importance of the local dynamics of the structure is depicted in the simulation results. Furthermore, attention is given to aspects such as the buoyancy calculation and methods of accounting for additional masses (i.e., hydrodynamic added mass). Finally, recommendations concerning the modeling of the jacket are given.

INTRODUCTION

The analysis of offshore wind turbines relies on aero-hydro-servo-elastic simulation codes. These coupled time-domain-based tools take into account an interaction of various environmental conditions and the entire structural assembly of the turbine, including its control system. Due to the complexity of the models, verification and validation of the codes is required. Limited availability of measurement data impedes the validation of these simulation tools. Therefore, there is a need to perform code-to-code comparisons (verification) instead. The first international project dedicated to verification of simulation tools for wind turbines, including hydrodynamic loads, was undertaken within the Offshore Code Comparison Collaboration (OC3) Project (Jonkman and Musial, 2010). The cooperation was focused on coupled simulations of an offshore wind turbine supported by a variety of support structures. Further research needs triggered a follow-up project, the Offshore Code Comparison Collaboration Continuation (OC4) Project. The OC4 project was formed under the International Energy Agency (IEA) Wind Task 30 in 2010 to investigate wind turbine coupled simulations with a jacket support structure and a semisubmersible platform. Complex hydrodynamics of the latter and local vibration phenomena of the former have not been broadly studied yet; therefore, their analysis is of interest.

A number of academic and industrial project partners from 10 countries participate in the task. Those actively involved in Phase I are: Fraunhofer Institute for Wind Energy and Energy System Technology IWES (Germany), the National Renewable Energy Laboratory (NREL) (USA), Technical University of Denmark, Department of Wind Energy, Risø campus, Roskilde, Denmark (Risø DTU) (Denmark), Fedem Technology AS (Norway), Garrad Hassan & Partners Ltd. (UK), Institute for Energy Technology (IFE) (Norway), Pohang University of Science and Technology (POSTECH) (Korea), Centre for Ships and Ocean Structures (CeSOS) at the Norwegian University of Science and Technology (NTNU) (Norway), National Technical University of Athens (NTUA) (Greece), Institute of Steel Construction at Leibniz Universität Hannover (LUH) (Germany), the Endowed Chair of Wind Energy at the Institute of Aircraft Design at Universität Stuttgart (SWE) (Germany), Norwegian University of Science and Technology (NTNU) (Norway), Knowledge Centre WMC (The Netherlands), Energy Research Centre of the Netherlands (ECN) (The Netherlands), American Bureau of Shipping (ABS) (USA), REpower Systems SE (Germany) and China General Certification (CGC) (China). Each one of the participants has their own area of expertise and, therefore, their own unique contribution to the project.

*ISOPE Member.

Received October 26, 2013; updated and further revised manuscript received by the editors December 9, 2013. The original version (prior to the final updated and revised manuscript) was presented at the Twenty-second International Offshore and Polar Engineering Conference (ISOPE-2012), Rhodes, Greece, June 17–22, 2012.

KEY WORDS: Offshore wind turbine, coupled simulation, aero-hydro-servo-elastic codes, jacket support structure, code verification, code-to-code comparison, OC4.

Appendix G Popko, W. et.al. (2012)

Offshore Code Comparison Collaboration Continuation (OC4), Phase I – Results of Coupled Simulations of an Offshore Wind Turbine with Jacket Support Structure

Wojciech Popko [1], Fabian Vorpahl [1], Adam Zuga [1], Martin Kohlmeier [1], Jason Jonkman [2], Amy Robertson [2], Torben J. Larsen [3], Anders Yde [3], Kristian Sæterøø [4], Knut M. Okstad [4], James Nichols [5], Tor A. Nygaard [6], Zhen Gao [7], Dimitris Manolas [8], Kunho Kim [9], Qing Yu [9], Wei Shi [10], Hyunchul Park [10], Andrés Vásquez-Rojas [11], Jan Dubois [11], Daniel Kaufer [12], Paul Thomassen [13], Marien J. de Ruiter [14], Johan M. Peeringa [15], Huang Zhiwen [16], Heike von Waaden [17]

1. Fraunhofer Institute for Wind Energy and Energy System Technology IWES, Bremerhaven, Germany; 2. National Renewable Energy Laboratory, Golden, USA; 3. Technical University of Denmark, Department of Wind Energy, campus Risø, Roskilde, Denmark; 4. Fedem Technology AS, Trondheim, Norway; 5. Garrad Hassan & Partners Ltd., Bristol, UK; 6. Institute for Energy Technology, Kjeller, Norway; 7. Centre for Ships and Ocean Structures at the Norwegian University of Science and Technology, Trondheim, Norway; 8. National Technical University of Athens, Zografou, Greece; 9. American Bureau of Shipping, Houston, USA; 10. Pohang University of Science and Technology, Pohang, Korea; 11. Institute of Steel Construction at the Leibniz Universität Hannover, Hannover, Germany; 12. Endowed Chair of Wind Energy at the Institute of Aircraft Design at Universität Stuttgart, Stuttgart, Germany; 13. Norwegian University of Science and Technology, Trondheim, Norway; 14. Knowledge Centre WMC, Wieringerwerf, The Netherlands; 15. Energy Research Centre of the Netherlands, Petten, The Netherlands; 16. China General Certification, Beijing, China; 17. REpower Systems SE, Osnabrück, Germany

ABSTRACT

In this paper, the exemplary results of the IEA Wind Task 30 "Offshore Code Comparison Collaboration Continuation" (OC4) Project – Phase I, focused on the coupled simulation of an offshore wind turbine (OWT) with a jacket support structure, are presented. The focus of this task has been the verification of OWT modeling codes through code-to-code comparisons. The discrepancies between the results are shown and the sources of the differences are discussed. The importance of the local dynamics of the structure is depicted in the simulation results. Furthermore, attention is given to aspects such as the buoyancy calculation and methods of accounting for additional masses (such as hydrodynamic added mass). Finally, recommendations concerning the modeling of the jacket are given.

KEYWORDS

Offshore wind turbine; coupled simulation; aero-hydro-servo-elastic codes; jacket support structure; code verification; code-to-code comparison; OC4

INTRODUCTION

The analysis of offshore wind turbines relies on aero-hydro-servo-elastic simulation codes. These coupled time-domain-based tools take into account an interaction of various environmental conditions and the entire structural assembly of the turbine, including its control system. Due to the complexity of the models, verification and validation of the codes is required. Limited availability of measurement data impedes the validation of these simulation tools. Therefore, there is a need to perform code-to-code comparisons (verification) instead. The first international project dedicated to verification of simulation tools for wind turbines, including hydrodynamic loads, was undertaken within the "Offshore Code Comparison Collaboration" (OC3) Project (Jonkman and Musial, 2010). The cooperation was focused on coupled simulations of an offshore wind turbine supported by a variety of support structures. Further research needs triggered a follow-on project, the "Offshore Code Comparison Collaboration Continuation" (OC4) Project. The OC4 project was formed under the International Energy Agency (IEA) Wind Task 30 in 2010 to investigate wind turbine coupled simulations with a jacket support structure and a semisubmersible platform. Complex hydrodynamics of the latter and local vibration phenomena of the former have not been broadly studied yet, and therefore, their analysis is of interest.

A number of academic and industrial project partners from 10 countries participate in the task. Those actively involved in Phase I are: Fraunhofer Institute for Wind Energy and Energy System Technology IWES (Germany), the National Renewable Energy Laboratory (NREL) (USA), Technical University of Denmark, Department of Wind Energy, campus Risø, Roskilde, Denmark (Risø DTU) (Denmark), Fedem Technology AS (Norway), Garrad Hassan & Partners Ltd. (UK), Institute for Energy Technology (IFE) (Norway), Pohang University of Science and Technology (POSTECH) (Korea), Centre for Ships and Ocean Structures (CeSOS) at the Norwegian University of Science and Technology (NTNU) (Norway), National Technical University of Athens (NTUA) (Greece), Institute of Steel Construction at the Leibniz Universität Hannover (LUH) (Germany), the Endowed Chair of Wind Energy at the Institute of Aircraft Design at Universität Stuttgart (SWE) (Germany),

Appendix H Popko, W. et.al (2012)

European Seminar OWEMES 2012

OC3 and OC4 projects – Verification benchmark exercises of the state-of-the art coupled simulation tools for offshore wind turbines

W. Popko[1], F. Vorpahl[1], J. Jonkman[2] and A. Robertson[2]
[1]*Fraunhofer Institute for Wind Energy and Energy System Technology IWES, Am Seedeich 45, 27572 Bremerhaven, Germany, wojciech.popko@iwes.fraunhofer.de*
[2]*National Renewable Energy Laboratory, Golden, CO 80401, United States of America, jason.jonkman@nrel.gov*

Abstract – This document briefly presents the activities of the Offshore Code Comparison Collaboration (OC3) and Offshore Code Comparison Collaboration Continuation (OC4) projects under the International Energy Agency (IEA) Wind Tasks 23 and 30, focused on advancing the overall accuracy of the coupled simulation tools for offshore wind turbines (OWT). These two projects focus on the verification of simulation tools performed by direct code-to-code benchmarking exercises. A methodology of the verification process and its outcome are briefly described. Also an introduction to the state-of-the art simulation of OWT is given.

1. Introduction

The enormous potential of offshore wind power and financial support from the European Union and its individual member states drive the offshore wind industry business. Offshore wind turbines (OWT) are becoming a significant source of renewable energy in Europe and also worldwide. However a large-scale development is hampered by dissimilar offshore conditions at diverse sites, which make the standardization of OWT design difficult. Offshore sites differ in terms of wind and wave conditions, water depth, seabed properties etc. This creates a need for the utilization of different types of sub-structures like bottom-fixed monopiles, gravity bases, space frames or floating structures. The price of an entire OWT can be significantly reduced by an appropriate choice of such a sub-structure and its cost-effective design, to which a robust load analysis is the key.

The analysis of OWT relies on aero-hydro-servo-elastic simulation tools and is performed in the time domain, as only this approach can incorporate non-linear dynamic effects and transient events of importance. The coupled tools take into account an interaction of various environmental conditions and the entire structural assembly of the turbine with its control system as shown in Figure 1. This includes various models describing: aerodynamics (aero), control systems (servo), hydrodynamics (hydro) and structural-dynamics of a wind turbine and its offshore support structure (elastic). The coupled approach is required by design standards and guidelines (e.g. International Electrotechnical Commission (IEC 2009) and Germanischer Lloyd (GL 2005)) for an accurate prediction of the system dynamic response and the extreme and fatigue loads of an OWT. Dynamic interaction should not be disregarded as it may result in a considerable loss of accuracy. As for example the aerodynamic damping coming from a rotor can, in some cases, significantly reduce hydrodynamic load effects on a support structure, which can only be captured in the coupled analysis.

Due to the high complexity and sophistication of these simulation tools, their verification and validation is required. The validation is currently impeded by the limited availability and high uncertainty of full-scale measurement data. However, the verification can be done by a

Appendix I Robertson, A. et.al (2013)

Definition of the Semisubmersible Floating System for Phase II of OC4

A. Robertson, J. Jonkman, M. Masciola, H. Song, A. Goupee, A. Coulling, and C. Luan

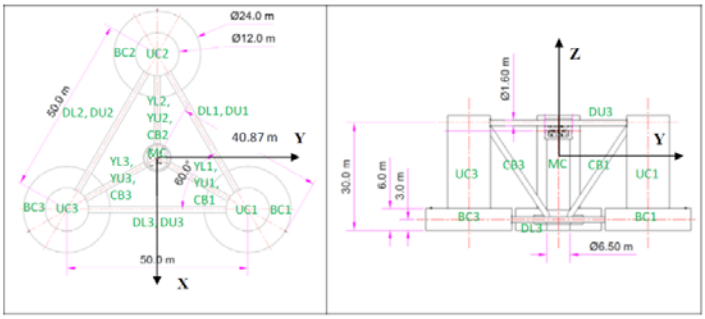

Appendix J Robertsen, A. et.al (2013)

Description of Load Cases for OC4, Phase II

May 18, 2013

1 Overview

This document defines the load cases to be run for Phase II of the OC4 project. Section 2 provides a list of the load cases and Section 3 defines the outputs to be reported. The remainder of this Overview section, Section 1, provides details of the simulations to be run, and information about the wind and wave excitation to be used.

1.1 Simulations

In Section 2, Tables 3-5 provide the details of each simulation to be run for the analysis of the OC4-DeepCwind semisubmersible. The first two columns in these tables provide the load case number and a general description of the load case. The third column (if present) gives any initial conditions that should be applied to the system and column four identifies which DOFs should be enabled in the simulation. The simulation length and wind/wave conditions are given in the following columns, with a description of the output to be reported in the final column.

The simulation length defined in these tables is the time to be reported after all transients have died out, with the exception of the free-decay cases. All of the stochastic cases are run with one seed and a simulation time of T_{stoch} = 3600 s (after transients die out) to get sufficient statistical information. Deterministic cases are run for only T_{det} = 60 s after transients, and the simulation time for the free-decay tests vary based on the DOF being analyzed. The time step for data output is set for all load cases to Δt_{out} = 0.05 s, providing a Nyquist frequency of 10 Hz.

With the exception of a few load cases, time-series responses should be reported for all load cases for the output measurements detailed in Section 3. The reported responses from all of the deterministic wave simulations should start with a wave elevation of 0 m at time = 0 s, with positive slope respective of time. All non-stochastic simulations should start with Blade 1 at 0 degrees azimuth (in the upright position). The deterministic load cases will be compared in terms of the time-series output. For the stochastic cases, time series should be supplied by the participants and NREL will process these for comparison in terms of statistics, probability density functions (PDFs), and power spectral densities (PSDs).

1.2 Wind

In all load cases, the turbine is facing perfectly upwind (no yaw error), towards the negative global X-axis. The turbulence description is based on the Mann turbulence model. Turbulent wind datasets are available for the 11.4 and 18 m/s wind cases on the OC4 SharePoint site (Team Site > Shared Documents > Task 30 OC4 > Phase I Jacket > Stochastic Wind Data). The 47.5 m/s dataset is available on the DTU ftp server at: ftp://ftp.risoe.dk/pub/pfv/tjul/, and will be loaded to the OC4 SharePoint site once the files are broken into smaller chunks, due to a file size limit on the SharePoint site. These datasets DO NOT include the mean value for the wind, or wind shear. Wind shear with a power law profile is to be applied to all load cases with the stochastic wind model, as specified in the load-case tables. In addition, the turbulence intensity must be scaled to the appropriate value given in the load-case tables.

Alternatively, participants can also generate their own wind files based on the parameters given in the load-case tables. In this case, the minimum resolution for the individually generated turbulence wind fields shall be 64 x 32 (lateral x vertical) with at least 5 m of grid spacing. A time step of Δt_{wind} = 0.05 s is to be used. The air density for all simulations is 1.225 kg/m^3. The wind load on the support structure shall be neglected.

1.3 Waves

In all but one load case, the direction of the waves are aligned with the wind, propagating in the direction of the +X-axis. The only exception to this is load-case 3.6, in which the waves are offset from the wind by 30 degrees. Wave direction measurements start with zero degrees in the +X direction, with positive rotation in the CCW direction when looking from above (about +Z).

Appendix K: Robertsen, A. et.al (2014)

Proceedings of the ASME 2014 33rd International Conference on Ocean, Offshore and Arctic Engineering
OMAE2014
June 8-13, 2014, San Francisco, California, USA

OMAE2014-24040

OFFSHORE CODE COMPARISON COLLABORATION CONTINUATION WITHIN IEA WIND TASK 30: PHASE II RESULTS REGARDING A FLOATING SEMISUBMERSIBLE WIND SYSTEM

Amy Robertson and Jason Jonkman
National Renewable Energy Laboratory
Golden, Colorado, USA

Fabian Vorpahl and Wojciech Popko
Fraunhofer Institute for Wind Energy and Energy Systems Technology IWES
Bremerhaven, Germany

Jacob Qvist and Lars Frøyd
4subsea
Hvalstad, Norway

Xiaohong Chen
American Bureau of Shipping
Houston, Texas, USA

José Azcona
National Renewable Energy Centre
Navarra, Spain

Emre Uzunoglu and Carlos Guedes Soares
CENTEC, Instituto Superior Técnico
Universidade de Lisboa, Portugal

Chenyu Luan
CeSOS and NOWITECH
Trondheim, Norway

Huang Yutong and Fu Pengcheng
China General Certification Center
Beijing, China

Anders Yde and Torben Larsen
Technical University of Denmark
Roskilde, Denmark

James Nichols and Ricard Builes
DNV GL
Høvik, Norway

Liu Lei
Goldwind
Beijing, China

Tor Anders Nygaard
Institute for Energy Technology
Kjeller, Norway

Dimitris Manolas
National Technical University of Athens
Athens, Greece

Andreas Heege
SAMTECH s.a.
Barcelona, Spain

Sigrid Ringdalen Vatne and Harald Ormberg
MARINTEK
Trondheim, Norway

Tiago Duarte[1] and Cyril Godreau
Instituto Superior Técnico,
Universidade de Lisboa
Lisbon, Portugal

Hans Fabricius Hansen and Anders Wedel Nielsen
DHI
Hørsholm, Denmark

Hans Riber and Cédric Le Cunff
PRINCIPIA NORTH
Svendborg, Denmark

Friedemann Beyer
University of Stuttgart
Stuttgart, Germany

Atsushi Yamaguchi
University of Tokyo
Tokyo, Japan

Kwang Jin Jung and Hyunkyoung Shin
University of Ulsan
Ulsan, Korea

Wei Shi and Hyunchul Park
POSTECH
Pohang, Korea

Marco Alves and Matthieu Guérinel
WavEC – Offshore Renewables
Lisbon, Portugal

ABSTRACT

Offshore wind turbines are designed and analyzed using comprehensive simulation tools (or codes) that account for the coupled dynamics of the wind inflow, aerodynamics, elasticity, and controls of the turbine, along with the incident waves, sea current, hydrodynamics, mooring dynamics, and foundation dynamics of the support structure. This paper describes the latest findings of the code-to-code verification activities of the Offshore Code Comparison Collaboration Continuation project, which operates under the International Energy Agency Wind Task 30. In the latest phase of the project, participants used an assortment of simulation codes to model the coupled dynamic response of a 5-MW wind turbine installed on a floating semisubmersible in 200 m of water. Code predictions were compared from load case simulations selected to test different model features. The comparisons have resulted in a greater understanding of offshore floating wind turbine dynamics and modeling techniques, and better knowledge of the validity of

[1]Present affiliation with EDP Inovacao

Appendix L:Larsen, T.J. et.al. (2014)

Benchmark comparison of load and dynamics of a floating 5MW semisub windturbine, using three different hydrodynamic approaches

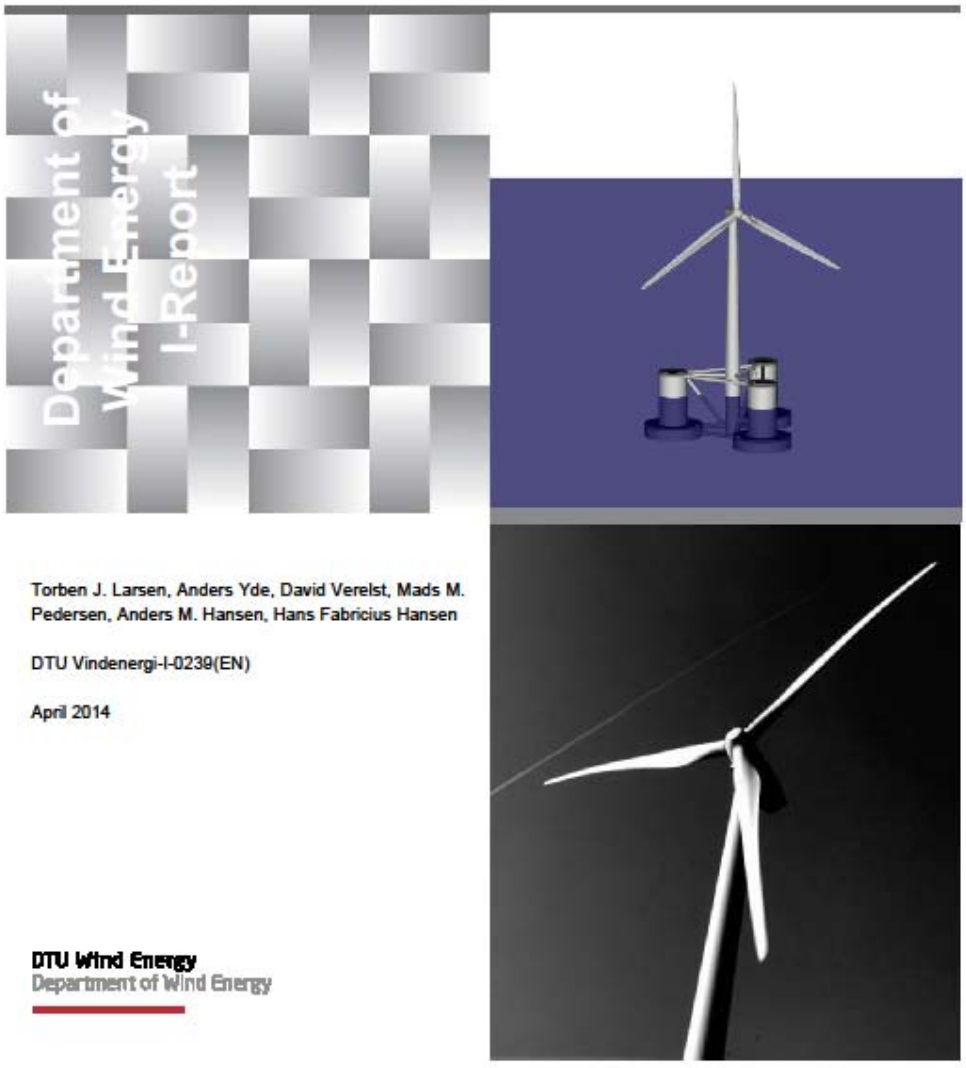

Torben J. Larsen, Anders Yde, David Verelst, Mads M. Pedersen, Anders M. Hansen, Hans Fabricius Hansen

DTU Vindenergi-I-0239(EN)

April 2014

DTU Wind Energy
Department of Wind Energy

Appendix M Robertsen, A. et.al. (2013)

Offshore Code Comparison Collaboration, Continuation: Phase II Results of a Floating Semisubmersible Wind System

Preprint

A. Robertson, J. Jonkman, and W. Musial
National Renewable Energy Laboratory

F. Vorpahl and W. Popko
Fraunhofer Institute for Wind Energy and Energy System Technology IWES

To be presented at EWEA Offshore 2013
Frankfurt, Germany
November 19–21 2013

NREL is a national laboratory of the U.S. Department of Energy
Office of Energy Efficiency & Renewable Energy
Operated by the Alliance for Sustainable Energy, LLC.

This report is available at no cost from the National Renewable Energy Laboratory (NREL) at www.nrel.gov/publications.

Conference Paper
NREL/CP-5000-60600
November 2013

Contract No. DE-AC36-08GO28308

DTU Wind Energy is a department of the Technical University of Denmark with a unique integration of research, education, innovation and public/private sector consulting in the field of wind energy. Our activities develop new opportunities and technology for the global and Danish exploitation of wind energy. Research focuses on key technical-scientific fields, which are central for the development, innovation and use of wind energy and provides the basis for advanced education at the education.

We have more than 240 staff members of which approximately 60 are PhD students. Research is conducted within nine research programmes organized into three main topics: Wind energy systems, Wind turbine technology and Basics for wind energy.

Technical University of Denmark
Department of Wind Energy
Frederiksborgvej 399
Building 118
4000 Roskilde
Denmark
Phone 46 77 50 85

info@vindenergi.dtu.dk
www.vindenergi.dtu.dk